CRCLEME
Cooperative Research Centre for
Landscape Evolution & Mineral Exploration

OPEN FILE
REPORT
SERIES

CSIRO
EXPLORATION
AND MINING

AMIRA
Australian Mineral Industries Research Association Limited ACN 004 448 266

GEOCHEMICAL EXPLORATION FOR PLATINUM GROUP ELEMENTS IN WEATHERED TERRAIN

P252 FINAL REPORT

Volume IIA

C.R.M. Butt, P.A. Williams, D.J. Gray, I.D.M. Robertson, K.H. Schorin, H.M. Churchward, J. McAndrew, S.J. Barnes and M.F.J. Tenhaeff

CRC LEME OPEN FILE REPORT 85

March 2001

(CSIRO Division of Exploration Geoscience Report 332R, 1992.
Second impression 2001)

AMIRA
Australian Mineral Industries Research Association Limited ACN 004 448 266

CRCLEME
Cooperative Research Centre for
Landscape Evolution & Mineral Exploration

CSIRO
EXPLORATION
AND MINING

GEOCHEMICAL EXPLORATION FOR PLATINUM GROUP ELEMENTS IN WEATHERED TERRAIN

P252 FINAL REPORT

Volume IIA

C.R.M. Butt, P.A. Williams, D.J. Gray, I.D.M. Robertson,
K.H. Schorin, H.M. Churchward, J. McAndrew,
S.J. Barnes and M.F.J. Tenhaeff

CRC LEME OPEN FILE REPORT 85

March 2001

(CSIRO Division of Exploration Geoscience Report 332R, 1992.
Second impression 2001)

CRC LEME is an unincorporated joint venture between The Australian National University,
University of Canberra, Australian Geological Survey Organisation and CSIRO Exploration and Mining
Headquarters: CRC LEME c/o CSIRO Exploration and Mining, Private Bag No 5, PO Wembley, Western Australia, 6913.

RESEARCH ARISING FROM CSIRO/AMIRA YILGARN REGOLITH GEOCHEMISTRY PROJECTS 1987-1996

In 1987, CSIRO commenced a series of multi-client research projects in regolith geology and geochemistry which were sponsored by companies in the Australian mining industry, through the Australian Mineral Industries Research Association Limited (AMIRA). The initial research program, "Exploration for concealed gold deposits, Yilgarn Block, Western Australia" had the aim of developing improved geological, geochemical and geophysical methods for mineral exploration that would facilitate the location of blind, buried or deeply weathered gold deposits. The program commenced with the following projects:

P240: Laterite geochemistry for detecting concealed mineral deposits (1987-1991). Leader: Dr R.E. Smith.
Its scope was development of methods for sampling and interpretation of multi-element laterite geochemistry data and application of multi-element techniques to gold and polymetallic mineral exploration in weathered terrain. The project emphasised viewing laterite geochemical dispersion patterns in their regolith-landform context at local and district scales. It was supported by 30 companies.

P241: Gold and associated elements in the regolith - dispersion processes and implications for exploration (1987-1991). Leader: Dr C.R.M. Butt.
The project investigated the distribution of ore and indicator elements in the regolith. It included studies of the mineralogical and geochemical characteristics of weathered ore deposits and wall rocks, and the chemical controls on element dispersion and concentration during regolith evolution. This was to increase the effectiveness of geochemical exploration in weathered terrain through improved understanding of weathering processes. It was supported by 26 companies.

These projects represented 'an opportunity for the mineral industry to participate in a multi-disciplinary program of geoscience research aimed at developing new geological, geochemical and geophysical methods for exploration in deeply weathered Archaean terrains'. This initiative recognised the unique opportunities, created by exploration and open-cut mining, to conduct detailed studies of the weathered zone, with particular emphasis on the near-surface expression of gold mineralisation. The skills of existing and specially recruited research staff from the Floreat Park and North Ryde laboratories (of the then Divisions of Minerals and Geochemistry, and Mineral Physics and Mineralogy, subsequently Exploration Geoscience and later Exploration and Mining) were integrated to form a task force with expertise in geology, mineralogy, geochemistry and geophysics. Several staff participated in more than one project. Following completion of the original projects, two continuation projects were developed.

P240A: Geochemical exploration in complex lateritic environments of the Yilgarn Craton, Western Australia (1991-1993). Leaders: Drs R.E. Smith and R.R. Anand.
The approach of viewing geochemical dispersion within a well-controlled and well-understood regolith-landform and bedrock framework at detailed and district scales continued. In this extension, focus was particularly on areas of transported cover and on more complex lateritic environments typified by the Kalgoorlie regional study. This was supported by 17 companies.

P241A: Gold and associated elements in the regolith - dispersion processes and implications for exploration (1991-1993). Leader: Dr. C.R.M. Butt.
The significance of gold mobilisation under present-day conditions, particularly the important relationship with pedogenic carbonate, was investigated further. In addition, attention was focussed on the recognition of primary lithologies from their weathered equivalents. This project was supported by 14 companies.

Most reports related to the above research projects were published as CRC LEME Open File Reports Series (Nos 1-74), with an index (Report 75), by June 1999. Publication now continues with release of reports from further projects.

P252: Geochemical exploration for platinum group elements in weathered terrain. Leader: Dr C.R.M. Butt.
This project was designed to gather information on the geochemical behaviour of the platinum group elements under weathering conditions using both laboratory and field studies, to determine their dispersion in the regolith and to apply this to concepts for use in exploration. The research was commenced in 1988 by CSIRO Exploration Geoscience and the University of Wales (Cardiff). The Final Report was completed in December 1992. It was supported by 9 companies.

P409: Geochemical exploration in areas of transported overburden, Yilgarn Craton and environs, WA.
Leaders: Drs C.R.M. Butt and R.E. Smith.
About 50% or more of prospective terrain in the Yilgarn is obscured by substantial thicknesses of transported overburden that varies in age from Permian to Recent. Some of this cover has undergone substantial weathering. Exploration problems in these covered areas were the focus of Project 409. The research was commenced in June 1993 by CSIRO Exploration and Mining but was subsequently incorporated into the activities of CRC LEME in July 1995 and was concluded in July 1996. It was supported by 22 companies.

Although the confidentiality periods of Projects P252 and P409 expired in 1994 and 1998, respectively, the reports have not been released previously. CRC LEME acknowledges the Australian Mineral Industries Research Association and CSIRO Division of Exploration and Mining for authority to publish these reports. It is intended that publication of the reports will be a substantial additional factor in transferring technology to aid the Australian mineral industry.

This report (CRC LEME Open File Report 85) is a second impression (second printing) of CSIRO, Division of Exploration Geoscience Restricted Report EG 332R, first issued in 1992, which formed part of the CSIRO/AMIRA Project P252.

Copies of this publication can be obtained from:
The Publication Officer, c/- CRC LEME, CSIRO Exploration and Mining, Private Bag 5, Wembley, WA 6913, Australia. Information on other publications in this series may be obtained from the above or from http://leme.anu.edu.au/
Cataloguing-in-Publication:

Geochemical exploration for platinum group elements in weathered terrain - Final Report.
ISBN vI: 0 64 3 06693 4 vIIA: 0 643 06694 2 vIIB: 0 643 06695 0 vIII: 0 643 06696 9 set: 0 643 06697 7
1. Geochemical prospecting 2. Weathering 3. Platinum ores
I. Butt, C.R.M. II. Title
CRC LEME Open File Report 85.
ISSN 1329-4768

TABLE OF CONTENTS

VOLUME I

VOLUME IIA

VOLUME IIB

VOLUME III

Addresses and affiliations of authors

C.R.M Butt
Division of Exploration Geoscience
CSIRO
Private Bag
Wembley 6014
Western Australia

D.J.Gray
Division of Exploration Geoscience
CSIRO
Private Bag
Wembley 6014
Western Australia

K.H.Schorin
Centro de Quimica
IVIC
Aptdo. 21827
Caracas 1020-A
Venezuela

J. McAndrew
Division of Exploration Geoscience
CSIRO
P.O. Box 136
North Ryde
NSW 2113
Australia

M.F.J. Tenhaeff
Institut fur Mineralogie und Lagerstattenlehre
Technische Hochschule
5100 Achen
Germany

P.A. Williams
Department of Chemistry
University of Western Sydney
P.O. Box 10, Kingswood
NSW 2747
Australia

I.D.M. Robertson
Division of Exploration Geoscience
CSIRO
Private Bag
Wembley 6014
Western Australia

H.M. Churchward
Division of Exploration Geoscience
CSIRO
Private Bag
Wembley 6014
Western Australia

S.J. Barnes
Division of Exploration Geoscience
CSIRO
Private Bag
Wembley 6014
Western Australia

CHAPTER 5 GEOCHEMICAL DISPERSION OF PLATINUM GROUP ELEMENTS IN LATERITIC REGOLITH, ORA BANDA SILL.

C.R.M. Butt, I.D.M. Robertson, K.H. Schorin and H.M.Churchward.

ABSTRACT

The Ora Banda sill is one of a number of highly differentiated sills in the Norseman-Wiluna Greenstone Belt known to contain anomalous concentrations of platinum group elements (PGE). The lower, ultramafic units of the sill have been deeply weathered and have given rise to lateritic enrichments of PGE similar to those of gold. The purpose of this investigation has been to describe these lateritic enrichments, to determine the manner in which they have formed in the context of landform evolution, to establish the nature of the geochemical dispersion of the PGE in this environment and to recommend appropriate exploration procedures for further such deposits or for concealed primary mineralization in lateritic terrain. The research concentrated on the Ora Banda prospect south of Ora Banda townsite, where Carbine Gold N.L. had tested the lateritic enrichments by shallow RAB drilling and possible primary mineralization by diamond drilling. A smaller study was conducted at Mt. Carnage, west of Ora Banda.

The Ora Banda sill is a 2 km thick high-magnesium mafic-ultramafic intrusive body. It consists of a basal peridotite (830 m thick) overlain by orthopyroxenite (165 m), norite and gabbro-norite (950 m) and an upper gabbro and granophyre (50-100 m). The pyroxenite are much richer in PGE (132 ppb Pt, 79 ppb Pd) than the peridotites (42 ppb Pt, 54 ppb Pd). There is a gradual increase in total PGE upwards through the peridotite, whereas in the pyroxenite, the PGE appear to be relatively enriched in the bottom 75 m and again towards the top. The sulphide distribution, indicated by Cu, suggests that sulphur saturation corresponds to the base of the pyroxenite, although the maximum occurs approximately centrally within the pyroxenite. No single horizon of PGE enrichment was located in the unweathered rocks by diamond drilling, although three RAB holes, close to the contact, intersected a narrow zone in the regolith rich in several PGE (maxima over 1 m: 1800 ppb Pt, 1200 ppb Pd, 52 ppb Ru, 114 ppb Rh, 6 ppb Os, 20 ppb Ir).

The region has moderate relief and variable preservation of lateritic regolith. Preservation is greatest over the pyroxenites, which are characterized by the presence of partly dissected lateritic duricrusts. The peridotites are less dissected, but there is no complete lateritic cover and the surface soils are developed on saprolite. Remnant Fe-rich duricrusts on the peridotite are partly transported and appear to be channel deposits. The pyroxenites and peridotites are weathered to depths of 40-60 m whereas, in contrast, the norite and gabbro-norite are essentially fresh at surface.

PGE contents in the regolith increase steadily towards the surface, with a total enrichment of three- to five-fold in the lateritic ferruginous zone over the pyroxenites. The highest concentrations occur in the ferruginous clays, lateritic horizons and calcareous lateritic soils on pyroxenite, and in calcareous saprolites and soils on peridotite. The maximum concentrations are up to 2000 ppb total PGE in clay-rich duricrusts at Mt. Carnage and 850-1150 ppb PGE at Ora Banda. The accumulations appear to be residual and are of the same order as other elements such as Cr, Zr and Cu that also appear to be immobile. The mean Pt/(Pt+Pd) ratio of unweathered rocks is approximately 45% in peridotite and 63% in pyroxenite. This difference

is maintained in the regolith, particularly comparing the pyroxenites in the south of the traverse with the peridotites towards the north and the relationship appears to distinguish the two lithologies reliably. There is an upward increase in the Pt/(Pt+Pd) ratio in the profile, with the highest values (75-88%) in the PGE-enriched horizons (mottled clay, lateritic duricrust and derived soil) developed from the pyroxenite; greater values still are found in the lag derived from these duricrusts. The increase may be due either to further chemical reworking during lag formation or because Pt is preferentially concentrated in those components of the duricrust, such as the most ferruginous nodules, that comprise the lag. Chemical studies indicate that Pt is strongly associated with Fe oxides in the regolith and therefore is immobile, whereas Pd is located in a slow-weathering phase and may be leached as this is weathered. However, it is evident from the diamond drill core, and from samples of the deep saprolite, that fresh and partly weathered pyroxenite may have ratios of 75-85%, though usually in rocks containing <150 ppb Pt and <40 ppb Pd, so that a high ratio is not unequivocal evidence for loss of Pd. There is minor concentration of PGE in calcareous soil and saprolite, similar to gold in this region, but the relationship with pedogenic carbonate was not confirmed either by analysis of hand-picked material or by selective extraction. Despite loss of Pd, lag sampling effectively delineates the lateritic zones of PGE enrichment and the petrography and geochemistry of lag both discriminate between peridotite and pyroxenite.

There is no evidence for significant chemical dispersion of PGE in the regolith at Ora Banda, with the minor exceptions of local concentrations in Mn oxides, loss of Pd in surface horizons and possible concentration in calcareous soils. The supergene behaviour of the PGE thus differ from gold in this region, for which secondary mobility has been quite pronounced, both during lateritization and subsequent arid periods, including the present. This has resulted in widespread dispersion of gold in lateritic horizons and some saprolite, secondary accumulation in pedogenic carbonates and leaching from the upper saprolite. Although economically significant enrichments of PGE have developed by residual accumulation during lateritic weathering, neither the concentrations nor the identified resource are sufficiently great to be exploitable. For supergene PGE concentrations in lateritic regoliths to be economic would probably require a rather higher initial PGE content and the possibility of chemical mobilization and reconcentration during weathering. Such mobility might be promoted in rocks that have a higher sulphide content, or in sites where the regolith is saturated by hypersaline groundwater, thus permitting mobilization as thiosulphate and chloride complexes, respectively. Such sites were not found on the Ora Banda sill.

GEOCHEMICAL DISPERSION OF PLATINUM GROUP ELEMENTS IN LATERITIC REGOLITH, ORA BANDA SILL.

C.R.M. Butt, I.D.M. Robertson, K.H. Schorin and H.M.Churchward.

1.0 INTRODUCTION

The Ora Banda sill is centred about 55 km NW of Kalgoorlie, at 121° 03' 50"E, 30° 24' 10"S (Figure 1). It is one of a number of highly differentiated sills in the Norseman-Wiluna Greenstone Belt known to have anomalous concentrations of platinum group elements (PGE). The lower, ultramafic units of the sill have been deeply weathered and are poorly exposed, but this has presented the possibility of the development of lateritic enrichments of PGE similar to those of gold. Much of the sill was explored by Carbine Gold N.L. during 1987-1990 at their Ora Banda and Mt. Carnage prospects south and west of Ora Banda, respectively (Figure 2). Initial exploration was by soil surveys for Au, Pt and Pd, followed by rotary air-blast (RAB) drilling (Menzies, 1988a, 1988b) which tested the lateritic enrichments present over the pyroxenites and possible primary mineralization at the pyroxenite-peridotite contact. Overlapping angle holes (inclination 50-65°) were drilled to a downhole depth of 40 m on selected lines across strike. At Ora Banda, the principal drill section was on line 12500E (Figure 3), which intersects the strike of the inferred contact at approximately 40°. This portion of the sill was further tested by two diamond drill holes, oriented approximately normal to the strike, drilled to intersect the contact beneath 12500E (Figure 4). Research at Ora Banda was concentrated on this section because of the availability of sample material suitable for studying PGE enrichment in complete lateritic profiles, good bedrock control and the possibility of establishing the surface expression of primary mineralization. Some detailed investigations were carried out on the profile sampled by one RAB hole at Mt. Carnage, in which the ferruginous horizons in the top 10 m contained 1000-1800 ppb Pt + Pd. Material from other holes in the section had been bulk sampled for metallurgical tests and no other profiles were complete.

2.0 SAMPLING AND ANALYSIS

2.1 Mapping and Surveying

Three lines of the 100x50 m grid, centred about line 12500 N, were re-established, surveyed and levelled using a Wild T100 electronic theodolite and a DIOR3002 laser distance measuring device (A.J. Snow, W.A. School of Mines, written communication, 1990). The GPS location of RAB drill collar OB 20, at grid position 12505 mE and 10470 mN, was 121° 03' 34"E and 30° 24' 05"S. The geology, geomorphology and regolith were mapped by stereoscopic interpretation of coloured air photographs (1:10,000 Ora Banda North ASA C955; 5/7/87) and by field observations of surface and near-surface materials and drill spoil.

2.1 Sampling

2.1.1 Lag

A limited lag survey was carried out at the Ora Banda prospect, centred over the area of strongest PGE enrichment. Lag was sampled at 20-40 m intervals on traverse 12500 E and at 50-100 m intervals on 12400 E and 12600 E. Using a nylon-bristled brush, the samples (1000-1500 g) were swept into a plastic dustpan from several randomly selected locations at each site. The lag sample inevitably contained some organic litter, soil and sand. Care was taken in selecting undisturbed and uncontaminated sample sites, particularly where drilling had been carried out. Where lag was scarce, or where the sample site was disturbed or contaminated, the area of search was extended up to 5 m along the sample line and up to 10 m across the line to collect an adequate and clean sample. Areas of sheetwash were avoided.

2.1.2 Drill cuttings and core

The RAB drill holes sampled the regolith at 1 m intervals. For most holes, Carbine Gold NL took 2 m composite samples but collected the top and bottom 1 m interval separately. For this multi-element study, the heaps of cuttings left on site beside each RAB hole were resampled. The cuttings were mostly in good condition, although some clay-rich samples, in the lower-lying sites (*e.g.*, holes OB 19-21, close to the peridotite-pyroxenite) contact, had been affected by sheetwash. Nevertheless, clean, apparently uncontaminated, material could be collected from most heaps. In general, 10-15 samples were taken from each hole, selected to represent the principal regolith horizons and/or any PGE enrichment shown by the earlier analyses. Carbine Gold NL had split the diamond drill core and analysed 1 m intervals; for this study, small samples of the split core were collected for petrographic examination and multi-element analysis. Two-metre composites of the percussion-drilled pre-collar of OBDDH2 were sampled to test for Pt and Pd concentrations at the norite-pyroxenite contact.

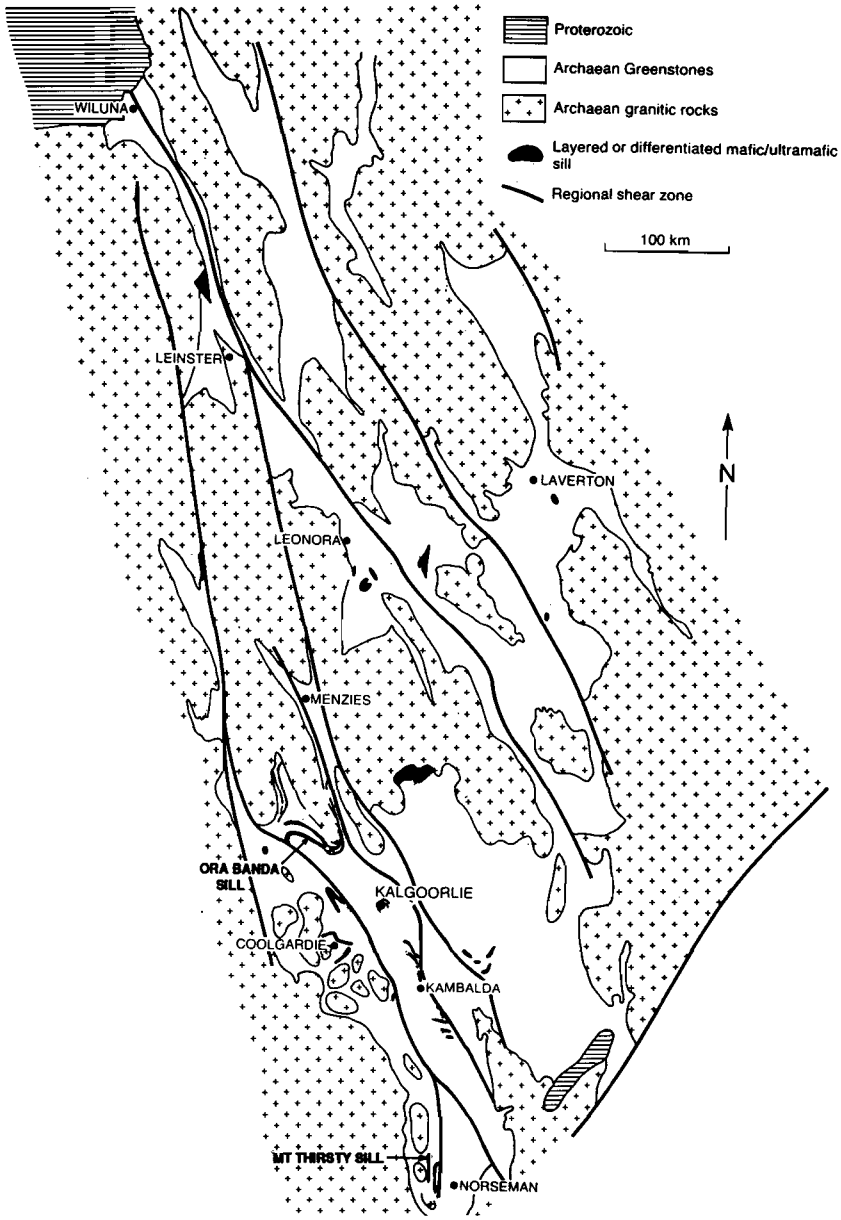

Figure 1. Geology of the Norseman-Wiluna greenstone belt, indicating the locations of the major layered intrusives (after Barnes *et al.*, 1991)

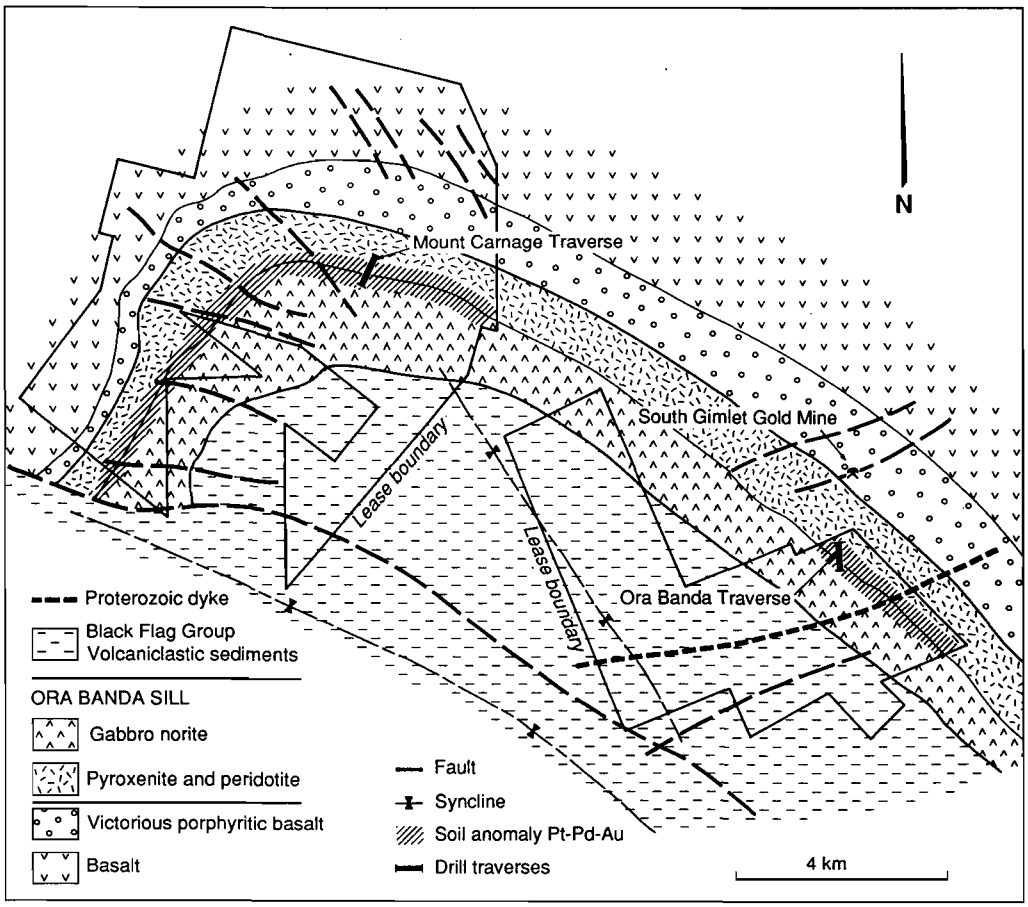

Figure 2: Geology of the Ora Banda Sill, showing locations of the Ora Banda and Mt. Carnage prospects of Carbine Gold N.L. and the drill traverses studied by AMIRA Project 252 (after Menzies, 1988a).

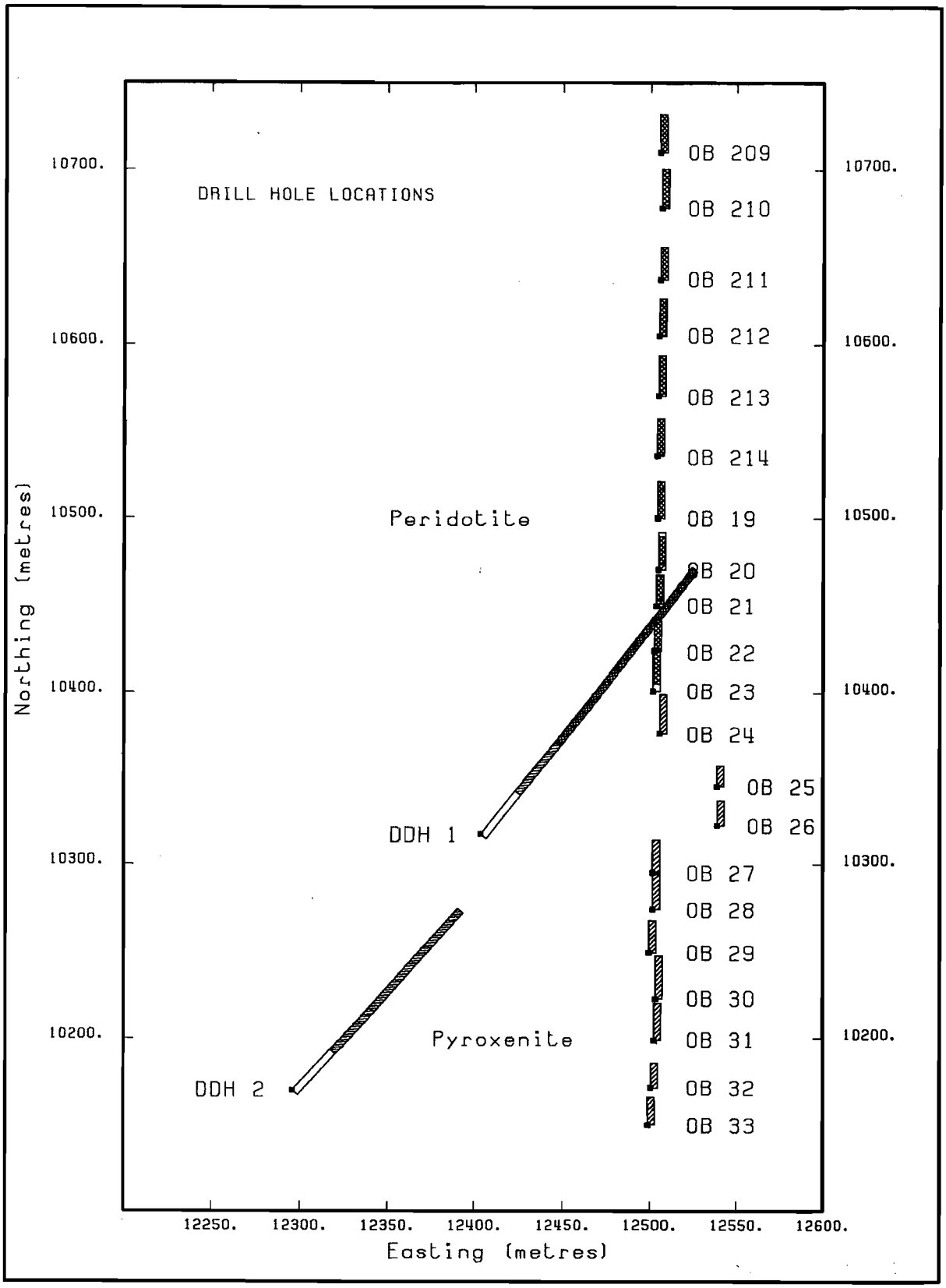

Figure 3: Locations of RAB and diamond drill holes, Ora Banda, with interpreted geology.

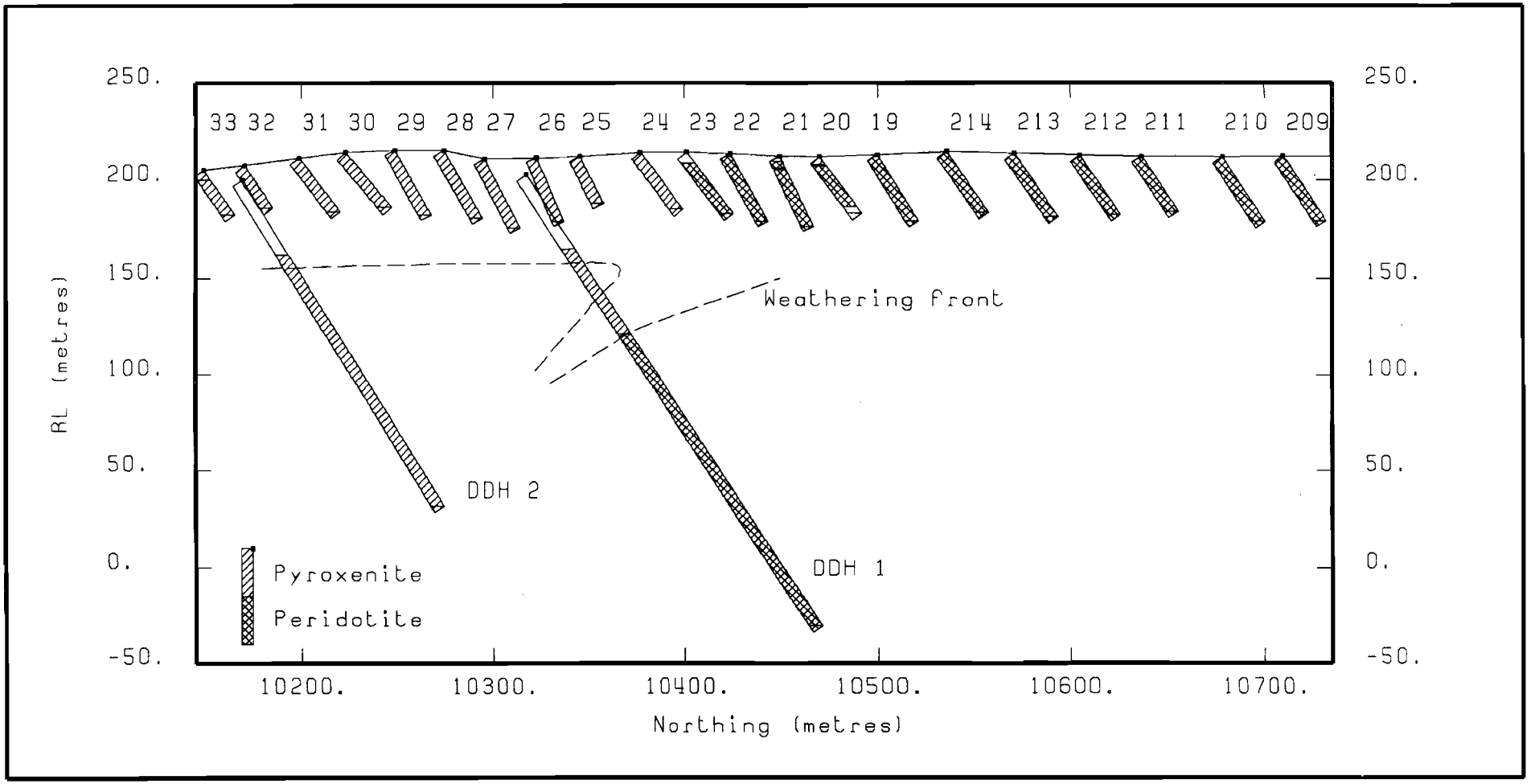

Figure 4: Section along RAB drill traverse at Ora Banda, with projected locations of diamond drill holes OBDDH 1 and OBDDH 2 (see Figure 3 for hole orientations).

2.2 Analysis

2.2.1 Sample preparation and chemical analysis

The lag samples were washed in the laboratory with agitation in tap-water on a 0.7-mm plastic sieve, to remove any dust; large organic debris was also removed. These and all other samples selected for analysis in this study were dried (40°C), a sub-sample taken for reference and the remainder jaw-crushed to 4 mm or smaller. The material was riffle split and a minimum of 100 g extracted for grinding to less than 75 μm in a hardened Mn steel ring mill, using a double sand clean and alcohol wipe of the mill components between samples. Samples were analysed as follows:

A. Inductively-coupled plasma emission spectroscopy (ICP-ES) on a Hilger E-!000 following fusion with Li metaborate and solution in dilute HNO_3 (RAB samples):
Al_2O_3, SiO_2, CaO and MgO.

B. X-ray fluorescence spectrometry (XRF) on pressed powders using a Philips PW1220C instrument by the methods of Norrish and Chappell (1977) and Hart (1989), with Fe determined for matrix correction (RAB samples):
As, Ba, Ce, Co, Cr, Cs, Cu, Fe, Ga, Ge, La, Mn, Na_2O, Ni, Pb, Rb, S, Sc, Se Sr, TiO_2, Y, Zr, Zn. Low abundance Se in lag samples was determined by longer (X5) counting times.

C. X-ray fluorescence spectrometry (XRF) using a Philips PW 1480 instrument samples fused in a Li borate flux (OBDDH and lag samples). Sample weight was 1.6 g for fresh rock samples and 0.7 g for lag samples due to the high Fe and Cr contents of the latter:
Al_2O_3, SiO_2, Fe_2O_3, K_2O, TiO_2, CaO, MgO, Na_2O, P_2O_5, Ba, Ce, Cl, Co, Cr, Cu, Ga, Mn, Ni, Rb, S, Sr, V, Y, Zn, Zr

D. Fire assay fusion. Carbine Gold NL had all samples analysed for Pt and Pd by fire assay fusion (Pb collection), aqua regia digestion and ICP-MS by Genalysis Pty. Ltd. Later inter-laboratory tests by CSIRO indicated that analyses by Genalysis appeared to be the most precise and accurate available, so that the original data have been accepted for this study and any additional analyses were by the same laboratory. Analyses of selected RAB and diamond drill core samples for the whole PGE suite were done by fire assay fusion (NiS collection), aqua regia digestion and ICP-MS, also by Genalysis.

E. Atomic absorption spectrometry (AAS). Carbine Gold NL had the diamond drill core samples analysed for Cr, Cu and Ni following digestion in an $HClO_4$-HF-HNO_3 acid mixture (Genalysis Pty. Ltd.)

Detection limits are shown in Appendix IV.

2.2.2 Mineralogy

The mineralogy of selected samples was determined by semi-quantitative X-ray powder diffractometry, using LiF diffracted beam monochromated Cu Kα radiation on a Sietronics-automated Philips PW1050 diffractometer. Each sample was scanned over the range 5-65° 2Θ, at 1°/min and data were collected on computer at 0.02° 2Θ intervals. Where Al-substitution in goethite and hematite was being determined, it was necessary to add small amounts of quartz as an internal standard, though some had sufficient naturally-occurring quartz.

Semi-quantitative major mineral abundances were estimated using the height above background of a selected diffraction peak for each mineral. The peaks were chosen so as to avoid overlap by peaks of other minerals. For the lag samples, the peaks selected are listed in Table 1 and the data were corrected for mass absorption, using the method of Brindley (1980). It must be

emphasized that these results are approximate and are influenced by the degree of crystallinity and mineral alignment as well as by abundance. They give an approximate comparison of the relative abundances of specific minerals between *samples*; they do not indicate the relative abundances of the different *minerals* in each sample.

TABLE 1
X-ray diffraction peaks used for semi-quantitative determination of lag mineralogy.

Mineral	Diffraction peak (hkl)	d-spacing (Å)
Quartz	101	3.343
Goethite	110	4.183
Hematite	110	2.51
Kaolinite	001	7.10
Maghemite	220	2.95

2.2.3 Estimation of Al substitution in goethite

The goethite XRD reflections of many samples show a slight displacement from that of pure FeOOH, indicating some Al substitution for Fe. The displacements are small but, if measured accurately, those of the d[110] and d[111] peaks give an estimate of the extent of substitution (Schulze, 1984). Study of a quartz standard indicated that error due to sample position in the goniometer is significant but variable at 4 Å, negligible at 1 Å and has an approximately linear distribution with d. The d[101] reflection of quartz was measured to estimate and correct goniometer error. Though the data are satisfactory, they must be regarded as indicating trends rather than being correct in an absolute sense.

2.2.4 Petrography

The polished sections were examined first under oblique reflected light with a binocular microscope and then under normally reflected light on a petrographic photomicroscope. Information gathered by both methods, one showing colour and overall fabric and the other mineralogy and fabric detail, are complementary. Mineral identification on the polished sections was aided by qualitative energy dispersive X-ray analysis using a JEOL GeoSEM 1. The results of such analyses are shown in the text so as to indicate approximate relative proportions, *e.g.* Fe>>Si=Al.

3.0 GEOLOGY, GEOMORPHOLOGY AND REGOLITH

3.1 Geological setting.

The Ora Banda sill is a 2 km thick high-magnesium, mafic-utramafic intrusive body emplaced near the contact between tholeiitic volcanic rocks and the felsic to intermediate volcaniclastic rocks of the Black Flag Group (Figure 2). The sill has six principal lithological zones (Table 2).

TABLE 2
Principal lithological units of the Ora Banda Sill (after Witt and Barnes, 1991)

Zone	Thickness (m)	Lithology
Top		
6.	50-100	Upper contact; includes pegmatoid gabbro, granophyre.
5.	540	Pigeonite-bearing gabbro-norite cumulate.
4.	315	Bronzite-bearing gabbro-norite cumulate. Some mm-scale layering; local lenses of anorthosite.
3.	90	Norite; massive equigranular plagioclase orthopyroxene adcumulate, grain size 1-2 mm.
2.	165	Orthopyroxenite; massive equigranular bronzitite adcumulate, grain size 1-2 mm.
1.	830	Peridotite. Olivine bronzite orthocumulate.
Base		

The sill is well exposed in its upper part, but deeply weathered towards the base. The basal peridotite and overlying pyroxenite rarely outcrop and are known principally from the two diamond drill cores (Figure 3). The correlation between the two holes is uncertain, but it is probable that they represent a complete section through the pyroxenite into the peridotite. Thus, the pre-collar of OBDDH2 passes through the norite-pyroxenite contact, so that coring commenced within 30 m of the top of the unit. The bottom of OBDDH2 is probably close to the base of the pyroxenite and hence overlaps the top of OBDDH1. The lower pyroxenite-peridotite contact, intersected at about 90 m true depth in OBDDH1, is sheared and oxidized. The contact is also intersected at 5.5 m in OB 20, and pyroxenite saprock outcrops. The contact is exposed in a small creek close to OB 20 and appears to be faulted and sheared. However, the regolith sampled by holes OB 21 and 22, and below about 10 m in OB 23, is derived from peridotite, so that it is deduced that the material in OB 20 is a small fault-block of pyroxenite emplaced in the peridotite. The lateritic gravels and duricrust in OB 23 are derived from pyroxenite but it is uncertain whether they are entirely *in situ*. If they are, then the contact is about 6-9 m downhole.

The rocks of the Ora Banda Sill sampled by drill holes OBDDH1 and 2 are very typical olivine cumulates and olivine-orthopyroxene cumulates, with accessory cumulus chromite. The olivine-orthopyroxene cumulates that form the Peridotite Zone are adcumulate to mesocumulate in fabric, with minor amounts of intercumulus plagioclase. Olivine and orthopyroxene form anhedral subequant grains with moderately annealed grain boundaries. Chromite grains, typically 100-500 μm in size, occur principally at olivine-pyroxene grain boundaries and less commonly enclosed within the cumulus silicates (see Figure 19A). Orthopyroxene (bronzite in composition) shows extensive fine-scale exsolution lamellae. Both olivine and orthopyroxene are mostly fresh, with some replacement of bronzite by talc, particularly towards the contact with the pyroxenite (Zone 2) and some serpentinization of olivine along irregular cracks.

The rocks of the Pyroxenite Zone are bronzite mesocumulates to orthocumulates, with intercumulus plagioclase (5-20%), large scattered oikocrysts of chromian augite (up to 5%) and minor olivine. Serpentinization of some olivine has occurred along narrow cracks, some pyroxene has been altered to talc and amphibole and some plagioclase is partially altered to chlorite (Figure 20A). Intercumulus phlogopite is present in accessory quantities throughout, typically at pyroxene-plagioclase grain boundaries. Chromite is present in very small quantities, typically less than 10 grains per thin section, as small (50 μm) commonly elongate grains, generally enclosed within bronzite.

Cryptic chemical variation is observed through the stratigraphic sequence sampled by the two drill holes, as indicated by the MgO/FeO ratio and Cr_2O_3 content of cumulus bronzite in Figure 5. These profiles are consistent with there being little stratigraphic overlap between the holes. The Peridotite Zone shows steady-state constant pyroxene compositions, implying regular replenishment of the magma chamber during crystallization. In comparison, the Pyroxenite Zone has an upward trend of Fe enrichment and Cr depletion, implying that the rate of magma supply to the chamber was less at this stage, resulting in *in situ* fractionation of magma within the chamber. Plots of Cr versus enstatite (MgO/(MgO+FeO) mole % in orthopyroxene show that the pyroxenites are generally more fractionated than the peridotites, as would be expected, and that the relatively orthocumulate pyroxenites have a wider within-sample spread in mineral chemistry, due to crystallization of the trapped intercumulus liquid.

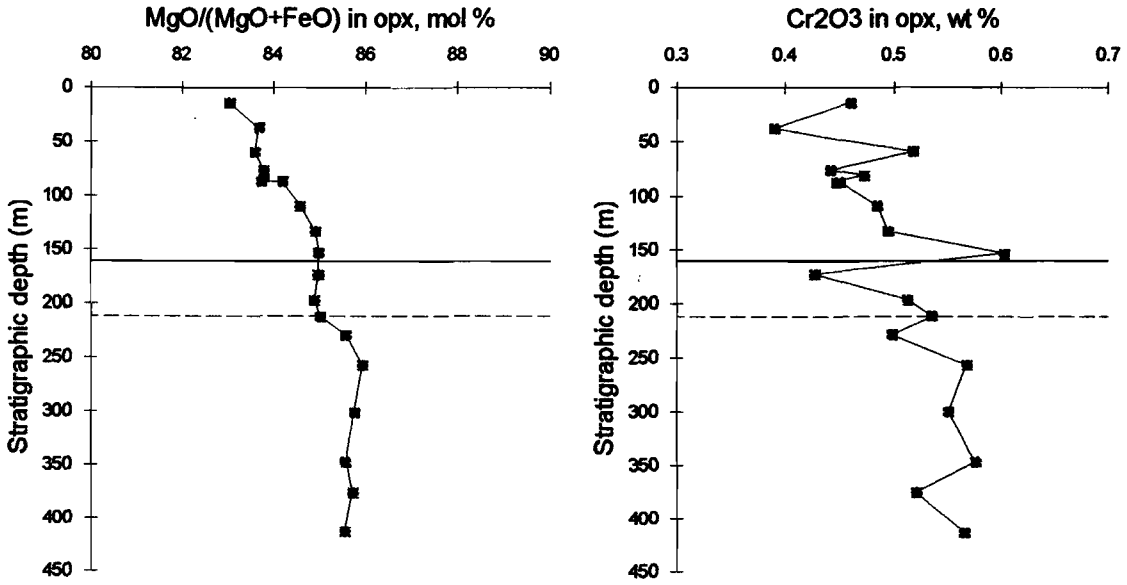

Figure 5. Profiles of sample averages of orthopyroxene compositions versus stratigraphic depth, assuming that the top of hole OBDDH 1 correlates with the base of hole OBDDH 2. Horizontal solid line is boundary between the two drill holes, dashed line is contact between peridotite and pyroxenite.

3.2 Geomorphology

3.2.1 Regional setting

The Ora Banda prospect is situated in a group of low hills and vales and has a moderate relief (Figure 6). Such belts of hills are common in the region, alternating with sheetflood plains such as that extending for 15 km along the Carbine road, from 5 km S of Ora Banda. Near Ora Banda, more extensively eroded areas are flanked by scattered residuals of a lateritized land surface. These relicts generally have gently sloping crests, inclined away from the more intensely eroded tracts, and are partly flanked by breakaways. Drainage from these erosional tracts passes through gaps between the cuesta-like residuals, moving detritus onto the extensive sheetflood plains that separate the main belts of hills.

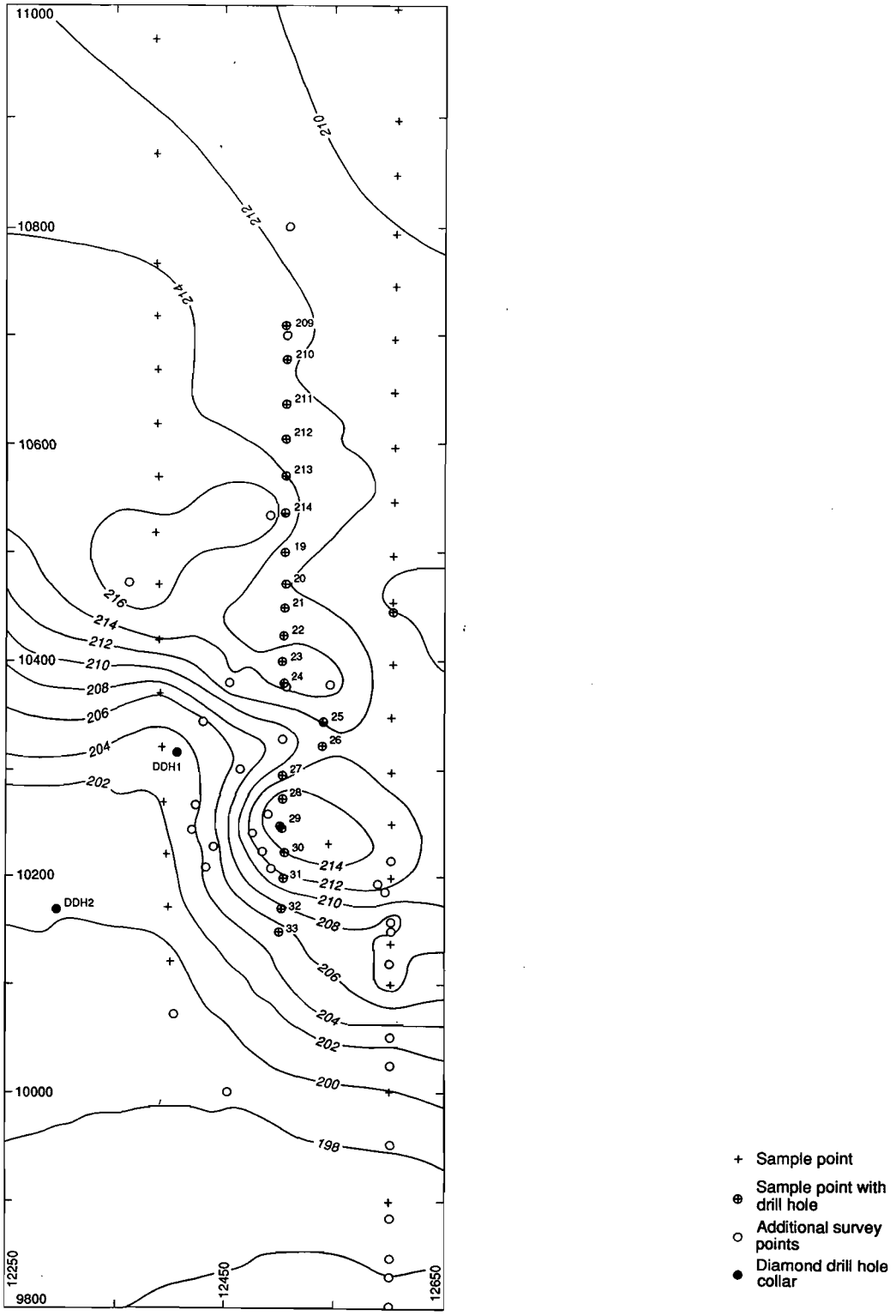

Figure 6. Contour plan of part of the Ora Banda prospect, showing drill hole and lag sample locations, and some additional topographic survey points.

The norite and gabbro-norites of the sill form prominent hills to the south and south west of the prospect. The hills have broadly convex crests that rise above the relicts of the lateritized surface and have extensive exposures of fresh rock. The pyroxenite is characterized by lateritic duricrust, which forms a low ridge, now partially dissected. This ridge becomes more prominent to the north. The breakaway slope at the south of the drill section may, in part, be a dip slope, marking the pyroxenite-norite contact. Weathered pyroxenite is present on the slope itself and fresh norite float is found towards the base. The old lateritic landsurface on the pyroxenite slopes gently north across the peridotite to broad-floored drainages north of the study area. The peridotites thus occupy slightly lower, less dissected ground. There are rare outcrops of saprolite and a few lenticular pods of Fe-rich duricrust form low rises, but there is no complete cover of duricrust similar to that on the pyroxenite. The area is covered with a low acacia woodland with scattered eucalypts; casuarinas are an important component of the vegetation, particularly on the duricrust exposures.

3.2.2 Regolith-landform units

Ten major regolith-landform units have been recognized (Figure 7) and are described below from SW to NE.

Unit 1. This is a prominent hill, with extensive exposure of relatively fresh norite, mainly south of the study area. It has a broadly convex crest and is flanked by steep slopes.

Unit 2. The area to the northeast of Unit 1 is cut by active, shallow, ephemeral stream channels flanked by sandy to loamy alluvium with minor occurrences of coarse, lithic, ferruginous lag. This is presumed to be underlain by norite.

Unit 3. This unit consists of moderate to gentle pediment slopes rising to the NE of Unit 2. Scattered outcrops and cobbles of variously weathered noritic rocks on the upper to mid slopes show through a shallow, stony, sandy, clay loam, or a colluvial lag-rich mantle with some pockets of soft calcium carbonate. The soils are shallow, neutral to alkaline, light brown to red brown earths. On the upper slopes, there is a covering of coarse lag, comprising iron-stained lithic fragments, ferruginous saprolite and vermiform lateritic duricrust.

Unit 4. This comprises scarps, dominated by the fall of the breakaway to the north-east of Unit 3, and characterized by very steep slope facets that are irregularly incised by narrow, steeply-graded gullies. Pyroxenitic saprolite is only rarely exposed; thick slabs and coarse blocks of brown duricrust are more common.

Unit 5. Numerous outcrops of a dark brown duricrust occur as large slabs and blocks on broadly convex crests, just above the breakaway of Unit 4. The unit is developed on pyroxenite. A lag of coarse, irregular, yellow-brown fragments (Figure 9B), with some fine (<20 mm), brownish black fragments, overlies a shallow, light-brown to red-brown, fine-grained, sandy to loamy soil. The brown duricrust (LT231; Anand *et al.*, 1989) has a complex, diffuse, light-brown mottling (Figure 9A). Some irregular, vermiform voids, reaching 5 mm in diameter, occur in the duricrust and are generally lined with pale yellow-brown goethite. Some voids are filled with red-brown clay which has an incipient pisolitic structure. In places the coarse voids have developed to such an extent that the crest is a fragmentary duricrust. Although some soils are neutral to acid, the duricrust is commonly infused with carbonate which is clearly visible where the lag-covered surface is only slightly disturbed (Figures 8E, 8F).

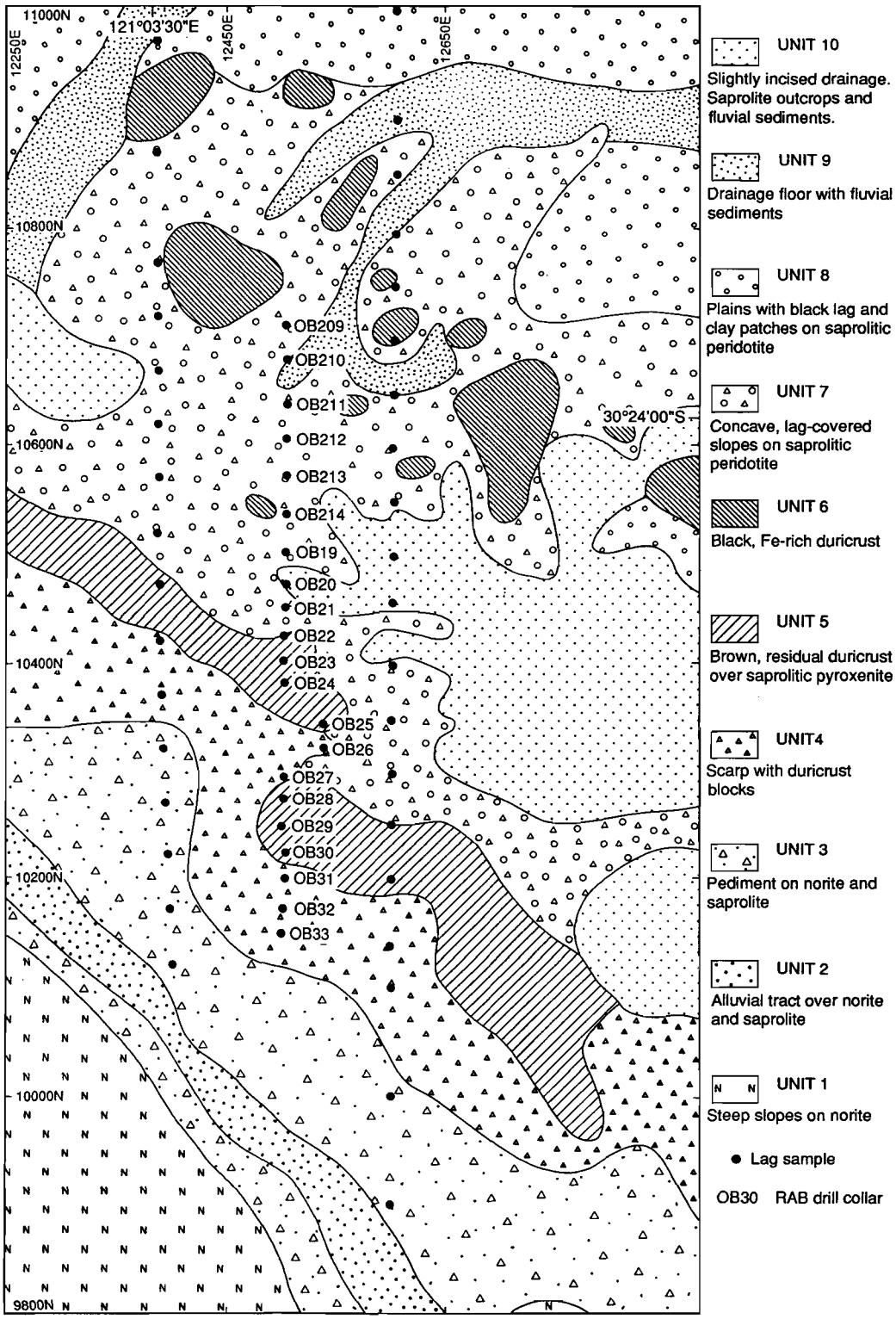

Figure 7. Geomorphology of part of the Ora Banda sill, showing the principal landform regolith units of the study area.

Unit 6. This forms crests and low rises, often broadly convex (Figure 8A), capped by black, Fe-rich duricrust, usually as a mass of coarse blocks (Figures 8C and G). The crests are generally small (Figure 8H), rising about 2 m above the adjacent linear to broadly concave slopes of Unit 7 onto which they shed rounded boulders. The black, Fe-rich, duricrust (LT228, Figure 9C) comprises dark brown to brownish black pisoliths and nodules with goethite cutans, set in a sparse, red-brown matrix. There are some vermiform voids, reaching 3 mm in diameter in the matrix, which are generally lined with yellow goethite. In places the matrix is porous and white; crypto-crystalline silica occupies some of the small voids. This unit is directly underlain by saprolitic peridotite.

Unit 7. These are very gentle, linear to slightly concave slopes (Figures 8A-C) that flank the crests of Unit 6 and generally truncate the drainage floors of Unit 8. The slopes are mantled by a black lag (Figure 9F) which is coarse upslope, on the fringes of the duricrust-capped crests, and becomes fine (< 10 mm) down slope. The lag on the slopes fringing Unit 6 also contain an appreciable amount of red-brown duricrust fragments (Figure 9D). The soils on Unit 7 are acid red earths, comprising a very friable, fine-grained, sandy, clay-rich loam over an incipient Wiluna hardpan at about 200 mm depth, although soft calcium carbonate and nodular magnesite generally occur within 300 mm of the surface. Peridotite saprolite appears below about 300-400 mm.

Unit 8. This is a gently sloping smooth plain that forms a down-slope continuum with Unit 7. It is extensively mantled by fine-grained, black lag and this overlies acid red earth or very friable, fine-grained, sandy, light clay with incipient hardpan at a depth of 250 mm. Saprolite, without hardpan, appears at about 300-450 mm depth. The soil, hardpan and upper saprolite are infused with carbonate from about 0.3 m to as much as 5 m depth. In addition, there are scattered pockets of well-structured red-brown clays that are self-mulching and, at the surface, have a finely patterned micro-relief. These areas of self-mulching clays have little or no lag.

Unit 9. Flat drainage floors, without defined channels, that appear to have been formed by active sheet flooding. These areas are occupied by red-brown to light brown sandy to loamy fluvial sediment, generally with no lag.

Unit 10. This comprises the slightly incised upper elements of a tributary drainage system (Figures 8B) and its flanking, often irregularly stripped slopes. Scattered outcrops of peridotite saprolite show through a shallow, stony, colluvial mantle (Figure 9E). There are also areas of soft calcrete and nodular magnesite (Figure 8D) as well as veins of moss agate and outcrops of pyroxenite saprock (Figure 9H).

Landform units 1-4 represent the zone where the regolith has been most strongly eroded. This zone strikes NW and approximately follows the contact between norite and pyroxenite. The remaining landform units (5-10) are subdivisions of a backslope terrain, developed upon strongly weathered regolith. The backslope is a very gently undulating tract with Fe-rich duricrusts (Unit 6) occupying the crest of low rises. The gentle slope (sometimes slightly concave) of Unit 7 connects with lower gradient Units 8 and 9. Saprolite is close to the surface in Units 7 and 8, mantled by residual soils or shallow colluvium. The change from coarse to fine lag away from each crest in Unit 7 indicates colluvial transport from the crests. The absence of laterite on these slopes and the shallow depth to saprolite indicates erosion has played an important role.

The duricrust of Unit 5 is probably the relict of a once extensive, residual, upper horizon of the regolith that has since largely eroded by shallow stripping and pediment development. The difference between these Units 5 and 6 reflects the underlying lithology; Unit 5 overlies pyroxenite and Unit 6 peridotite. Nevertheless, although pedimentation is clearly expressed on the present land surface, it is not clear whether the Fe-rich duricrust of Unit 6 was once a more continuous member of the regolith or a very localized development. Its clastic, pisolitic and

apparently polymictic nature, and the presence of numerous fossil wood fragments (Section 5.2) strongly suggests that it is not residual but probably represents a small depositional regime. The origin of these materials is discussed further in Section 8.1.5.

The land surface, dominated by pediment slopes, is itself being modified by local incision of minor tributaries. Such areas are represented by Unit 10. The minor tributaries terminate as local fans, beyond the study area. The more striking erosional terrain in the SW of the study area is also caused by streams that drain onto extensive alluvial plains. This erosional activity is not related to any clear major drainage rejuvenation. The erosion is more likely due to landsurface instability caused by both decreased vegetation and the incidence of episodic rainfall, rather than by regional drainage rejuvenation. Aggradation of the valleys has perhaps been proceeding, in a cyclic manner, since the mid-Tertiary, since palaeochannels in the region have been infilled by Eocene and more recent deposits.

3.3 Regolith

3.3.1 Regolith stratigraphy

The peridotites and the pyroxenites are generally weathered to 40-60 m depth, although some nearly fresh pyroxenite is present in the top 6 m of hole OB 20 and exposed in an adjacent gully. Essentially complete lateritic profiles are extensively preserved over the pyroxenites, giving rise to the tracts of lateritic duricrusts and derived soils of Unit 5. Duricrust is rare or absent over the peridotites, and soils are derived from saprolite. The massive, blocky duricrusts of Unit 6 developed locally on the peridotites were not drilled. These appear to lie directly on saprolite and may be partly transported in origin. They have an assemblage of fossil plants that includes wood, leaf, moss and fern, suggesting humid conditions of formation, such as swampy depressions (see Section 8.1.5). The top 1 to 4 m of the regolith over both lithologies contain pedogenic carbonate.

Typical profiles are shown on Table 3. The principal horizons are identified on the geochemical drill sections (Appendix I) by the informal codes given in parentheses.

The regolith stratigraphy is shown on the drill sections (Appendix I) which also illustrate that the distribution of duricrust is controlled by the occurrence of pyroxenite. The most complete profiles are present over the upper (southern) part of the pyroxenite unit (10200 to 10400N); the lateritic duricrust and gravels become thinner and are absent to the north over the peridotite. This change is reflected in the nature of the underlying regolith. Thus, over the pyroxenite, the regolith is generally shallower, for although the profile is essentially complete, the strongly leached clay-rich horizons are thin and deeper zones (below 20-25 m) consist of relatively fresh saprolite/saprock. In contrast, over the peridotite, despite being partly stripped, the regolith is deeper and is increasingly clay-rich in the upper saprolite and silica- and magnesite- rich in the lower saprolite. Little near-fresh rock was present in RAB drill samples north of 10400N. An exception is the fault-block of almost fresh pyroxenite (saprolite/saprock) in the top 6 m of OB 20, overlying clay-rich saprolite derived from peridotite. The weathering front, as shown by minor oxidation in the diamond drill core, is at approximately 55 m depth in the upper part of the pyroxenite but below 85 m depth in the lower part, close to the contact; it is probably at 60-70 m on the peridotite.

Figure 8. Geomorphology and surface geology (see over page)

A. Land surface on weathered peridotite on the Ora Banda Sill, covered by blue-black lag and red earth soil. It comprises the slightly concave slopes of Unit 7, below a tree-covered (eucalypts and acacias) crest of Fe-rich duricrust of Unit 6. View to the west from near 12600E 10600N.

B. A slope over weathered peridotite covered with a coarse lag of Fe-rich duricrust. This comprises Unit 7 in the foreground which has been incised by the head of a small drainage channel of Unit 10 beside the vehicle. View to the south from 12500E, 10550N.

C. A small outcrop of Fe-rich duricrust of Unit 6 forming the crest of a rise. Below it are lag-covered slopes of Unit 7 forming a thin veneer over peridotite saprolite covered with acacias. View to the north from 12500E, 10500N.

D. Nodules of magnesite lying in a friable, acid brown earth of Unit 8, near 12600E, 10600N; 150 mm scale.

E. A tree-covered crest of lateritic duricrust overlying pyroxenite (Unit 6). The foreground is a slope, developed by local incision, mantled by calcrete-cemented saprolite under a very thin veneer of lag. Spoil heaps from hole OB 26 show the deep weathering of the pyroxenite. View south from near 12510E, 10350N.

F. Detail of calcrete-permeated duricrust with thin lag veneer. Vicinity of OB 26, near 12510E, 10320N. 150 mm scale.

G. Detail of an outcrop of Fe-rich duricrust on a small but prominent crest (Unit 7). The black boulders have a rough surface but, where broken, are dark brown and goethite-rich. 12491E 10535N.

H. A very small bouldery outcrop of Fe-rich duricrust (Unit 7) on a very low rise near 12600E, 10850N. Here the duricrust has a marked pebbly surface and is surrounded by a coarse lag derived from this duricrust. 150 mm scale.


A


B


C


D


E


F


G


H

Figure 9. Detail of lag and duricrust (see over page).

A. Detail of brown duricrust of Unit 5 with some coarse vermiform voids and minor yellow-brown mottling, overlying pyroxenite. Location 12600E, 10200N.

B. Coarse, relatively pale, yellow-brown, nodular lag derived from the duricrust of Unit 5 (compare with Figure 5 A). Location near 12500E, 10250N.

C. Detail of surface of Fe-rich duricrust of Unit 6. This shows a mass of subrounded, hematite-rich pebbles, ranging from 2-40 mm, with a clast-supported, conglomeratic appearance, set in a goethitic cement. Location 12720E, 10640N.

D. A deep, red-brown goethite coated buckshot lag, with a wide size range, characteristic of the Fe-rich duricrust. Location close to 12500E, 10750N.

E. A small drainage channel of Unit 10 has incised weathered peridotite which is mantled by a very thin veneer of characteristic blue-black buckshot lag. Location east of the grid.

F. A thin soil, largely masked by a shiny, blue-black buckshot lag, typical of that overlying peridotitic rocks. Location close to 12500E, 10800N.

G. Fragments of Fe-rich duricrust in calcrete-cemented peridotitic saprolite at the base of a Fe-rich duricrust outcrop exposed by earthmoving. North-west corner of grid near 12400E, 10950N.

H. The knobbly surface of a pyroxenite outcrop exposed at the head of a small drainage channel of Unit 10. The knobbly surface is probably due to large oikocrysts of either augite or plagioclase enclosing Mg silicate chadacrysts. Location to the east of 12500E, 10470N.


A
0 cm 5


B


C
ASAHI
PENTAX


D


E


F

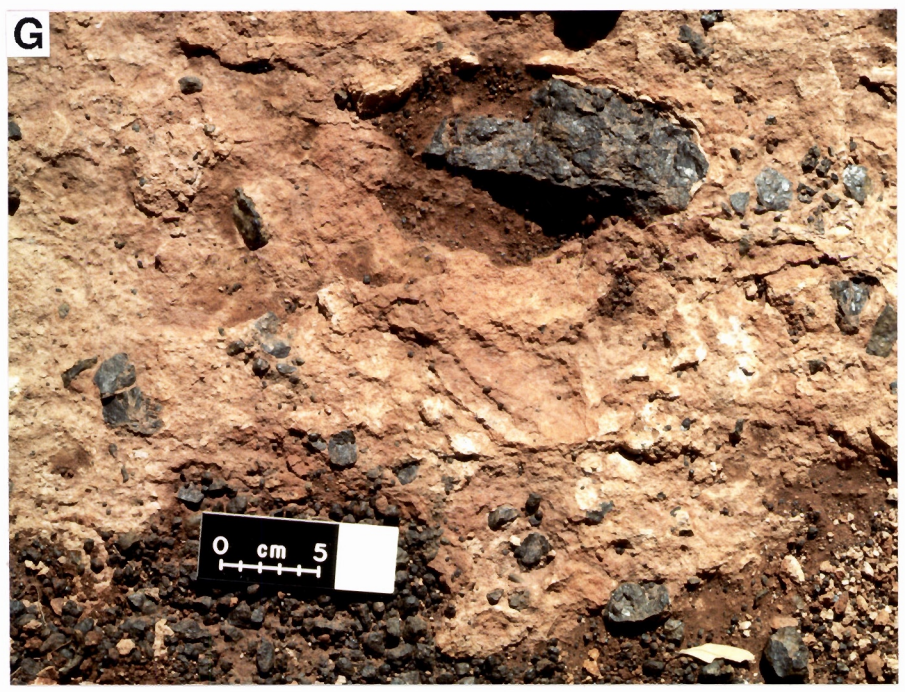
G
0 cm 5


H

TABLE 3
Regolith profiles developed over pyroxenite and peridotite. Informal codes in parentheses identify horizons on drill sections (Appendix I).

Pyroxenite	
0-2 m	Gravelly, calcarous soils *(Ak,)* commonly with numerous lateritic nodules and pisoliths. *(Ank)*
2-7 m	Massive, nodular and pisolitic duricrust (*L, Lpn)*, calcareous near the surface *(Lk)*. Tending to be cemented at the top, but friable with depth.
7-13 m	Strongly oxidized mottled and plasmic clays, the former containing ferruginous pisoliths and nodules. *(Mc)*
13-16 m	Clay saprolite, commonly ferruginous with some nodules, but containing some green clays. *(Sc)*
> 16 m	Saprolite; yellow green, soft and clay-rich *(Sc)* near the top, becoming harder with depth *(S)*. Fabrics well preserved. Silica present in some clay-rich samples. *(Ss, Scs)*
> 35 m	Saprock *(Sr)*; slightly weathered rock, present to about 55 m depth in cores OBDDH1 and OBDDH2, but deeper (> 100 m) near the sheared contact with the peridotite
Peridotite	
0-2 m	Calcareous, clay-rich red earths *(Ak)*
2-5 m	Non-calcareous red earths *(Mc)*
5-11 m	Clay saprolite; red clays becoming brown and green with depth *(Sc)*. Saprolite at shallower depths may be calcareous *(Sk)*.
> 11 m	Clay saprolite; brown, khaki and yellow-green *(Sc)* commonly with abundant magnesite and silica, including moss agate *(Scs)*. Harder and less clay-rich saprolite with depth in some holes, locally silicified (*S, Ss)*.

3.3.2 Lag

Most of the study area has a partial uncemented cover of lag, comprising gravels and coarser fragments derived from the breakdown of lateritic duricrust, saprolite and derived soils and the removal of the finer fractions by wind and water. Ferruginous lag is a valuable and widely used geochemical sampling medium (Carver *et al.*, 1987) because of its relative resistance to erosion and because key indicator elements are readily adsorbed by Fe oxides, especially goethite. In addition, lag may preserve recognizable rock fabrics which may assist geological mapping (Robertson, 1989). As discussed below, two main types of lag occur at Ora Banda, identifiable by attributes that can be seen in the field with the aid of a hand lens.

The size distribution of the lag is variable, with that around outcrops of Fe-rich duricrust (Unit 6) and fragmental duricrust (Unit 5) being particularly coarse. Ants (probably the Mulga Ant, *Polyrhachis* sp) bring lag particles of specific sizes to the surface to surround the exits of their nests. The particle size appears to be peculiar to the ant species. Material from deserted ant middens is gradually dispersed, resulting in small 'pools' on the surface, one or two m in diameter, of a particular lag size. Dispersion of ant midden material is likely to be minor, even though the grain size is small.

Type A Lag - generally overlying peridotitic rocks. The area underlain by peridotite is strewn with a lag containing a variety of fragments, including dominant ferruginous granules and pebbles and lesser amounts of calcrete, magnesite (Figure 8D), moss agate, and minor saprolite and vein quartz. The ferruginous lag (LG201, LG203; Anand *et al.*, 1989) consists of dark brown, dense, angular and roughly equant clasts with generally resinous to slightly vitreous

surfaces (Figure 9F). These possibly represent the remnants of a pre-existing laterite and ferruginized saprolite developed on the peridotites, whereas some pisolitic lag with glossy goethitic coatings among them may be material shed from outcrops of the Fe-rich duricrust (Unit 6). Where this material is dominant, the lag has a distinctive, deep red-brown colour (Figure 9D) due to the coating of goethite. Together these are described as lag type A.

Type C Lag - generally overlying pyroxenitic rocks. Lag overlying the pyroxenitic rocks is commonly coarser than that over peridotite and is generally nodular, lighter brown and less dense. The fragments are angular, variable in size and have a dull and in places cellular surface texture (Figure 9B); some have a ferruginized lithic fabric. Although internally most of these lag fragments are dark brown to deep red-brown, some surfaces have a patina of yellow brown clay. This nodular lag is morphologically related to the outcrops of fragmental duricrust (LT205) among which the lag occurs (Figure 9A).

Type B Lag. Where both peridotitic and pyroxenitic sources have contributed to the lag, the resultant mixture is referred to as lag type B.

3.3.3 Regolith mineralogy

The mineralogy of the regolith profile, determined by X-ray diffraction, is summarized for each lithology on Figure 10. Of the principal primary minerals, only olivine and plagioclase are not found in the regolith. Over pyroxenite, tremolite, orthopyroxene and talc persist to the mid-saprolite, the base of the clay saprolite and base of the mottled zone, respectively. Saponite (magnesian smectite) is the principal clay mineral, derived from olivine and orthopyroxene. It is present throughout the saprolite but is not found above the mottled zone. Kaolinite is also present throughout the saprolite but is only a minor phase due to the low abundance of aluminium; it is most abundant in the clay-rich saprolite and into the mottled and lateritic horizons but, rather surprisingly, gibbsite is the principal Al mineral (apart from Al-goethite) at the top of the laterite and in the soil. Quartz and magnesite are minor phases in the saprolite. The ferruginous horizons are dominated by goethite and hematite, but pedogenic calcite and dolomite are important near the surface. Broadly similar mineral assemblages are present over peridotite, although the regolith is more clay-rich and strongly weathered. Nevertheless, because there is no ferruginous horizon, goethite, hematite and gibbsite are at low abundances or absent from the surface horizons, whereas orthopyroxene, talc and saponite persist to the surface and are present in some soils. In comparison with pyroxenite, the saprolite on peridotite locally contains abundant cryptocrystalline quartz (*e.g.*, as moss agate) and magnesite. Small pebbles and cobbles of these materials occur throughout the profile and are present in the surface lag.

The lag consists largely of hematite and goethite, with minor quantities of kaolinite and quartz (Appendix X). The type A lags, overlying the peridotite, are particularly rich in hematite, whereas type B and C lags, on the pyroxenite, are correspondingly goethite-rich (Figure 11A). These major oxide components are antipathetic (Figure 12A). Maghemite is present in small amounts in the type A lag and in lag at the base of the breakaway to the south end of the central traverse (Figure 11C). Maghemite may thus characterize lag derived from relatively low in the weathered profile (saprolite). Quartz occurs sporadically in the type A lag, presumably due to small chips of agate or vein quartz (Figure 11B). Kaolinite is present as a minor component of each type of lag (Figure 11B).

The Fe-rich duricrust (Unit 6) is richer in both goethite and hematite (Figure 12A) than the lags and forms a separate group, but with a parallel antipathetic trend in these minerals. The range of hematite contents is similar to that of the type A lag but their goethite content is significantly higher, due to their goethite-rich cutans. All Fe-rich duricrusts also contain maghemite and quartz but no detectable kaolinite.

The degree of Al substitution in the goethite is greater in the Fe-rich duricrust (10-11 mole%) than most lag samples, particularly the type C lag (1-4 mole%). A few type A and B lag samples have anomalously high Al substitution in the goethite (12-18 mole%, Figure 12B) due to the presence of material shed from outcrops of the Fe-rich duricrusts.

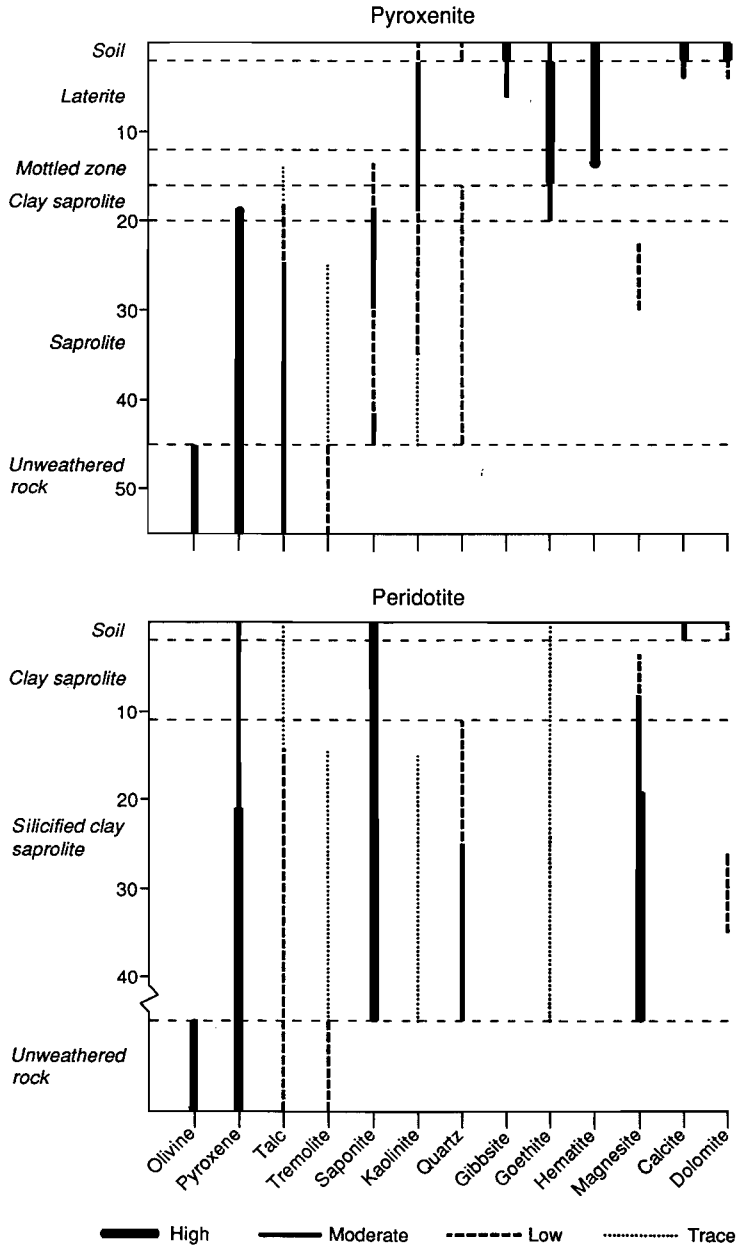

Figure 10. Mineralogy of the main horizons of the regolith over pyroxenite and peridotite, Ora Banda, determined by X-ray diffraction.

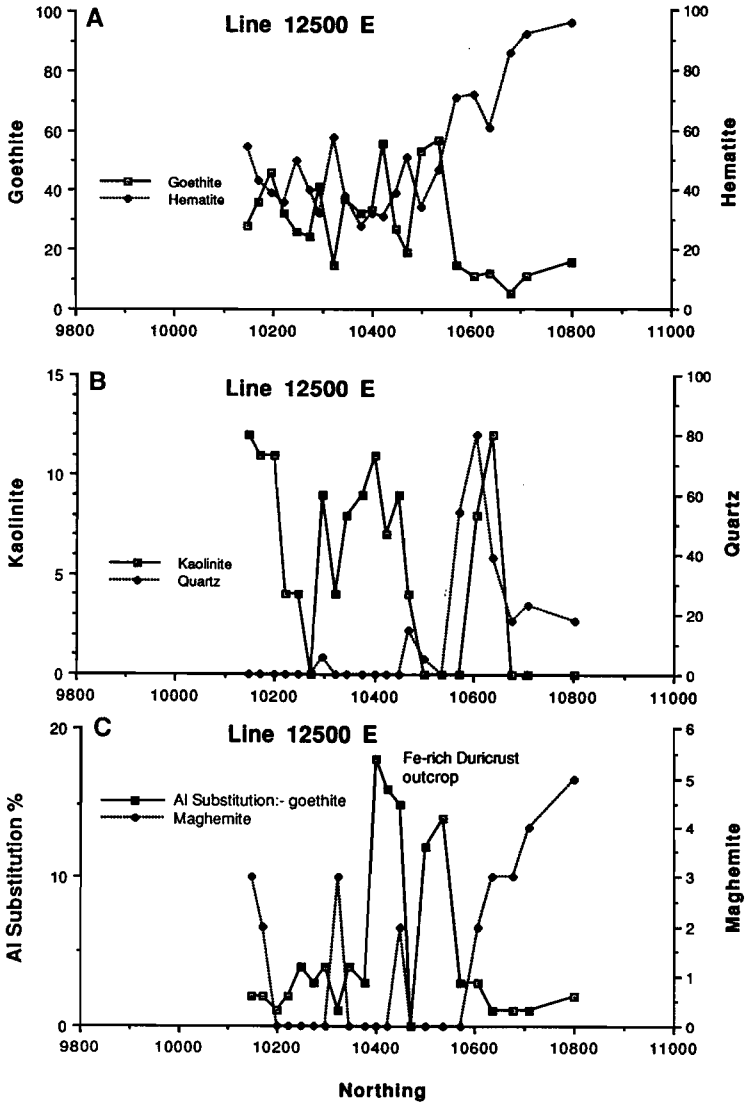

Figure 11. Mineralogy of lag on traverse 12500E. A: goethite and hematite. B: kaolinite and quartz. C: Maghemite and the level of Al-substitution in goethite. Data in arbitrary units that portray variations in the abundance of each mineral between samples, not the relative abundance of different minerals in each sample.

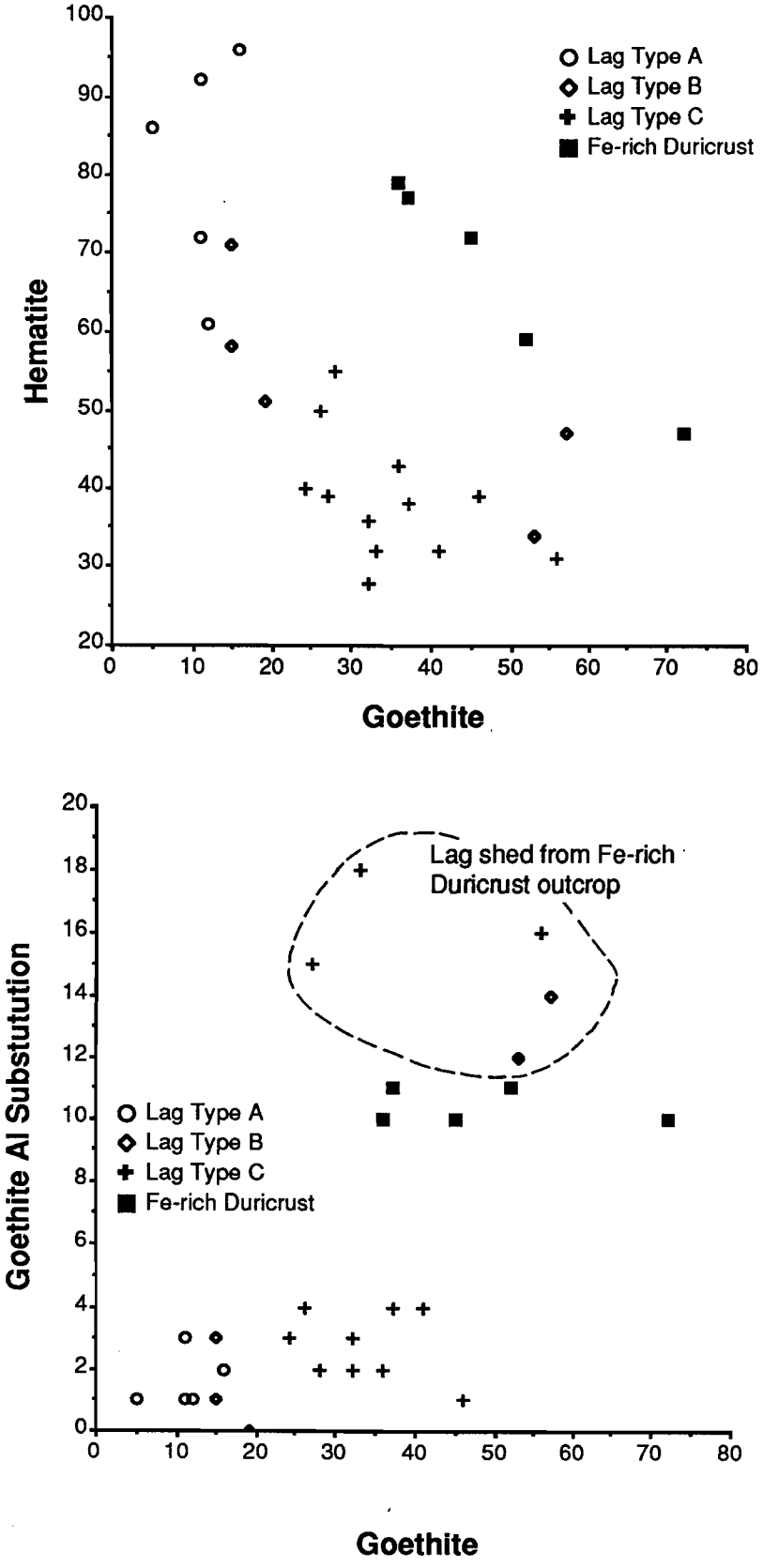

Figure 12. Binary plots showing mineral inter-relationships. A: Goethite and hematite. B: Al-substitution and goethite.

4.0 GEOCHEMISTRY OF THE UNWEATHERED ROCKS

The geochemical data for Pt, Pd, Cr, Cu and Ni in drill core from holes OBDDH1 and OBDDH2, obtained by Carbine Gold N.L., are shown on Figures 13, 14, 15 and 16 and listed in Table 1, Appendix III. Detailed analyses for a range of major and trace elements on sub-samples of the core are listed in Table 2, Appendix III). Data from both sources are summarized in Table 4.

Major elements. The major element data illustrate the less magnesian and more siliceous composition of the pyroxenites compared to the peridotites and also show that these rocks are richer in Al, other alkaline earths (Ca, Ba, Sr) and Na.

Platinum, palladium and copper. The pyroxenites are much richer in Pd and, in particular, Pt, and have a higher Pt/(Pt+Pd) ratio (Pt%) than the peridotites. There are gradual increases in total PGE content and Pt% throughout the peridotite, with a suggestion of cyclicity. In the pyroxenite, the PGE appear to be enriched in the lower 75 m and again towards the top; the trend of increasing Pt%, evident in the peridotite, continues into the pyroxenite, in which it rises from about 55% at the base to about 68% above 75 m, although with some maxima of 80-85% close to the top of the unweathered section in OBDDH2. The original data showed a maximum concentration of 980 ppb Pd in the basal 1 m of the pyroxenite in OBDDH1. However, re-analysis of the contact zone (105-107 m) showed that although some of the highest PGE concentrations occur in this zone, this peak value could not be repeated (Table 5), the maximum being 360 ppb Pd and 420 ppb Pt.

The distribution of sulphides (principally chalcopyrite) is indicated by that of Cu, which shows mostly low concentrations (~10 ppm) through much of the peridotite, rising abruptly to 50 ppm about 60 m below the contact with the pyroxenite. This increase corresponds to a rise in Pt% from <40-45% to >50-55%. The Cu content again increases sharply at the contact to >200 ppm through the lower half of the pyroxenite, but decreasing gradually towards the top. There is a concomitant increase in Pt% to 55-68% at the contact but, whereas the Cu content then declines, Pt% remains high and locally increases upwards, as described above. The maximum Cu concentrations occur approximately centrally within the pyroxenite, with maxima of 1000-1025 ppm at 146-149 m in OBDDH2. A 15 cm sample at 147 m contained 3940 ppm Cu (XRF analysis). Examination of the core indicates that the base of the pyroxenite corresponds to the onset of sulphur saturation and the first appearance of cumulus sulphides. However, the data from this core show that there is no single horizon of PGE enrichment occurring at the first appearance of sulphides, as might be expected and as reported at Munni Munni (Hoatson and Keays, 1989), but a broader zone of moderate PGE and sulphide enrichment. Nevertheless, data from the weathered zone suggest that there may be some thin zones of PGE enrichment but these are either discontinuous or cut by faulting (Section 6.2).

Ruthenium, rhodium, osmium and iridium. Several samples, including those close to the contact, were analysed for the minor PGE in order to determine their approximate concentrations and to investigate whether the apparently stratigraphic enrichment intersected in the regolith, which has elevated minor PGE, could be traced into the found in the bedrock. The results (Table 5) show that the minor PGE are at essentially background concentrations, with some minor Rh and perhaps Os enrichment where Pt and/or Pd are also elevated, but not to the same extent as in the regolith. It was assumed that concentration of the minor PGE would only occur where Pt and Pd are also enriched, so that only a few samples have been analysed.

TABLE 4
Comparative compositions of unweathered peridotite and pyroxenite, Ora Banda Sill.
(See also Table 3, Appendix III).

Major and alkali elements

Lithology		Obs	SiO_2%	Al_2O_3%	Fe%	CaO%	MgO%	Sr ppm	Ba ppm
Peridotite	Mean	8	42.57	1.83	12.18	2.39	32.40	10	16*
	SD		2.71	0.45	1.98	1.91	5.22	5	8*
Pyroxenite	Mean	12	53.76	3.30	11.11	3.04	26.55	17	36*
	SD		1.01	0.65	0.66	0.64	3.01	6	23*

Elements associated with mineralization

Lithology		Obs	Pt ppb	Pd ppb	Pt%	Cu ppm	Ni ppm	S%	
Peridotite	Mean	198	42	54	45.21	30	1092	-	#
	SD		35	55	9.15	34	152	-	#
	Mean	8	-	-	-	33	1191	0.0414	*
	SD		-	-	-	62	199	0.0636	*
Pyroxenite	Mean	160	132	79	63.30	217	545	-	#
	SD		132	79	6.99	131	195	-	#
	Mean	12	-	-	-	612	1112	0.1761	*
	SD		-	-	-	1072	938	0.3407	*

Lithophile transition elements

Lithology		Obs	TiO_2%	Cr ppm	Sc ppm	Ga ppm	Zr ppm	
Peridotite	Mean	198	-	4398	-	-	-	#
	SD		-	752	-	-	-	#
	Mean	8	0.09	4568	-	3	6	*
	SD		0.03	973	-	1	3	*
Pyroxenite	Mean	160	-	2692	-	-	-	#
	SD		-	376	-	-	-	#
	Mean	12	0.19	2965	-	3	12	*
	SD		0.04	316	-	1	8	*

Base and transition metals

Lithology		Obs	As ppm	Pb ppm	Zn ppm	Mn ppm	Co ppm	Ni ppm
Peridotite	Mean	8	-	-	74	1351	132	1092*
	SD		-	-	10	224	19	152*
Pyroxenite	Mean	12	-	-	69	1586	102	1191*
	SD		-	-	4	27	33	199*

Alkali and rare earth elements

Lithology		Obs	Na_2O%	Cs ppm	Rb ppm	Ce ppm	La ppm	Y ppm
Peridotite	Mean	8	0.15	-	3	7	-	2*
	SD		0.10	-	2	4	-	2*
Pyroxenite	Mean	12	0.36	-	3	9	-	5*
	SD		0.19	-	2	5	-	2*

- Not determined. SD standard deviation.
* Analysis by XRF fusion (CSIRO)
# PGE analysis by fire assay; Cu, Cr, Ni by mixed acid/AAS (Genalysis, for Carbine Gold N.L.)

Chromium and nickel. The Cr and Ni distributions are, of course, rather different to those of Cu and the PGE. They are relatively enriched in the peridotites (means 4400 ppm Cr, 1090 ppm Ni) compared to the pyroxenites (2690 ppm Cr, 545 ppm Ni), both tend to decrease upwards through each unit, and are much less variable, Cr in particular. The maximum Ni contents in the pyroxenites (1000-1075 ppm) correspond to the Cu maxima, with a peak of 3855 ppm in the same 15 cm sulphide-rich sample at 147 m in OBDDH2.

TABLE 5
Platinum group metals in fresh and partly weathered rocks, including the pyroxenite-peridotite contact intersected in OBDDH 1.

Sample	Depth m		Pt ppb	Pd ppb	Pt%	Ru ppb	Rh ppb
Hole OBD 1							
00-5442	64.0- 64.1	Px	160	20	89	4	14
00-5443	71.0- 72.0	Px	58	140	29	1	9
00-5444	94.1- 94.2	Px	8	10	44	8	3
00-5445	105.5-106.0	Px	130	78	63	4	7
00-5446	106.0-106.2	Px	8	8	50	4	2
00-5447	106.2-106.5	Px	420	360	54	8	15
00-5448	106.5-106.7	Po	170	118	59	6	11
00-5449	106.7-107.0	Po	22	22	50	6	3
00-5497	126.9-128.0	Po	28	14	67	8	5
00-5498	141.0-142.0	Po	46	56	45	10	5
Hole OBD 2							
00-5450	97.15- 97.25	Px	175	88	67	2	9
00-5451	146.85-147.00	Px	112	80	58	4	14
00-5452	202.40-202.46	Px	195	116	63	1	13

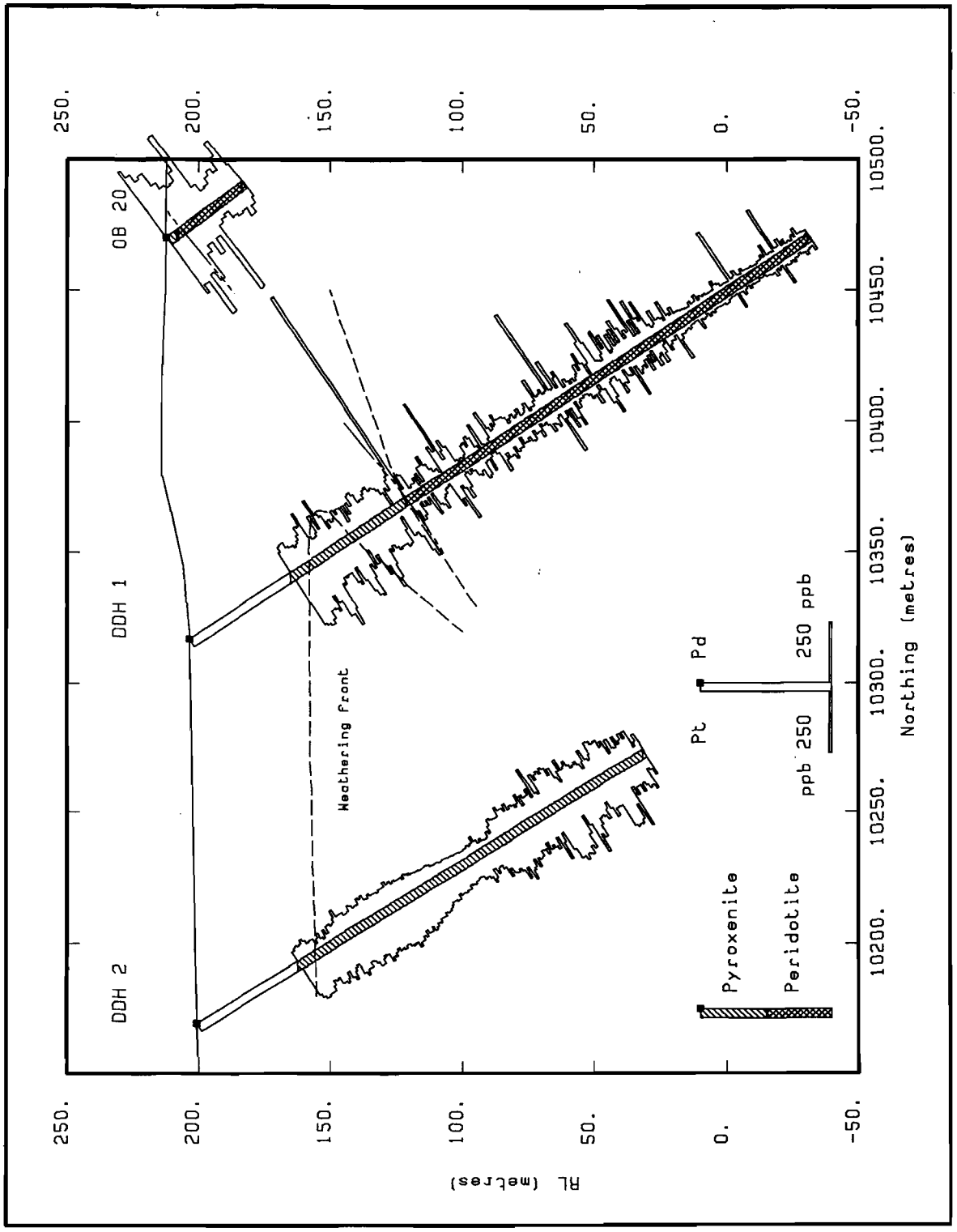

Figure 13. Platinum and palladium distributions in predominantly unweathered pyroxenite and peridotite, Ora Banda. Diamond drill core sampled at 1 m intervals (data from Carbine Gold N.L.).

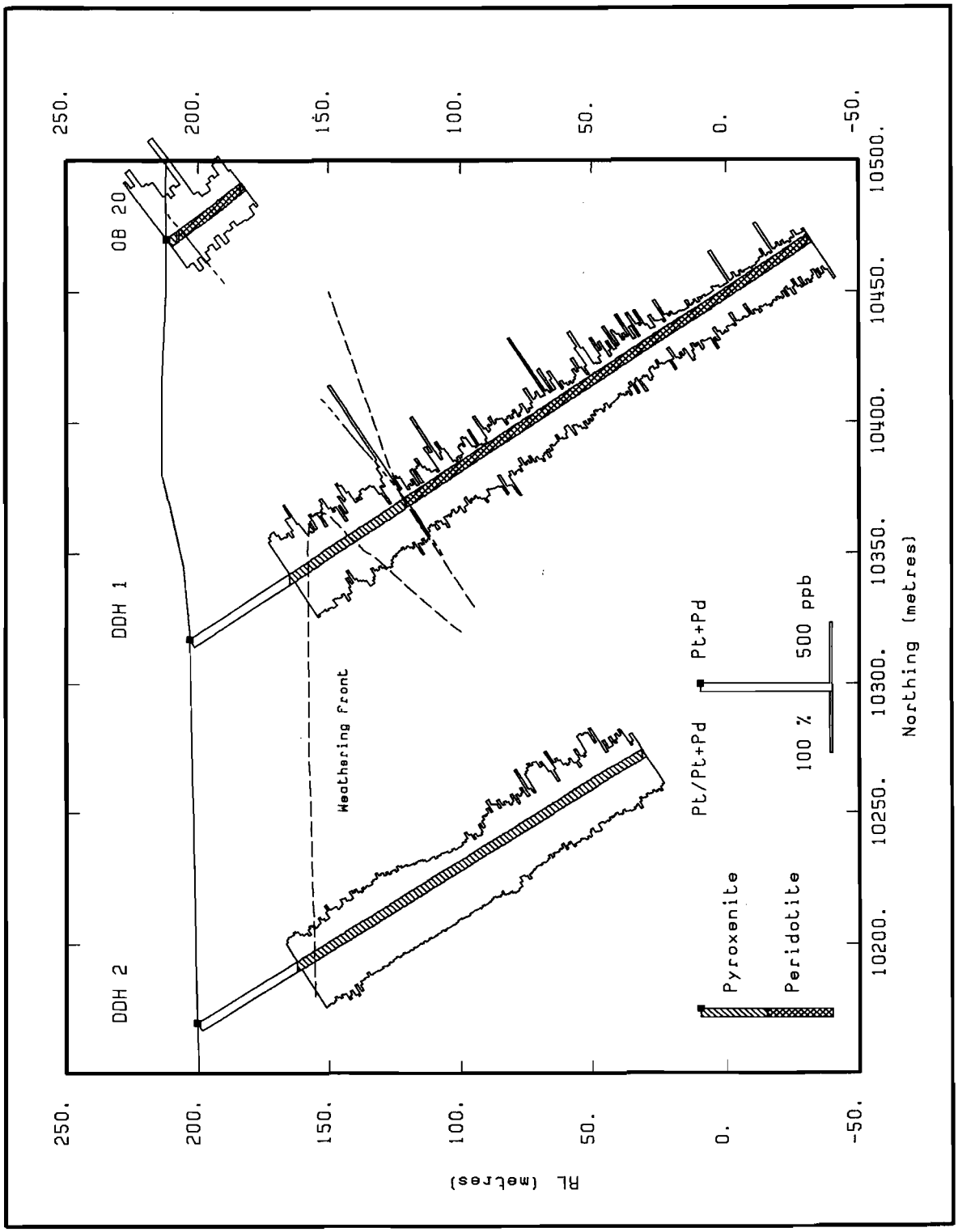

Figure 14. Platinum ratio and total platinum plus palladium distributions in predominantly unweathered pyroxenite and peridotite, Ora Banda. Diamond drill core sampled at 1 m intervals (data from Carbine Gold N.L.).

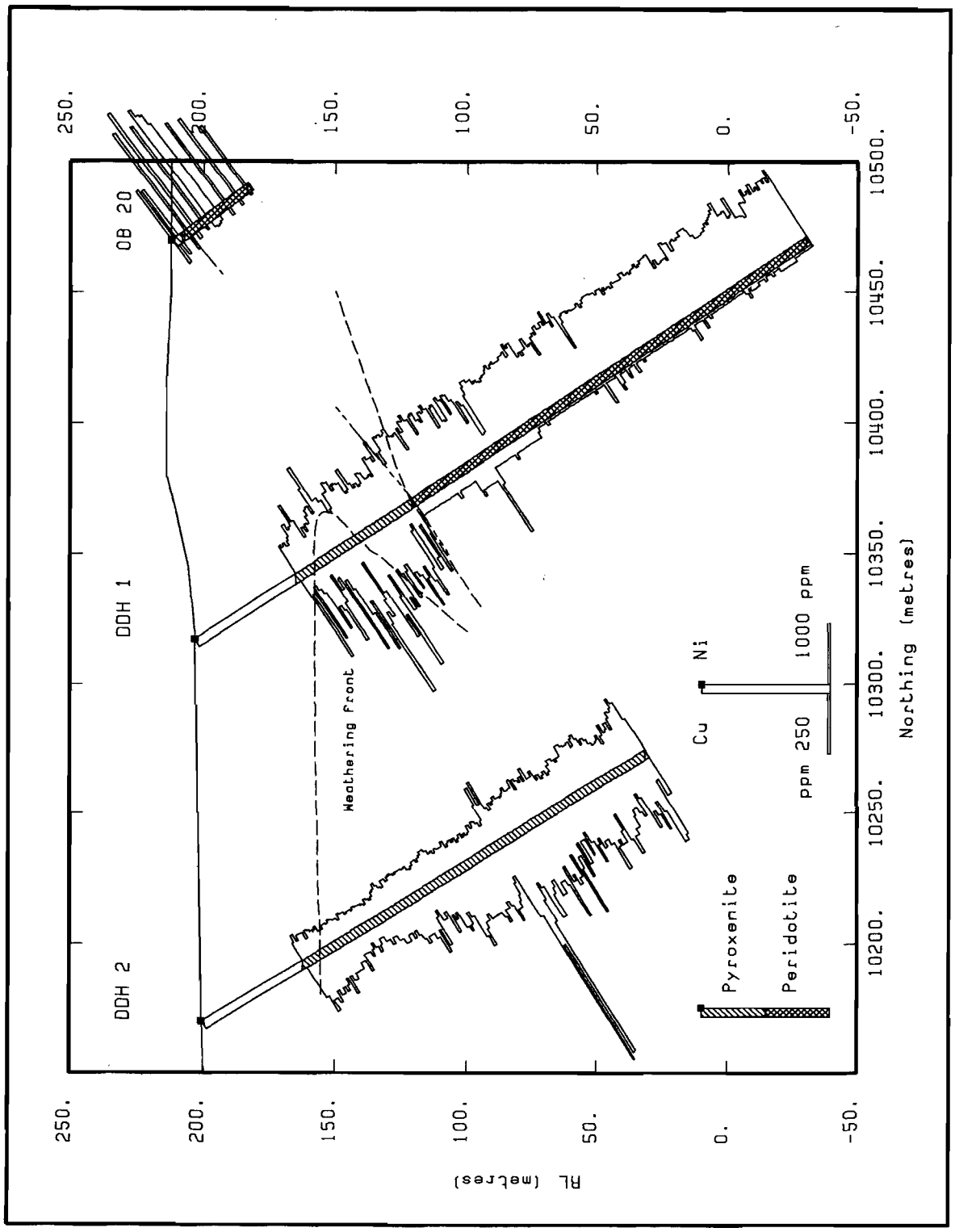

Figure 15. Copper and nickel distributions in predominantly unweathered pyroxenite and peridotite, Ora Banda. Diamond drill core sampled at 1 m intervals (data from Carbine Gold N.L.).

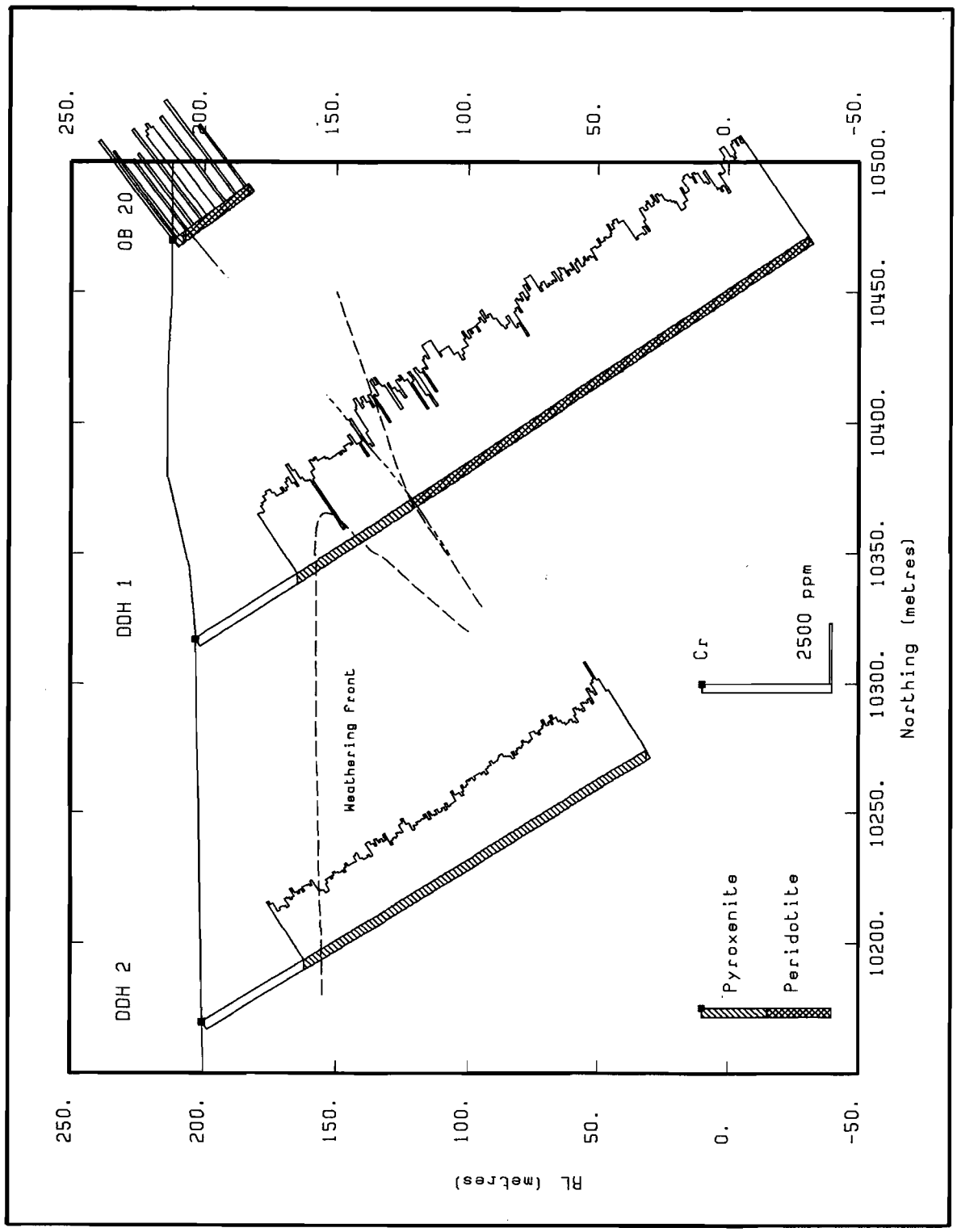

Figure 16. Chromium distribution in predominantly unweathered pyroxenite and peridotite, Ora Banda. Diamond drill core sampled at 1 m intervals (data from Carbine Gold N.L.).

5.0 PETROGRAPHY OF DURICRUSTS AND LAGS

5.1 Introduction

The objectives of the petrographic study were to provide a better understanding of the origins of the lag and duricrust and to determine any features that indicate underlying lithologies. Because of inhomogeneities due to variations in parent material, weathering, degrees of Fe oxide replacement and provenance, three sections of lags were made from each location. Many of the fragments of the duricrust and lag contain lithorelics. Much of their original fabric has been destroyed by massive to slightly porous Fe oxide, mainly goethite, although this has, in part, been dehydrated to hematite, probably reflecting dry, near-surface conditions. Where the fabric has been preserved, the original minerals have been almost completely replaced and pseudomorphed by Fe oxides, although some relict chromite is still present. The most distinctive pseudomorphs are those after olivine and pyroxene; others are after amphibole, serpentine, talc and even smectite and kaolinite, and some are very difficult to identify. The principal findings are described below and illustrated in Figures 9 and 17 to 20. Detailed descriptions of each specimen are given in Appendix V.

5.2 Duricrust

Duricrust overlying pyroxenite (Unit 5). This duricrust, which is deep red-brown to yellow-brown, contains numerous cavities and vesicles, is comparatively rich in kaolinite and goethite, poor in hematite and lacks quartz. The vesicles are largely filled with several generations of ferruginous clay which cement and coat fragments of duricrust, in places forming oolitic and pisolitic structures (Figures 20E-F, H). Vesicles within this clay cement are coated and filled with goethite which has a cuspate or occasionally a colloform appearance. Relic lithofabrics are generally difficult to recognize among a mass of secondary goethite, though the fine-scale cleavage of pyroxene, amphibole and talc are apparent in places (Figure 20G). This duricrust has an identical mineralogy and fabric to the lag derived from it.

Fe-rich duricrust overlying peridotite (Unit 6). The Fe-rich duricrusts have a pisolitic fabric (Figures 17A-D, F). Many of the pisoliths consist of round to subangular, apparently clastic fragments coated by banded goethite. The fragments are composed of bright Fe oxides, some clearly being lithorelics whereas others have no recognizable fabric (Figures 17D, F). Some pisoliths have dehydration cracks in which goethite has, in part, altered to hematite. The pisoliths are generally set in a goethite cement that was either incomplete or, less probably, has been partly dissolved to leave cavities and vesicles. These cavities are now coated or partly infilled by goethite-stained clay (Figures 17A-B), some with a colloform or cuspate-structured goethite (Figure 17E) and a very few with agate. Some of the clasts themselves have an internal clastic fabric which has been cemented by bright, Fe oxides (Figure 17A). Some pisoliths, and the cutans formed upon them, have been broken and recemented (Figure 17B), indicating several detrital phases, interspersed with cycles of Fe oxide cementation. Many contain drop-like and, in part, weathered chromite crystals (Figure 17H) and a few have pseudomorphs after weathered, serpentinized olivine (Figure 17G) and minor pyroxene, typical of the peridotitic rocks, and less distinct layer silicate pseudomorphs, probably after saprolitic clays. Others have no chromite at all. In places the total assemblage is polymictic, with some lithorelics having fabrics suggesting argillaceous rocks, implying a wider provenance of the Fe-rich detritus than the Ora Banda Sill.

The Fe oxide of the fragments is dark grey in oblique reflected light (Figures 17A-B) but it is bright, yellowish white in normally reflected light (Figures 17C-H) and consists of an intimate hematite-goethite mixture. Its brightness appears to be related to its hematite content. The banded goethite, coating the fragments and forming the cement, is a deep honey-brown in oblique reflected light (Figures 17A-B) and a lead-grey in normally reflected light

(Figures 17D, F). The cutans on the clasts are generally banded and continuous (Figures 17D, F), suggesting some slight movement in a low energy environment during the coating process. Some goethitic cements are a continuation of the individual coatings around pisoliths (Figure 17B) and sand- and silt-sized quartz grains (Figure 17C), forming a solid mass; others have formed around and others impregnate ferruginous clay.

Fossil plant material has been identified in much of the Unit 6 Fe-rich duricrust. The scale, regularity and organization of the void patterns, and the variability of wall thicknesses and void shapes are all consistent with cell structures. Identification of specific plant organs is, at this stage, speculative, though it is possible to note similarities with present-day plant material. Most of the fossil plant matter has been preserved as early bright goethite in the centres of pisoliths, though some is preserved by later, lead-grey goethite. In all instances, the cell walls are preserved as Fe oxides but the interiors (cell lumen) are now void.

Plant organs that have been tentatively identified are:-

1. The tip of a stem, showing lines and whorls of cells, suggesting overlapping bud scales (Figure 18A).
2. Fragments of leaf material including stomata (Figure 18C), vein (Figure 18E) , elongate midrib cells and supporting tissues (Figure 18G). One has rectangular cells suggestive of a moss leaf (Figure 18B).
3. A seed, with a clear, linear, banded arrangement of cells in two directions and the suggestion of the remnants of the smaller enveloping cells (Figure 18D).
4. A web of thin-walled cells, suggesting a fragment of corky bark tissue (Figure 18F).
5. A triangular structure that could be a section through the rachis of a filmy fern (Figure 18H).

Similar cell structures have been observed in the channel iron deposits of the Pilbara (Ramanaidou *et al.*, 1991) and the oolitic Fe-rich duricrusts of the Lawlers District (Anand *et al.*, 1990; Anand *et al*, 1991).

5.3 Lag

5.3.1 Lag overlying peridotite

Many of the subangular fragments consist of hematite or hematitic goethite, in which hematitic pseudomorphs after olivine (Figures 19B, E, F, H), and a few goethitic pseudomorphs after talc-altered pyroxene (Figures 19B, F), may be distinguished in various states of preservation. In some fragments, serpentinized cracks in the olivine have been faithfully pseudomorphed by hematite, but the olivine is now void, leaving only an outline. The preservation of the primary fabric depends on ferruginization occurring before destruction of the saprolite structure. If this does not occur, the most that may be found are disaggregated olivine pseudomorphs (Figure 19H) or only very indistinct relics, probably after smectitic clays.

Some lead-grey goethite has pseudomorphed probable kaolinitic accordion structures (Figure 19G). The relics are set in bright, secondary goethite, which has been altered, in part, to hematite, leaving characteristic dehydration cracks. Some lag fragments themselves have a clastic fabric and contain a breccia of hematite- and goethite-rich lithorelics, some pisoliths, derived from the Fe-rich duricrust and shards of secondary hematite, cemented by a bright hematitic goethite.

Abundant, drop-like crystals of weathered, pinkish-grey chromite are characteristic of these lags. The polished surfaces of some of these crystals are extensively pitted (Figure 19D), others have a reticular pattern of goethite-filled cracks which penetrate the crystal from its margin (Figure 19C). These cracks appear to reflect weathering of the chromite and become progressively

narrower towards the centre of the grain. This crack pattern has almost destroyed the outline of some small chromite crystals.

5.3.2 Lag overlying pyroxenite

The primary fabrics of the pyroxenes are not nearly as well preserved as those of olivine. In general all that can be discerned is a fine-scale, parallel, goethite structure (Figures 20B, D, G) which appears to be after amphibole, talc or, rarely, after pyroxene. There are a few indistinct pseudomorphs after sheet silicates, probably smectites and vermiculites (Figure 20C). This is generally set in dark, spongy goethite. This lag is significantly poorer in hematite and richer in goethite than that overlying the peridotites. It is also much poorer in chromite and the chromite grains are generally much smaller, characteristic of the pyroxenites. Some have bright hematitic rims interposed between the weathered chromite and the surrounding goethite.

These lag fragments have numerous vesicles and voids that have been filled with several generations of pisoliths (Figures 20E-F) of similar material to that enclosing the vesicles. Some pisoliths are coated thinly in iron oxides and are set in goethite and goethite-rich clay. Some voids have been coated with colloform goethite (Figure 20H) or with goethite showing a layered, cuspate structure, suggesting accumulation at the bottom of the void with minor deposition on the walls.

Figure 17. Fabrics of Fe-rich duricrust (see over page).

A. Goethite-coated ferruginous lithorelic granules (l) set in an incomplete goethite cement (g). Cavities in this cement are filled with iron-stained clay (cl). Varied fabrics emphasize the polymictic nature and diverse provenance of the granules. One fragment (a) shows an earlier clastic fabric indicating a previous sedimentary episode. Close up photograph of polished section - oblique reflected light. Specimen HMC-OB2B. Co-ordinates 12400E 10700N.

B. Lithorelic granules (l) coated with varying thicknesses of a banded goethite cement (g). One fragment has had part of its goethite coat chipped off (a), suggesting moderate energy in the sedimentary environment. Close up photograph of polished section - oblique reflected light. Specimen 08-1553. Co-ordinates 12600E 10700N.

C. Ooliths containing hematitic lithorelic cores (h), coated in goethite (g), rich in inclusions, and angular quartz shards (q), set in a goethitic cement. Polished section photomicrograph. Specimen HMC-OB1D. Co-ordinates 12491E 10535N.

D. A hematitic pisolith (h) coated with lead-grey goethite (g). The core of the pisolith consists of massive hematite set with a few drop-like, pitted crystals of chromite (cr). Polished section photomicrograph. Specimen 08-1553. Co-ordinates 12600E 10700N.

E. The clastic, Fe-rich matrix of a Fe-rich duricrust has a small cavity filled with cuspate layers of secondary goethite (sg). Polished section photomicrograph. Specimen 08-1554. Co-ordinates 12400E 10850N.

F. A pisolith core of massive, secondary goethite (sg) coated in banded lead-grey goethite (gc). Polished section photomicrograph. Specimen 08-1553. Co-ordinates 12600E 10700N.

G. A poorly-preserved relic of olivine (ol) and a chromite grain (cr) set in slightly spongy secondary goethite (sg). Polished section photomicrograph. Specimen 08-1553. Co-ordinates 12600E 10700N.

H. Weathered drop-like chromite grains (cr) set in hematitic goethite (hg). The chromite shows a rectangular pattern of penetrating iron oxides. Polished section photomicrograph. Specimen 08-1556. Co-ordinates 12400E 10850N.

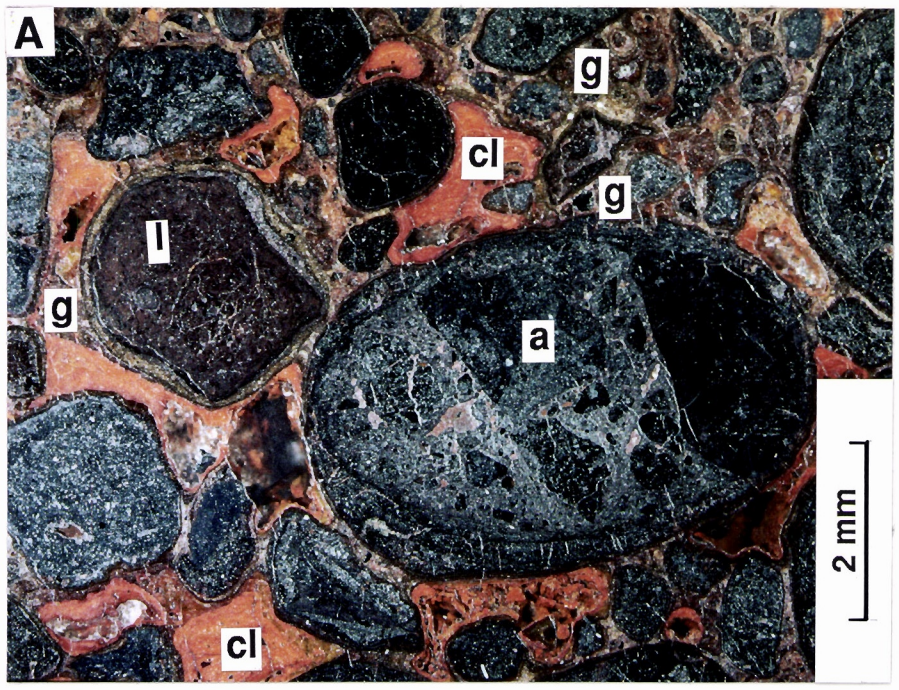
A
g
cl
g
l
g
a
cl
2 mm

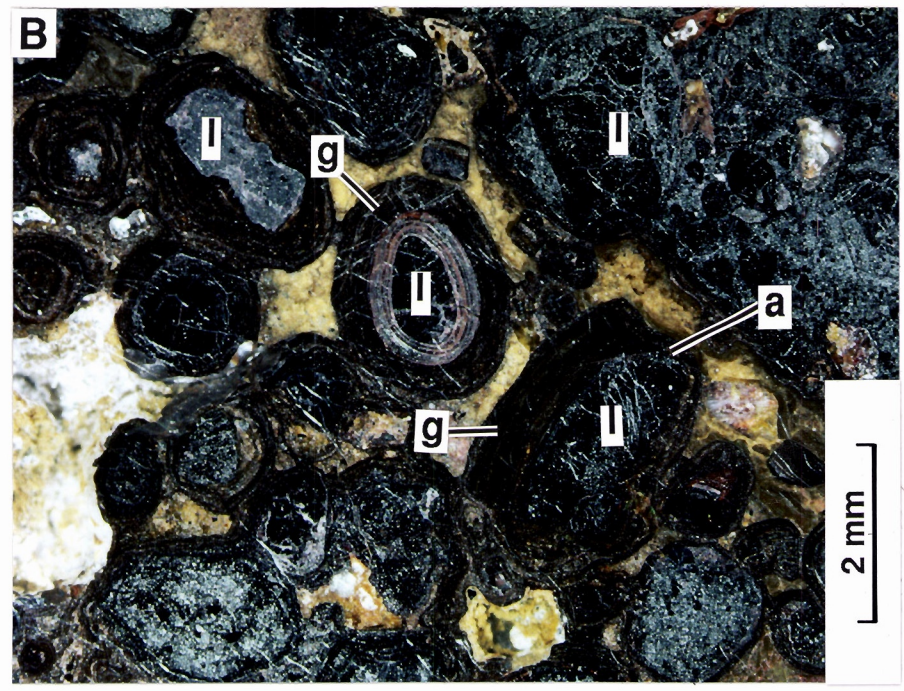
B
l
g
l
l
a
g
l
2 mm

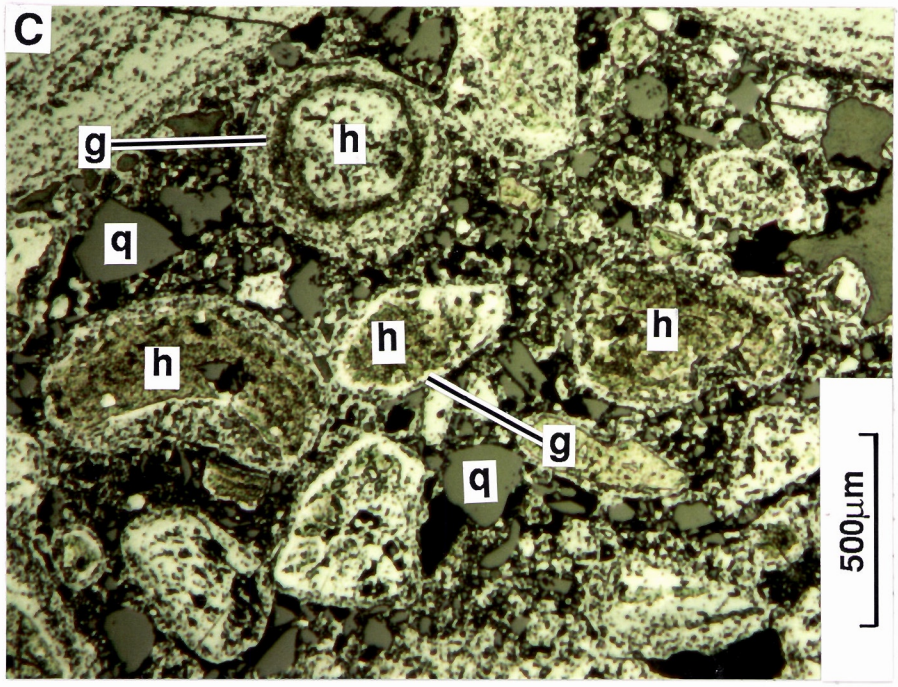
C
g
h
q
h
h
h
g
q
500µm

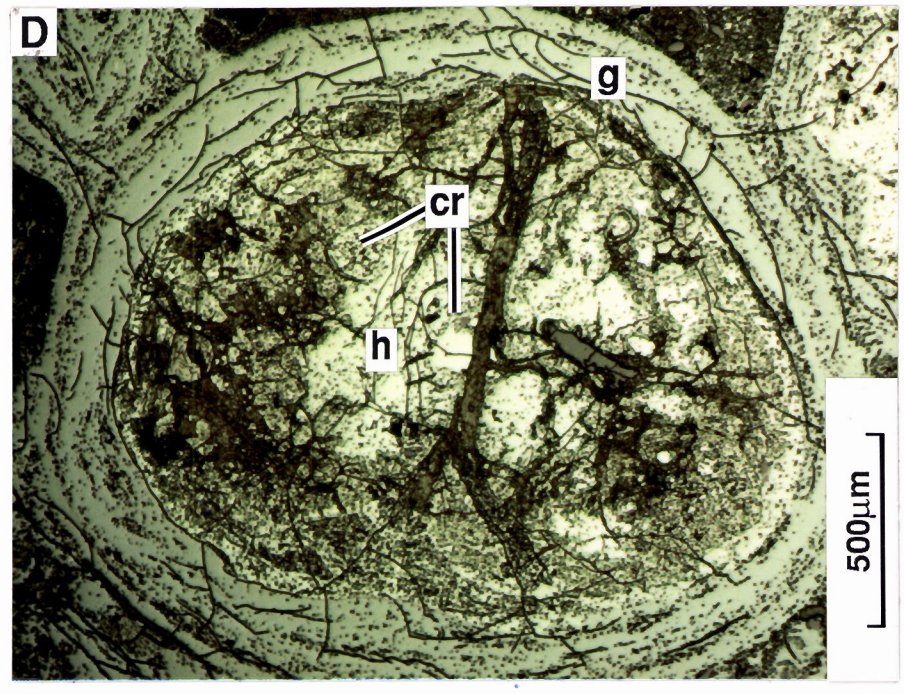
D
g
cr
h
500µm

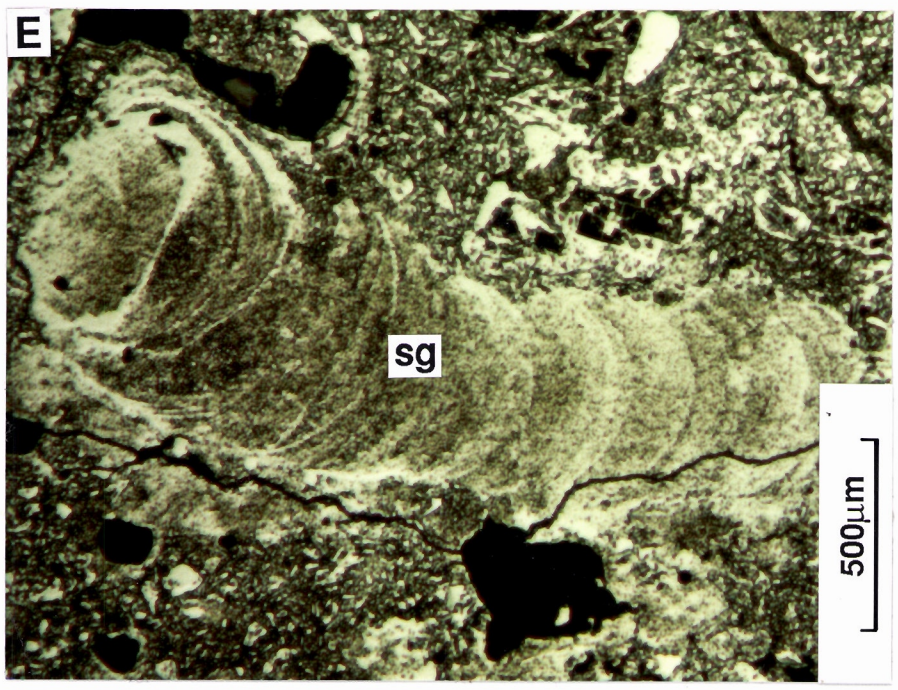
E
sg
500µm

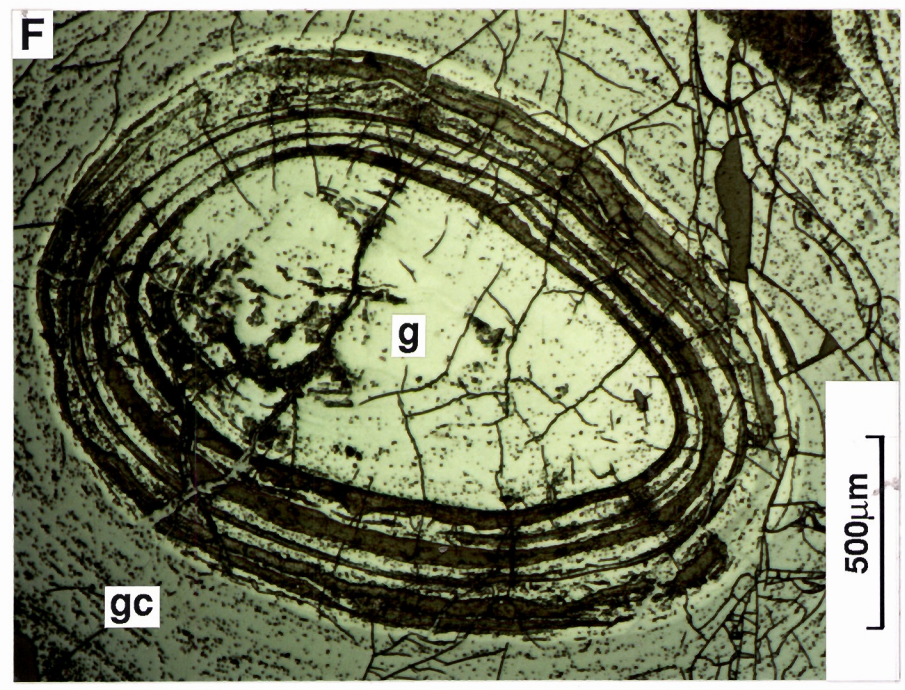
F
g
gc
500µm

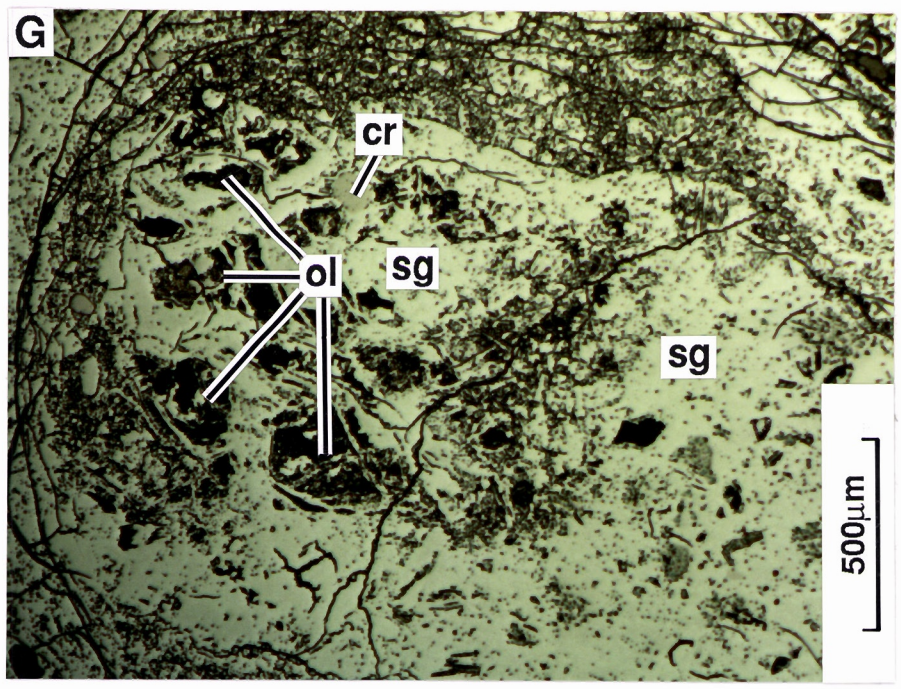
G
cr
ol
sg
sg
500µm

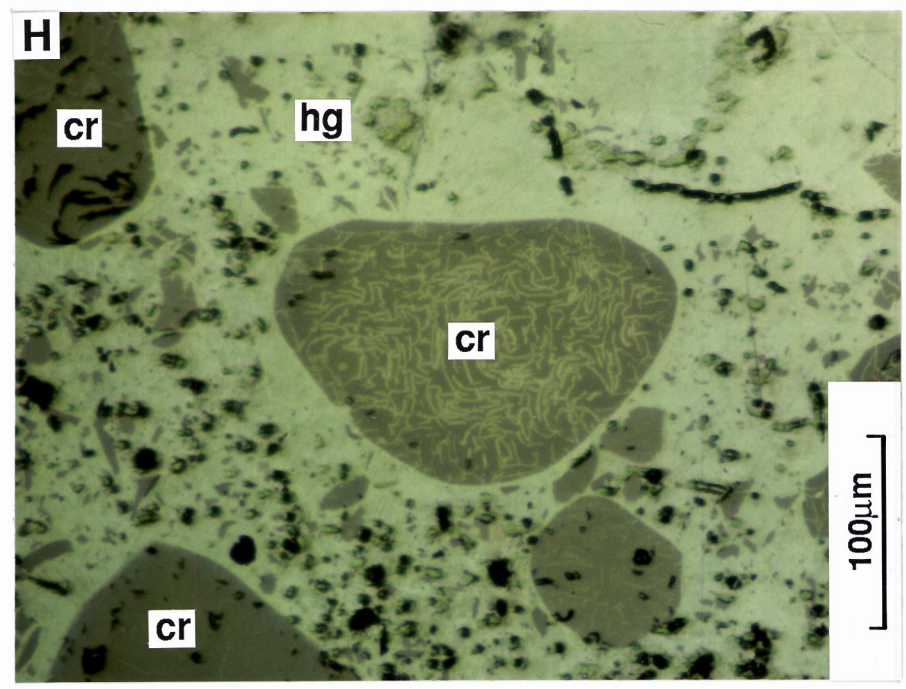
H
cr
hg
cr
cr
100µm

Figure 18. Fossil plant material in Fe-rich duricrust (see over page).

A. Interior of a rounded, hematitic clast shows a possible tip (a) of a stem with lines and whorls of cells suggesting overlapping bud scales. This is coated in goethite (g) and cemented by goethite (s). Specimen 08-1553. Co-ordinates 12600E 10700N.

B. A goethite clast with an internal rectangular and square cell structure suggesting part of a moss leaf. Specimen HMC-OB2B. Co-ordinates 12400E 10700N.

C. A lozenge-shaped fragment of leaf fossilized in goethite, showing preserved stomata (s) but the cell pattern is indistinct and possibly distorted. Specimen 08-1555. Co-ordinates 12600E 10750N.

D. The alignment of cells in two directions suggests the inner part of a seed and there is a suggestion of some of the enveloping cells. The shape of its enclosing pisolith may have in part been dictated by the shape of the plant organ. Specimen HMC-OB2B. Co-ordinates 12400E 10700N.

E. A rounded hematitic clast with an internal cell structure suggesting the vein structure of a leaf (v) with surrounding supportive tissue (s). This fragment is surrounded with a thin, bright goethite cutan (c). Specimen 08-1553. Co-ordinates 12600E 10700N.

F. A plant fragment, showing a mass of thin-walled, irregular cells (c), indicative of corky bark tissue, preserved in goethite. Specimen HMC-OB3A. Co-ordinates 12400E 10700N.

G. Elongate cells of a leaf midrib (m) and equant cells of the attached supporting tissue (s) preserved in hematite. Specimen HMC-OB3A. Co-ordinates 12400E 10700N.

H. A triangular section and typical cell structure of the rachis of a filmy fern, preserved in hematite. Specimen HMC-OB3A. Co-ordinates 12400E 10700N.

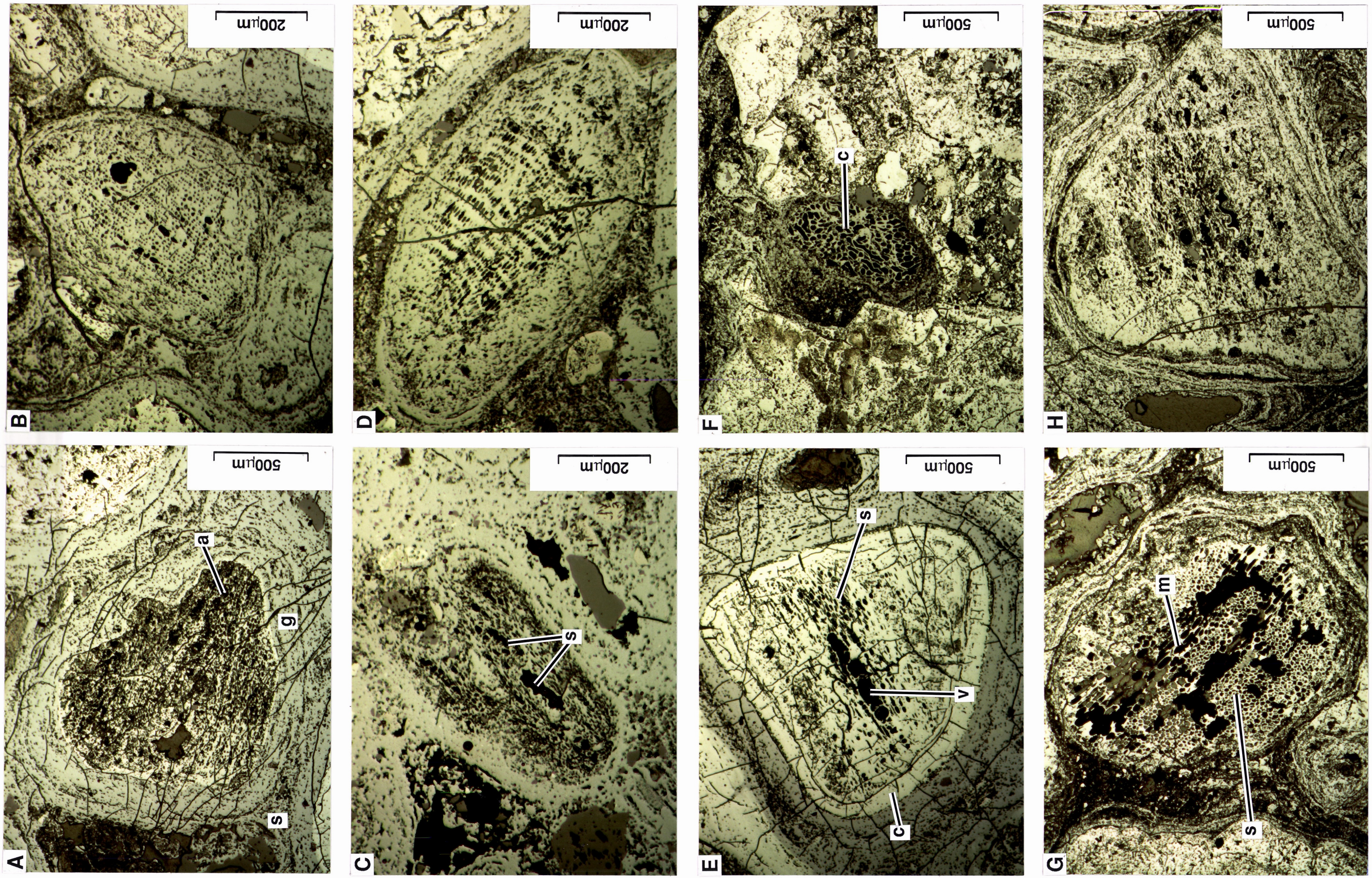
A
a
g
s
B
200µm
C
s
200µm
D
200µm
E
c
s
v
500µm
F
c
500µm
G
m
s
500µm
H
500µm

Figure 19. Fabrics of peridotite and equivalent lags (see over page).

A. Polygonal crystals of fresh olivine (ol) and intercumulus bronzite (br) in an olivine-bronzite cumulate. A few drop-like chromite crystals (cr) occur near the edges of the olivines and within the pyroxene. Thin section photomicrograph - crossed polarizers. Specimen from diamond core OBDDH1, down hole depth 236.5 m.

B. Olivine (ol) and pyroxene (px) pseudomorphed in a lag sample near the top of the peridotite. The serpentinized cracks in the olivine are preserved by hematite (he) but the olivine has been dissolved and is now void (vo). The outline and cleavage of the pyroxene are both preserved in goethite (gt). Polished section photomicrograph. Specimen 08-1498. Co-ordinates 12504E 10450N.

C. A crystal of weathered chromite (cr) set in goethite (gt). Goethite has followed rectangular cracks (c) from the outside of the chromite, becoming progressively thinner to its centre and the outline of the chromite grain largely has been lost. Polished section photomicrograph. Oil immersion. Specimen 08-1511. Co-ordinates 12606E 10997N.

D. Pitted, drop-like chromite crystals (cr), typical of lags derived from peridotitic rocks, set in dehydration cracked hematite (hm). Polished section photomicrograph. Specimen 08-1516. Co-ordinates 12604E, 10696N.

E. An olivine pseudomorph in goethite. Thin serpentinized cracks in the olivine are now preserved in hematite (hm). Polished section photomicrograph. Specimen 08-1498. Co-ordinates 12504E, 10450N.

F. Serpentinized olivine (ol) and talc-altered pyroxene (px) fabric perfectly preserved in goethite and hematite. Close up photograph of polished section - oblique reflected light. Specimen 08-1498. Co-ordinates 12504E 10450N.

G. An accordion structure (ac) probably after kaolinite now pseudomorphed by slightly bluish goethite, set in goethite, hematite and some relict pitted chromite (cr). Polished section photomicrograph. Specimen 08-1499. Co-ordinates 12502E 10424N.

H. Olivine pseudomorphs (ol), now preserved in hematite and goethite, and fragments of massive, secondary goethite (gt) in a lag from near the top of the peridotite. Close up photograph of polished section - oblique reflected light. Specimen 08-1498. Co-ordinates 12504E, 10450N.

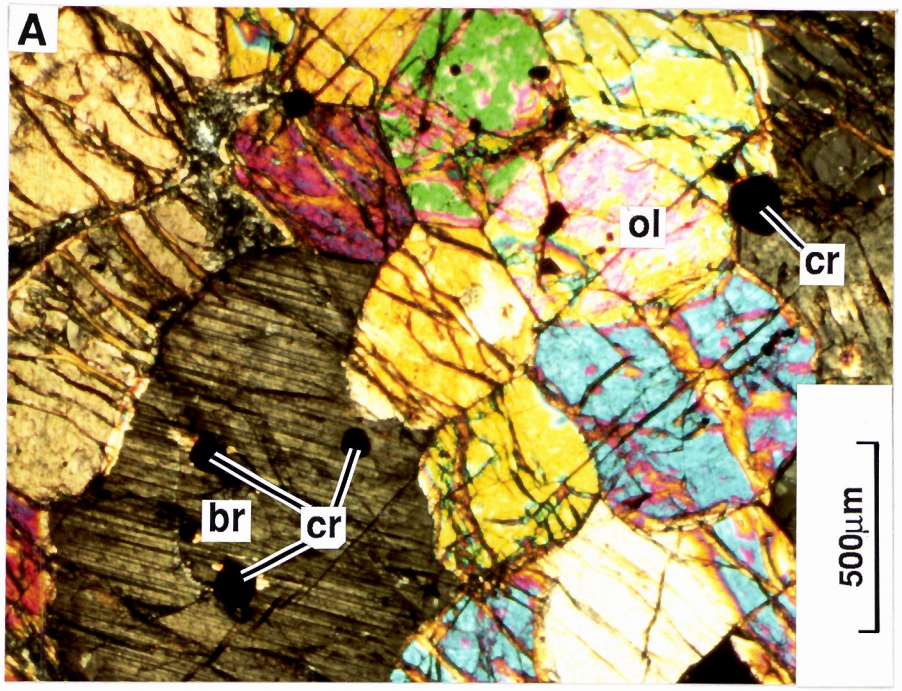
A
ol
cr
br
cr
500µm

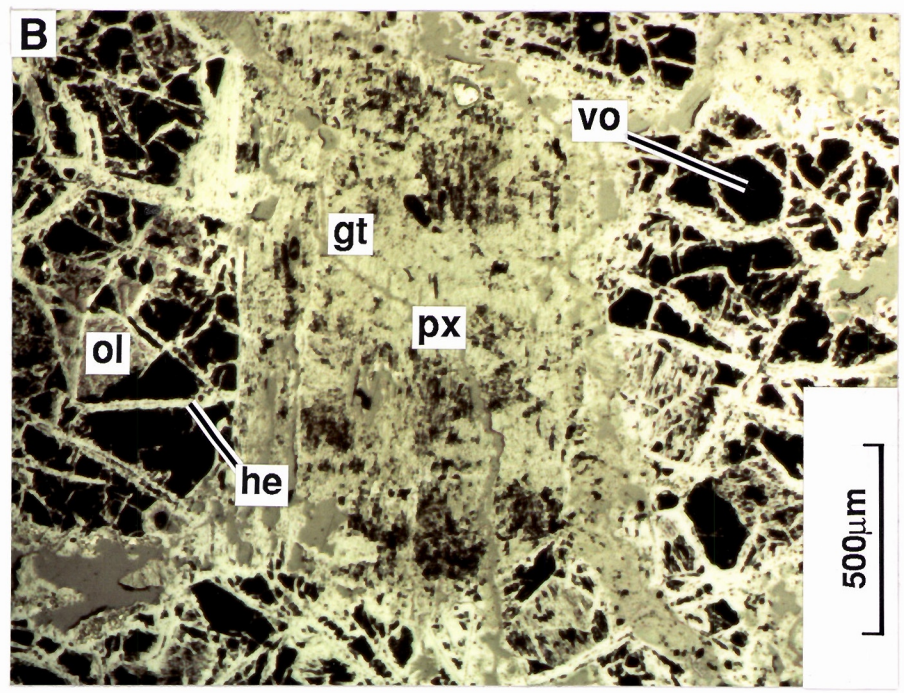
B
vo
gt
px
ol
he
500µm

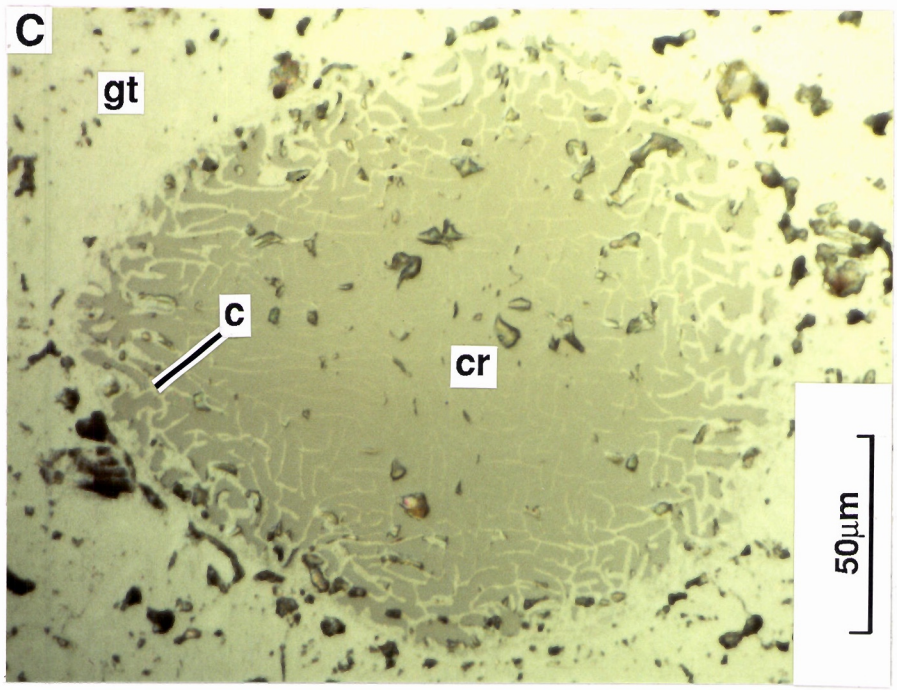
C
gt
c
cr
50µm

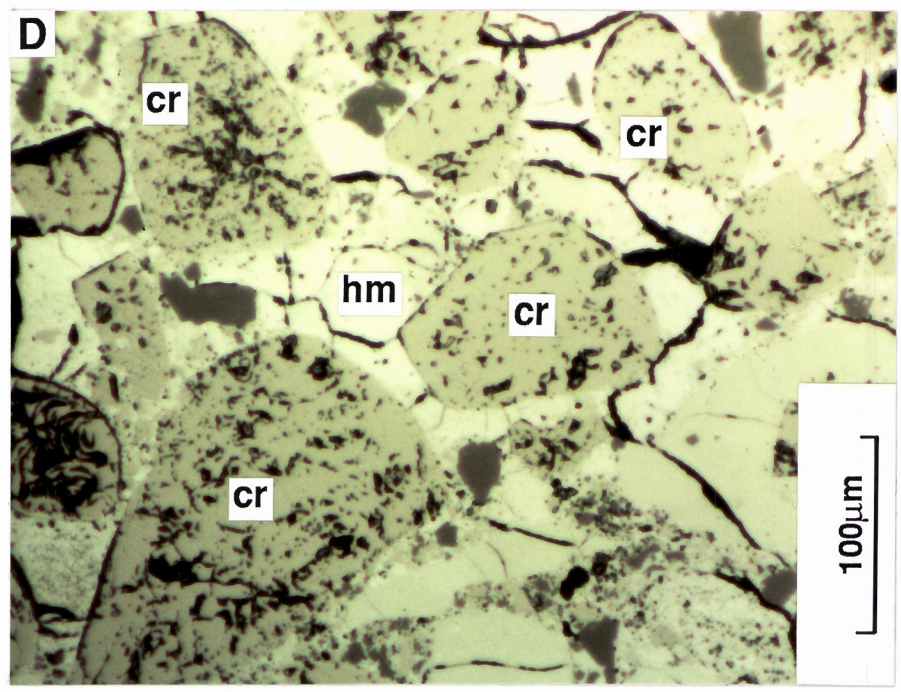
D
cr
cr
hm
cr
cr
100µm

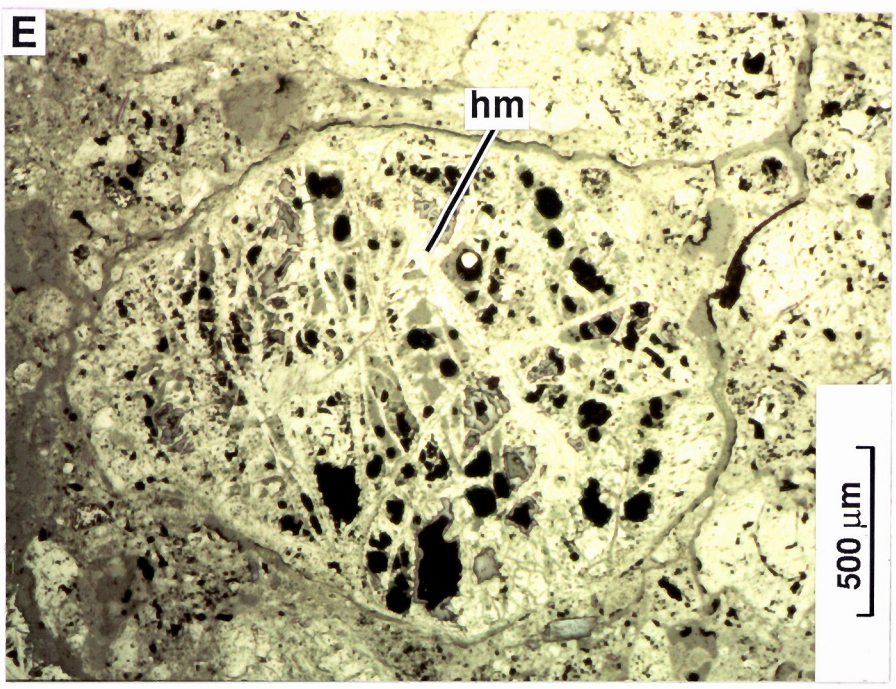
E
hm
500 µm

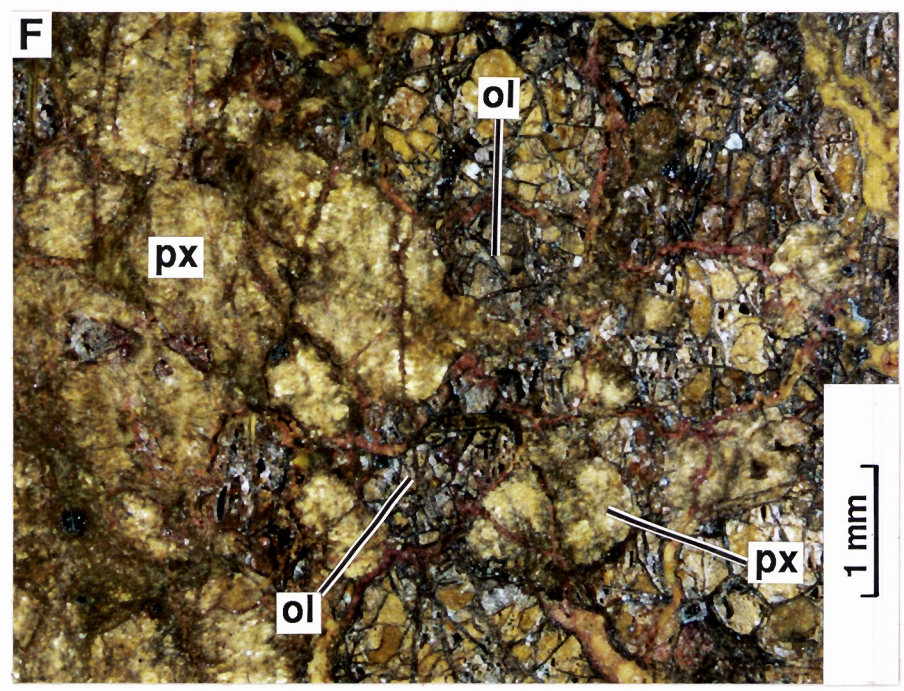
F
ol
px
ol
px
1 mm

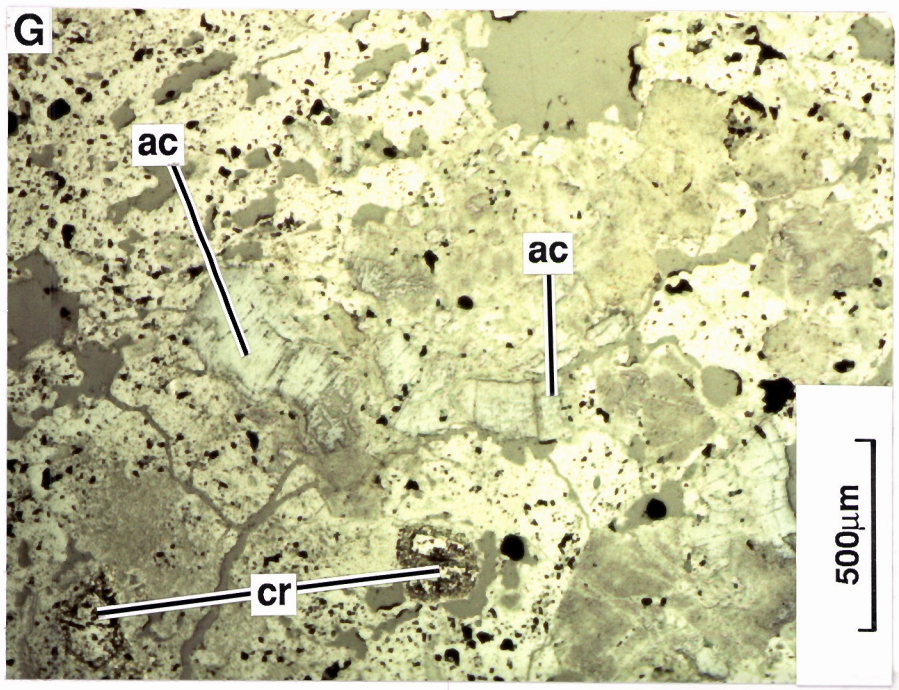
G
ac
ac
cr
500µm

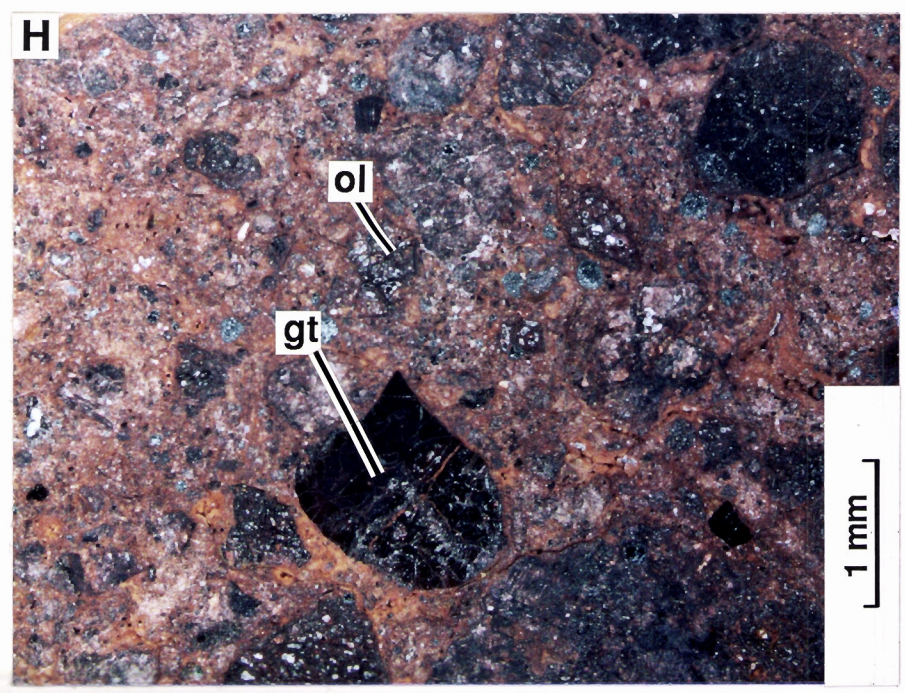
H
ol
gt
1 mm

Figure 20. Fabrics of pyroxenite , Unit 5 duricrust and derived lag (see over page)

A. Crystals of fresh olivine (ol) and amphibolitized pyroxene (px) with a few ragged crystals of chromite in a pyroxenitic rock from the base of the bronzite cumulate (see Witt and Barnes, 1991). Thin section photomicrograph - crossed polarizers. Specimen from diamond drillhole OBD1, down hole depth 98.0 m.

B. A pyroxene cleavage (pc) perfectly preserved in goethite. Lag overlying pyroxenitic rocks and Unit 5 duricrust. Polished section photomicrograph. Specimen 08-1499. Co-ordinates 12502E 10424N.

C. A wavy layer silicate fabric (ls) after either vermiculite or smectite, now preserved in goethite. Lag overlying pyroxenitic rocks and Unit 5 duricrust. Polished section photomicrograph. Specimen 08-1522. Co-ordinates 12601E 10397N.

D. Goethite pseudomorph after pyroxene or amphibole cleavage. Lag overlying pyroxenitic rocks and Unit 5 duricrust. Polished section photomicrograph. Specimen 08-1527. Co-ordinates 12601E 10150N.

E. Unit 5 duricrust. Lithorelics of ferruginized pyroxenite (px) which has been partly dissolved. The cavities have been filled with two oolitic phases of goethitic clay. The earlier ooliths (p1) are cemented by goethitic clay and the later ooliths (p2) by hematite. Close up photograph of polished section - oblique reflected light. Specimen HMC-OB12A. Co-ordinates 12600E 10250N.

F. Unit 5 duricrust. An early cavity filling of iron-stained, clay-rich ooliths (p1) with a later cavity filled with ooliths coated and partly cemented by goethite (p2). Polished section photomicrograph. Specimen HMC-OB6B. Co-ordinates 12500E 10375N.

G. Unit 5 duricrust. Larger talc-filled shears (ts) and fine-scale pyroxene or amphibole cleavage (pc) preserved in hematite. Polished section photomicrograph. Specimen HMC-OB5C. Co-ordinates 12500E 10275N.

H. Unit 5 duricrust. Lithorelics of an indeterminate fabric that have been partly dissolved to form cavities now infilled with clay-rich ooliths set in an iron-rich clay cement. A few vesicles remain unfilled. Close up photograph of polished section - oblique reflected light. Specimen HMC-OB6A. Co-ordinates 12500E 10375N.

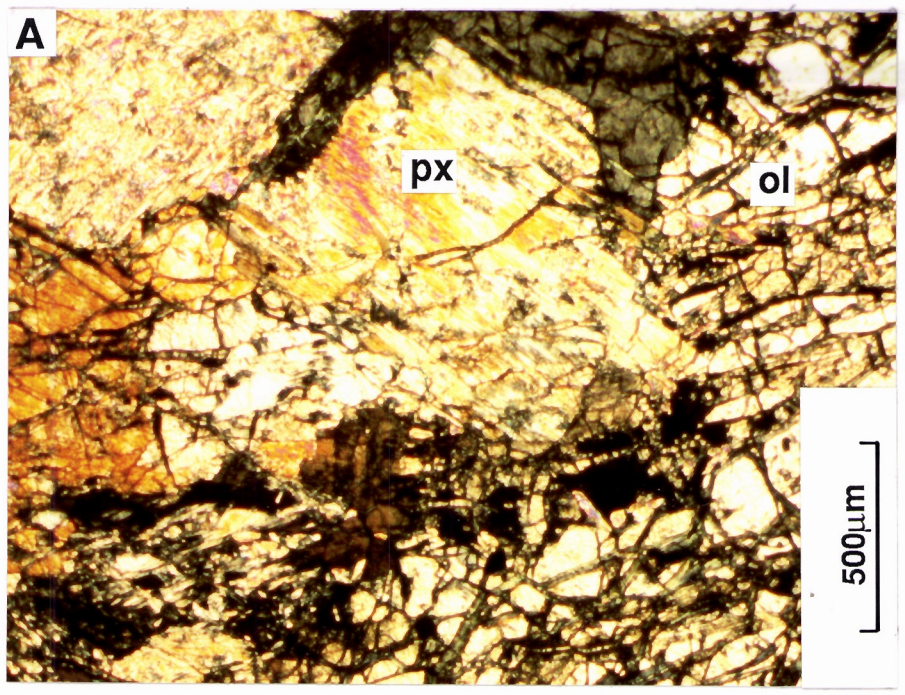
A
px
ol
500µm

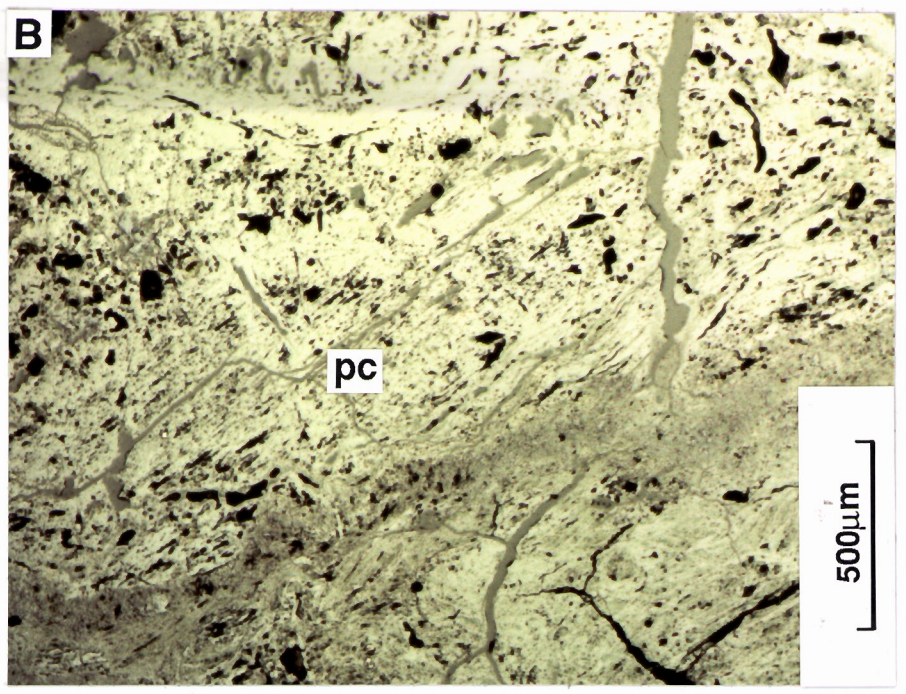
B
pc
500µm

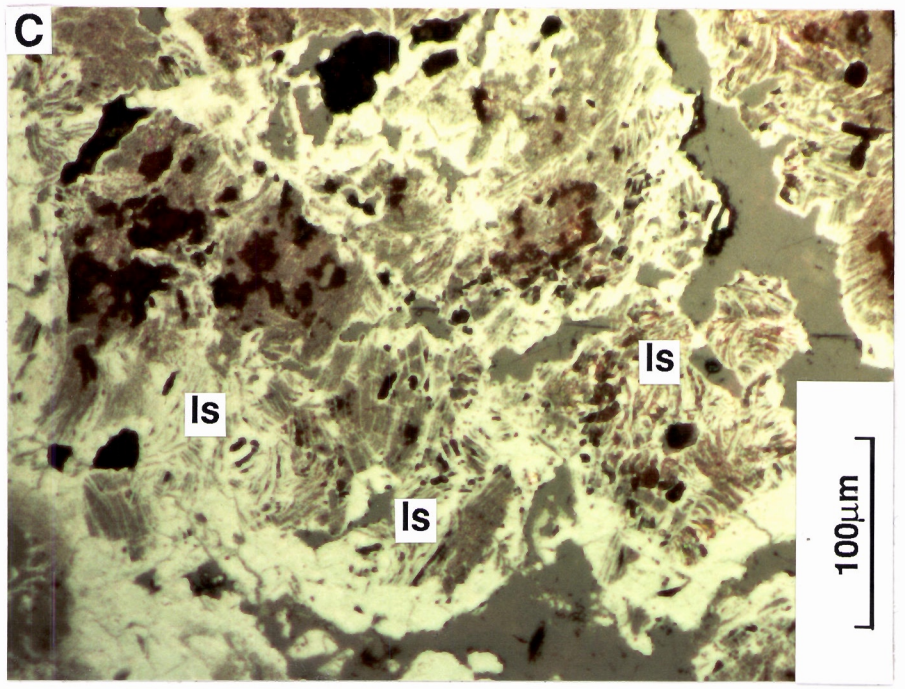
C
ls
ls
ls
100µm

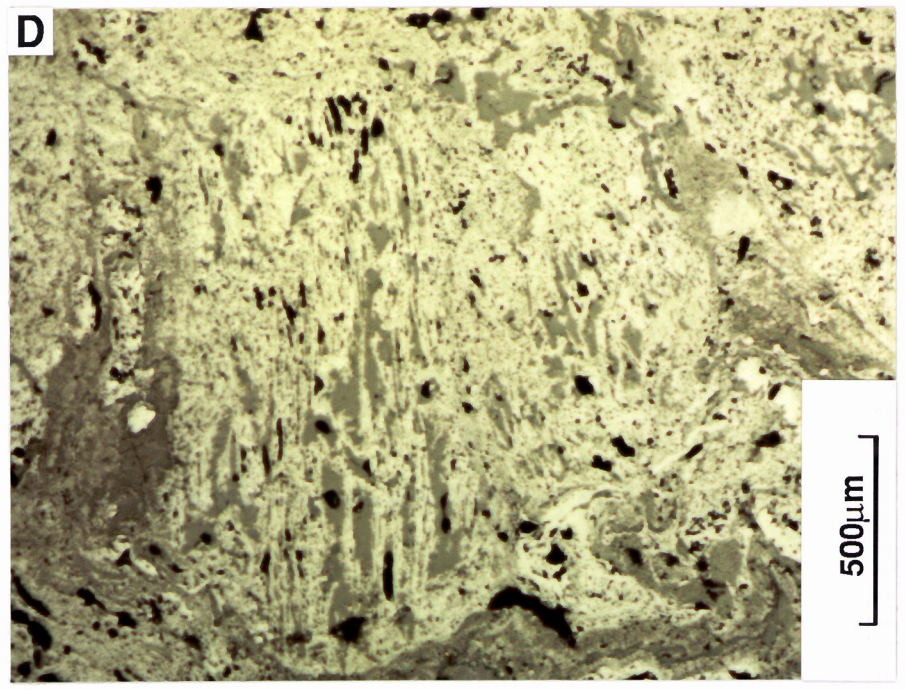
D
500µm

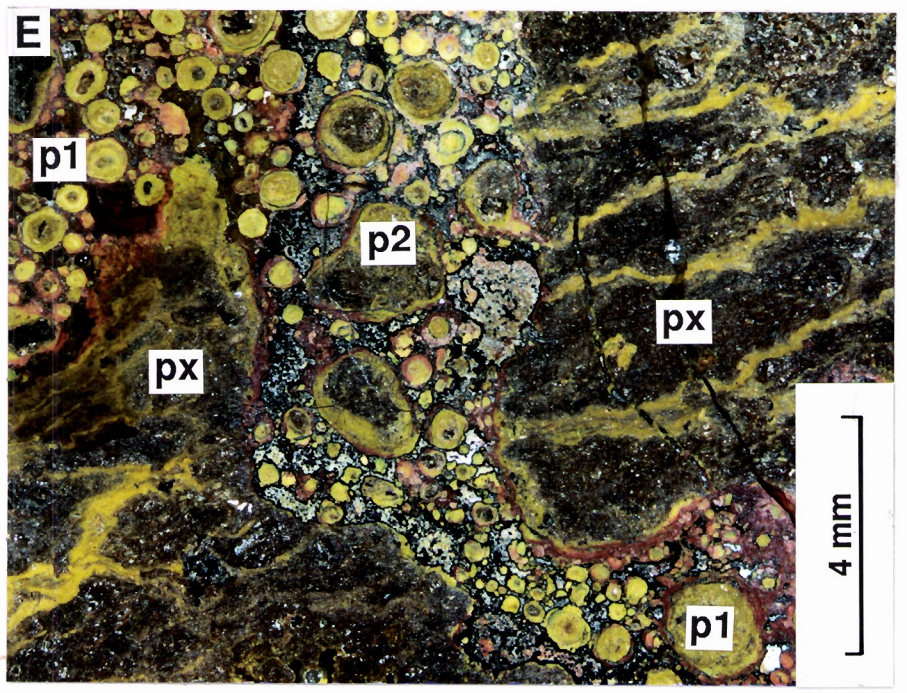
E
p1
p2
px
px
p1
4 mm

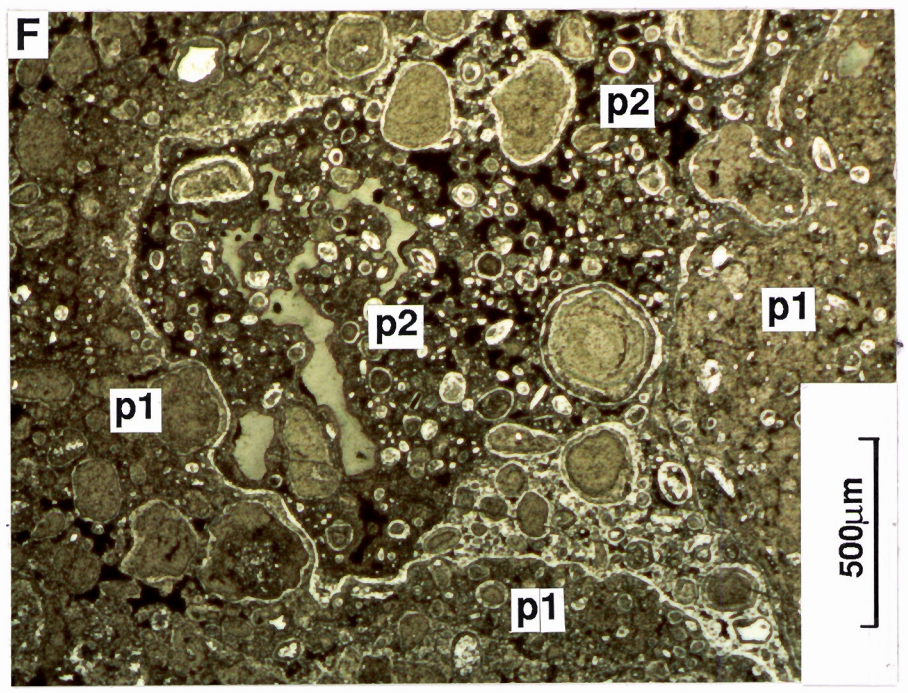
F
p2
p1
p2
p1
500µm

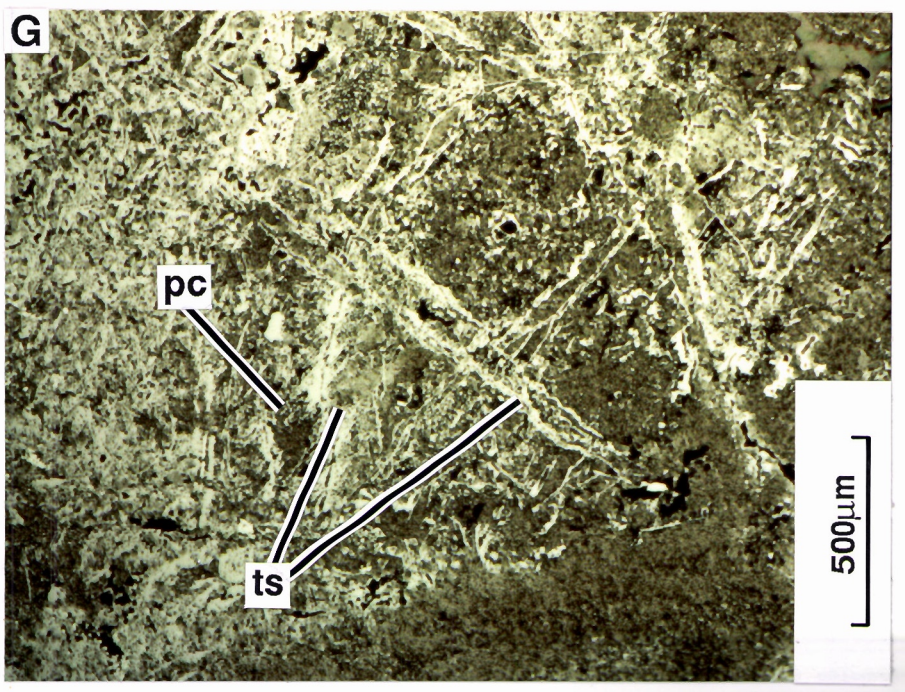
G
pc
ts
500µm


H
2 mm

6.0 GEOCHEMICAL DISPERSION IN THE REGOLITH.

6.1 Introduction

The distributions of each element in the regolith along the drill section are shown as symbol plots in Appendix I; in addition, the Pt and Pd data are also shown in Figures 21-25 as "histogram" plots. The plotting intervals for the former were selected on the basis of the principal populations evident in histograms and cumulative frequency graphs of the whole data set. For clarity, the data for each element are shown in three contiguous plots - south, centre and north. In the text, elements having similar geochemical affinities are discussed together. Comparative statistical data for each group of elements in the main regolith horizons over the peridotites and pyroxenites are given in Tables 1 to 5, Appendix II. The data are listed in full in Appendix IV. It should be noted that in the following discussions, "enrichment" and "depletion" are apparent terms, based on mass concentration data. The description is adequate in the saprolite, in which weathering has been largely isovolumetric but, in overlying horizons, this does not apply, so that apparent enrichment of a component may occur because it is less strongly leached than other components. Corrections may be applied by assuming certain components to be evenly distributed in the parent rock and immobile during weathering.

Element and ignition loss distributions shown by the lag on the three traverses are plotted in Appendix VI and the data listed in Appendix X. The data for Pd, Pt, Cu, Cr and Ni are also displayed as contour plots in Appendix VII. All data for La and Rb are below the detection limits (50 and 5 ppm respectively) and the Ge and Nb data are marginal. The frequency distributions for the lag data (Appendix IX) show that Ti, Ce, Ga, Se, Y, Zn and Zr have approximately normal distributions, suggesting that they may not be useful for distinguishing between different rock or lag types. For the other elements, bimodal (Fe, Mn, Co, Cr, Mn), polymodal (Si, Al, S, LOI, Ba, Pd, Pt, Sr) and positively skewed (Mg, Ca, Na, K, P, Cu, Ni, Pb, V) distributions are apparent and some of these may be characteristic of specific rock or lag types or of mineralization. Correlations of the raw (untransformed) data are given in Appendix VIII. Interpretation of the lag geochemistry needs to account for the influence of lithology and the position in the profile. Thus, type C lag is present over pyroxenite and is derived from a well-developed duricrust horizon whereas type A lag occurs over peridotite and may be derived in part from pre-existing laterite and mottled zone, and in part from saprolite.

6.2 Elements related to PGE mineralization: Pt, Pd, Rh, Ru, Os, Ir, Cu, S

These elements are commonly associated in PGE mineralization in layered complexes and are considered together, although the association is only tenuous at this site. The data for Pt, Pd, Pt% and Pt+Pd are shown in Figures 21-25 and, for Pt, Pd, Cu and S, as symbol plots in Appendix I. Comparative statistical data for these elements in the main regolith horizons over each lithology are given in Table 2, Appendix II. The data for the lag on the traverses are plotted in Appendix IV and as contour plans in Appendix VII.

Platinum and palladium. The Pt and Pd data were derived from analyses obtained by Carbine Gold NL. Unfortunately, it has not been possible to retrieve the individual Pt and Pd analyses for the northern part of the drill section and only total Pt+Pd has been plotted. The principal features of the distribution of these elements in the regolith are as follows:

1. The overall abundances in the regolith reflect the primary distributions, namely that weathered pyroxenites are PGE-rich in comparison with equivalent horizons of weathered peridotite. This can be deduced from the distribution plots for Pt+Pd but is not immediately evident from the statistical data in Tables 2, Appendix II because of the absence of individual Pt and Pd analyses for the northern part of the section. Most of the

tabulated data for peridotite are derived from RAB holes OB 19 to 21 in which primary enrichment close to the contact is subcropping, resulting in high PGE concentrations in surface horizons.

2. There is marked enrichment in both elements upwards through the regolith, with maxima in the ferruginous clays, lateritic horizons and calcareous lateritic soils over the pyroxenites and in calcareous soils and saprolites on the peridotites (lateritic horizons being absent over this lithology). The peak value in the majority of profiles is at the surface, in the soil, exceptions being holes OB 20 and 21 in which there are highly enriched samples in the saprolite, probably reflecting primary concentrations (see 4, below), and in OB 24 and 25, where peak enrichment is at the base of the lateritic duricrust. Maximum concentrations of 800-1150 ppb Pt+Pd occur in the south (holes OB 29 to 32), where the mean enrichment in the lateritic horizons and derived soils, represent a concentration factor of three- to four-fold, relative to the primary abundance in the pyroxenite. This surface enrichment may simply reflect residual concentration as an immobile element, but it is possible that some of the surface enrichment is due to an association with pedogenic carbonate, as noted for gold in this region (Butt *et al.*, 1991). The data from carefully handpicked material are equivocal, since enhancement of the PGE contents is relatively minor (Table 6) and chemical extraction does not indicate preferential leaching from the calcareous fraction (see Volume III, Chapter 6, Section 2). Nevertheless, there are significant enhancements of Pt and, particularly, Pd in the calcareous fractions of surficial lateritic materials, compared to the whole sample of the ferruginous fraction, and a consistent decrease in the Pt/(Pt+Pd) ratio (Pt%).

TABLE 6
Platinum and palladium contents of fractions of calcareous surface samples

Hole	Depth m	Rock	Horizon	Material	CaO %	Fe %	Pd ppb	Pt ppb	Pt/Pt+Pd %
OB 212	3	Po	Saprolite	Whole	11.3	10.0	185	120	39.3
				Carbonate	23.9	2.18	205	130	38.8
OB 23	2	Px?	Nodular soil	Whole	6.58	18.7	290	450	60.8
				Carbonate	22.8	2.52	550	650	54.2
OB 24	1	Px	Laterite	Whole	8.67	17.6	31	110	78.0
				Carbonate	27.6	2.67	150	270	64.3
				Ferruginous	0.16	30.2	12	92	88.5
OB 25	1	Px	Laterite	Whole	7.16	19.3	58	190	76.6
				Carbonate	18.1	7.50	90	190	67.9
OB 26	1	Px	Laterite	Whole	19.9	8.5	88	260	74.7
				Carbonate	24.8	3.62	84	195	69.9
OB 27	1	Px	Laterite	Whole	10.8	12.7	80	285	78.1
				Carbonate	18.3	10.1	90	290	76.3
				Ferruginous	nd	nd	52	455	89.7

3. The mean Pt/(Pt+Pd) ratio (Pt%) of unweathered rocks is approximately 45% in peridotite and 63% in pyroxenite although, towards the base of the pyroxenite, the ratio declines to 50-55% in many samples. This difference is maintained in the regolith, particularly comparing the pyroxenites in the south of the traverse with the peridotites towards the north and the relationship appears to distinguish the two lithologies reliably. The values of 30-50% in most samples in holes OB 19 to 23 indicate that these are probably derived from peridotite, as corroborated by multivariate analysis (Section 8.3.3) and analyses of chromites.

Inspection of the data from holes OB 24-29 (Appendix IV and Figures 22 and 24) suggests that there is an upward increase in Pt%, with the highest values (75-88%) in the PGE-enriched horizons (mottled clay, lateritic duricrust and derived soil) developed from the pyroxenite (see also Table 7). Such an increase is expected, due to preferential leaching of Pd, and greater values still are found in the lag derived from these duricrusts (see 6, below). This may be due either to further chemical reworking during lag formation or carbonate precipitation (see 2 above), or because Pt is preferentially concentrated in those components of the duricrust, such as the most ferruginous nodules, that comprise the lag. Chemical studies (Volume III, Chapter 6, Section 5.6) have indicated that Pt is strongly associated with Fe oxides in the regolith and therefore is immobile, whereas Pd is located in a slow-weathering phase and may be leached as this phase is weathered. However, it is evident from the diamond drill core, and from samples of the deep saprolite, that fresh and partly weathered pyroxenite may have Pt% values of 75-85%, though usually in rocks containing < 150 ppb Pt and < 40 ppb Pd, so that a high ratio is not unequivocal evidence for loss of Pd.

TABLE 7
Platinum group metal concentrations of enriched zones intersected in RAB holes OB 19, OB 20 and OB 21, and possible source intervals in diamond hole DDH1.
(Analysis by fire assay, NIS collection)

Hole or sample n	Depth m	Lithology	Pt ppb	Pd ppb	Pt%	Ru ppb	Rh ppb	Os ppb	Ir ppb
OB 19	**0- 1**	**Po**	**250**	**640**	**28**	**20**	**10**	**2**	**4**
OB 19	**1- 2**	**Po**	**270**	**500**	**35**	**22**	**9**	**2**	**4**
OB 19	**2- 3**	**Po**	**300**	**440**	**41**	**22**	**11**	**2**	**2**
OB 19	**3- 4**	**Po**	**215**	**320**	**40**	**20**	**13**	**4**	**4**
OB 19	5- 6	Po	185	255	42	26	26	4	4
OB 20	16-17	Po	200	240	45	16	19	4	2
OB 20	**17-18**	**Po**	**820**	**440**	**65**	**34**	**49**	**2**	**10**
OB 20	19-20	Po	44	118	27	16	9	2	2
OB 20	20-21	Po	70	106	40	16	12	2	2
OB 21	24-25	Po	46	116	28	16	10	2	2
OB 21	25-26	Po	120	180	40	18	18	2	6
OB 21	**26-27**	**Po**	**1800**	**1200**	**60**	**52**	**114**	**6**	**20**
OB 21	27-28	Po	82	135	38	18	14	2	4
DDH 1									
00-5445	105.5-106.0	Px	130	78	63	4	7	4	2
00-5446	106.0-106.2	Px	8	8	50	4	2	2	1
00-5447	**106.2-106.5**	**Px**	**420**	**360**	**54**	**8**	**15**	**6**	**4**
00-5448	106.5-106.7	Po	170	118	59	6	11	4	2
00-5449	106.7-107.0	Po	22	22	50	6	3	2	2
00-5497	126.9-128.0	Po	28	14	67	8	5	4	-
00-5498	141.0-142.0	Po	46	56	45	10	5	4	-

Bold type indicates enriched zones

4. There are intersections of strongly PGE-enriched units in three RAB holes, OB 19-21, close to the pyroxenite-peridotite contact. Re-analysis confirmed these enrichments, which are confined to one-metre intervals in OB 20 and 21, but occupy 3 m in OB 19 (Table 7). These appear to define a continuous "stratigraphic" unit, sub-parallel to the inferred pyroxenite-peridotite contact. However, whereas the minor PGE (Ru, Rh and Ir) are relatively enriched in holes OB 20 and 21, they are not in OB 19. In addition, Pt% is similar in the enriched samples in OB 20 and 21 (65%, 60%), but <50% in the almost all other samples in these holes. No similarly PGE-rich interval was intersected by the diamond drill holes. These data suggest, therefore, that some minor PGE concentrations are present in the sill but that they either form discontinuous lenses or have been cut out by faults associated with the contact. The low abundances of the minor PGE at the surface in OB 19 may indicate that this enrichment reflects generally higher Pt+Pd abundances in bedrock, rather than a specific "mineralized lens".

5. The minor PGE (Ru, Rh, Os, Ir) were determined to provide background data on their distribution in lateritic regoliths. Each shows upward concentration through the regolith (Table 8) although Os and Ir are at such low abundances in the pyroxenite (at the detection limit (2 ppb)) that the data must be considered semi-quantitative at best. The highest contents occur in the ferruginous horizons (mottled clay zone and laterite) and are probably due to residual accumulation as immobile elements. The enrichment is of the same order as for Cr, Zr and Cu that also appear to be immobile in this environment. Similar results were obtained at Mt. Carnage (Table 9), where the abundances of all these elements other than Os are greater. The degree of enrichment of the PGE in these profiles, however, is rather lower than the factors of 10-15 reported by Travis *et al.*, (1976) from a profile on serpentinized dunite at Gilgarna, near Kalgoorlie (see Volume I, Chapter 2). There, concentrations of 20-25 ppb Pd and 30-32 ppb Ir occur in the ferruginous horizon. The enrichment is ascribed to very strong leaching of the major elements, but the Ir content is exceptionally high.

TABLE 8
Platinum group elements in a complete laterite profile developed on pyroxenite (hole OB 27). (Analysis by fire assay, NIS collection)

Depth m	Horizon	Pt ppb	Pd ppb	Pt/Pt+Pd %	Ru ppb	Rh ppb	Os ppb	Ir ppb
1	Calcareous laterite	285	80	78	6	14	2	2
3	Laterite	440	124	78	8	26	4	4
5	Mottled clay	310	82	79	8	16	4	4
9	Mottled clay	170	52	77	8	17	4	6
14	Saprolite	145	64	69	4	7	2	2
20	Saprolite	215	82	72	4	10	2	2
25	Saprolite	300	98	75	4	10	-	2
30	Saprolite	145	84	63	6	9	4	2
35	Saprolite	116	70	62	4	8	2	2
40	Saprolite	150	90	62	4	10	2	2

6. In lag, the Pt and Pd contents clearly indicate the enrichment of these elements in the laterite overlying the pyroxenite. On line 12500N, maximum Pt and Pd concentrations occur at the southern end of the traverse by holes OB 31 and 32 (Figure 26). The Pt enrichment extends about 70 m downslope from the duricrust at OB 23 (10400N), which is presumed close to the pyroxenite-peridotite contact, to the creek at OB 20. The lag in this

zone is noted as being of mixed provenance (type B), which is consistent with this interpretation. The relative depletion of Pd compared to Pt from lag derived from the laterite is evident between 10200N and 10400N; Pd contents increase in the mixed lag, with a local maximum at 10500N (100 ppb) corresponding to the enrichment found in the top few metres of OB 19 (Table 7).

Copper. The Cu distribution in the regolith reflects the abundances in the unweathered rock, although strongly influenced by the nature of the regolith itself. Thus, Cu content in the regolith developed on the peridotite is commonly <30 ppm, with a few higher values in soils close to the contact with the pyroxenites - particularly where these may contain lag derived from the lateritic duricrust. In comparison, all regolith units on the pyroxenites have Cu contents >200 ppm and concentrations increase upwards through the saprock (mean 205 ppm) and saprolite (mean 315 ppm), reaching maxima of 700-1095 ppm in the saprolitic and mottled clays and the lower (nodular) horizon of the laterite. Some narrow intervals in the fresh pyroxenite contain >3000 ppm Cu, but these are not recognized in the weathered zone, although not all sample intervals were analysed. The highest Cu concentrations form an approximately sub-horizontal zone of enrichment and are thus attributed to secondary accumulation with Fe oxides, a phenomenon observed elsewhere over ultramafic rocks containing disseminated sulphides (Butt and Nickel, 1981) and attributed in part to the tendency for Cu to catalyse the oxidation of ferrous iron and coprecipitate with Fe oxides (Thornber and Wildman, 1979). Higher in the profile, the Cu content declines, presumably due to leaching during the further evolution of the lateritic duricrust and, ultimately, soil formation. Some of the leached Cu may contribute to the underlying enrichment. The Cu distribution is accordingly similar to those of Fe, with which it is associated, and Al, which also concentrates in the lateritic horizons, as gibbsite and in aluminous goethite and hematite.

The Cu distribution shown by lag sampling clearly distinguishes pyroxenite and peridotite, with concentrations of 400 ppm to over 1000 ppm reflecting similar enrichments in the lateritic duricrust over the pyroxenites. There is a close correlation between Cu and Pt and, on line 12500N, high Cu concentrations, like those of Pt, extend downslope across the peridotite in the zone characterized by the mixed lag.

Sulphur. Sulphur in the unweathered rocks is present principally as disseminated sulphides, with concentrations rarely exceeding 1%. Sulphides are commonly some of the first minerals to alter during weathering, with S being leached. This is evident at Ora Banda, where saprolite is generally contains $<0.03\%$ S. Sporadic higher concentrations, to $>1\%$ S, in some laterites and soils over the pyroxenites, are probably due to gypsum.

6.3 Major elements: Si, Fe, Al.

Comparative statistical data for these elements in the principal regolith horizons over the two lithologies are given in Table 1, Appendix II. These elements commonly form the principal residual products of deep chemical weathering, occurring as oxides (*e.g.*, goethite, hematite, maghemite, gibbsite, quartz, hyalite), or as aluminosilicates (*e.g.*, kaolinite, halloysite) following the alteration of primary silicates and carbonates and the leaching of other components, particularly the alkalis and alkaline earth elements. Silicon, Fe and Al tend to show minor residual enrichment in the saprolite and further remobilization causes the concentration of one or more of them in the upper horizons although, due to closure, the abundances and distributions are generally interdependent. At Ora Banda, leaching is incomplete in the saprolite and the magnesian smectite, saponite, is the dominant clay mineral, so that residual enrichment of Si, Fe and Al is only minor below the lateritic and mottled zones of the profile.

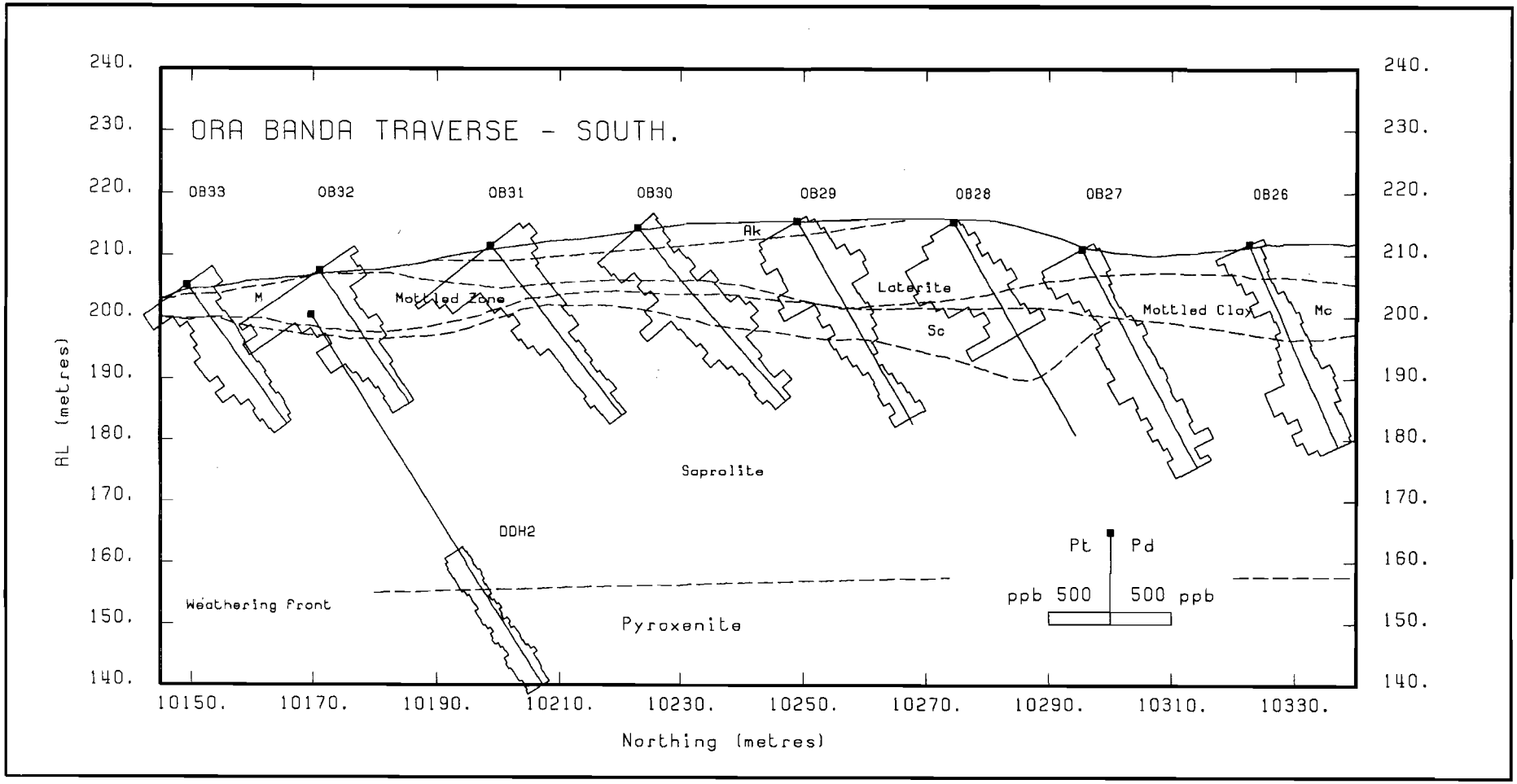

Figure 21. Distributions of platinum and palladium in the regolith, Ora Banda traverse south. Data from Carbine Gold N.L.

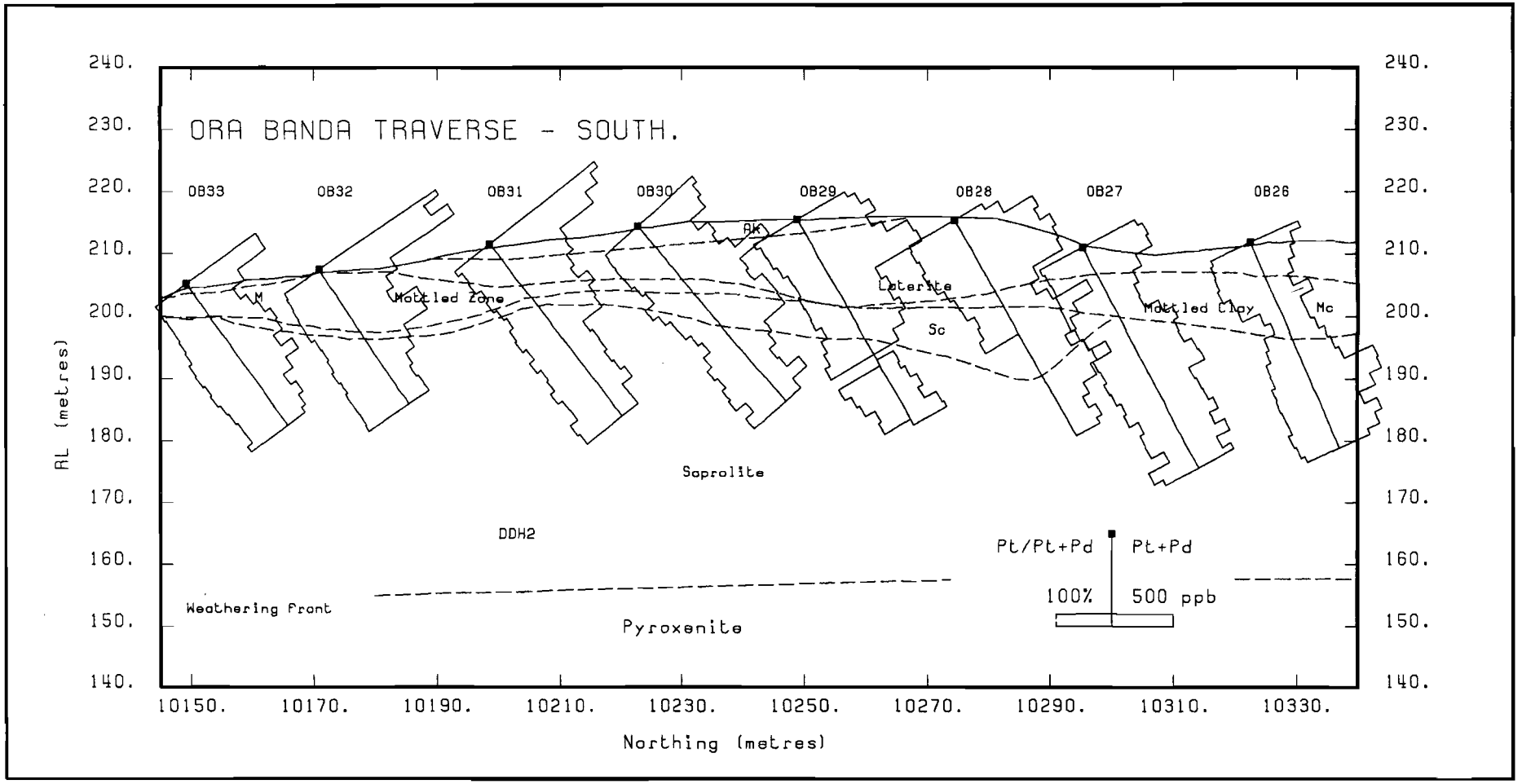

Figure 22. Distributions of platinum ratio (Pt/Pt+Pd%) and total platinum plus palladium in the regolith, Ora Banda traverse south. Data from Carbine Gold N.L.

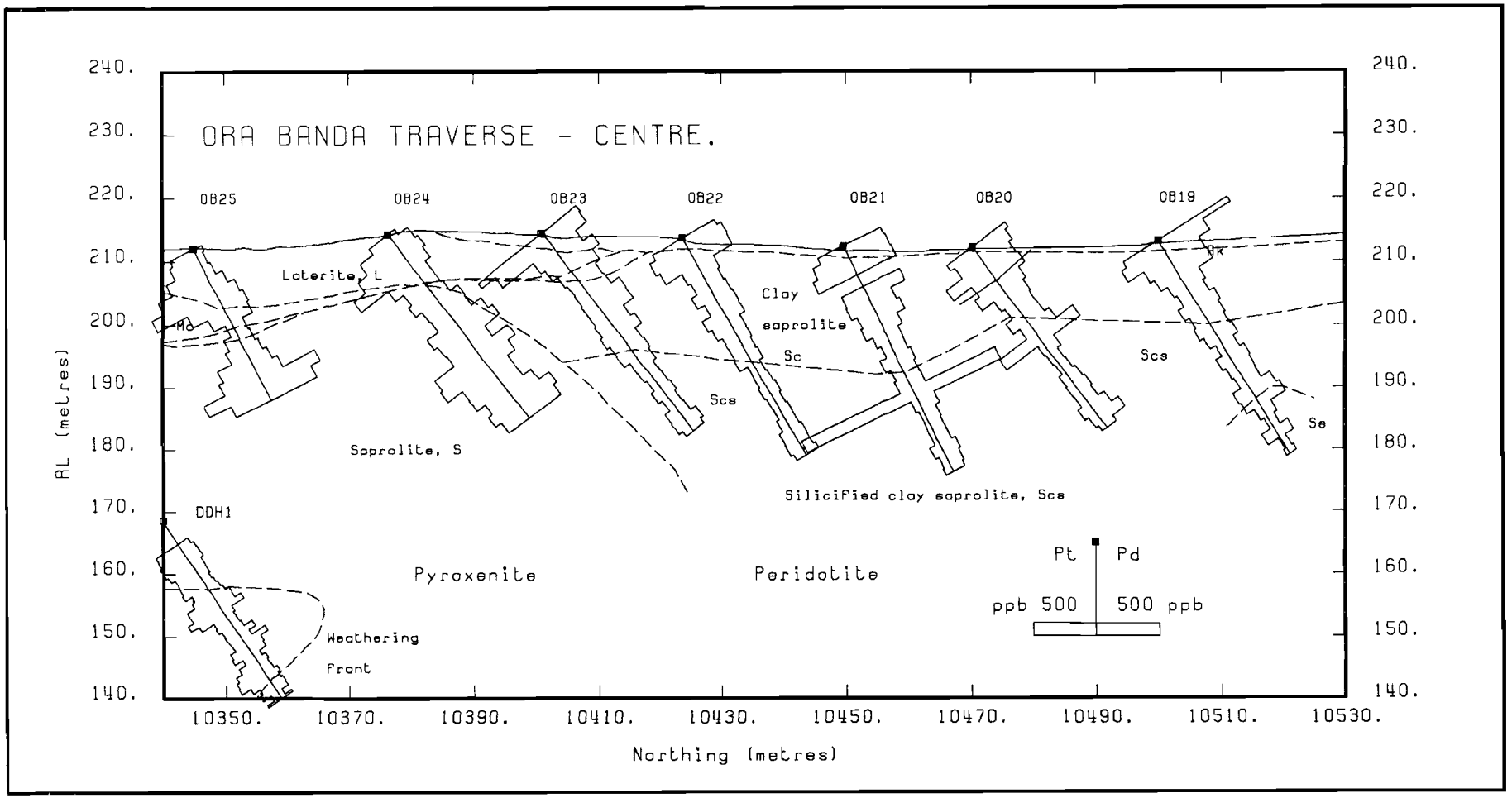

Figure 23. Distributions of platinum and palladium in the regolith, Ora Banda traverse centre. Data from Carbine Gold N.L.

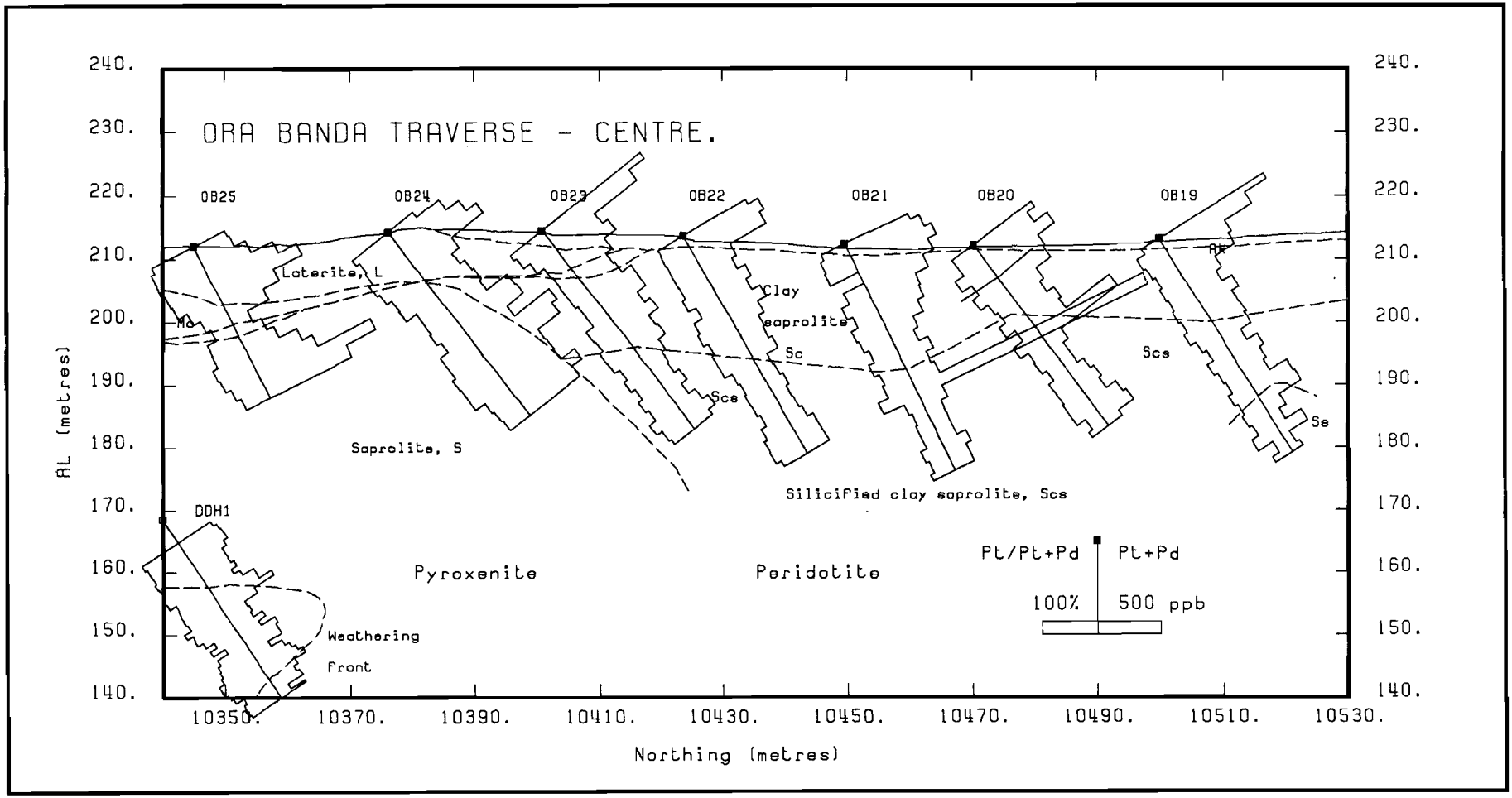

Figure 24. Distributions of platinum ratio (Pt/Pt+Pd%) and total platinum plus palladium in the regolith, Ora Banda traverse centre. Data from Carbine Gold N.L.

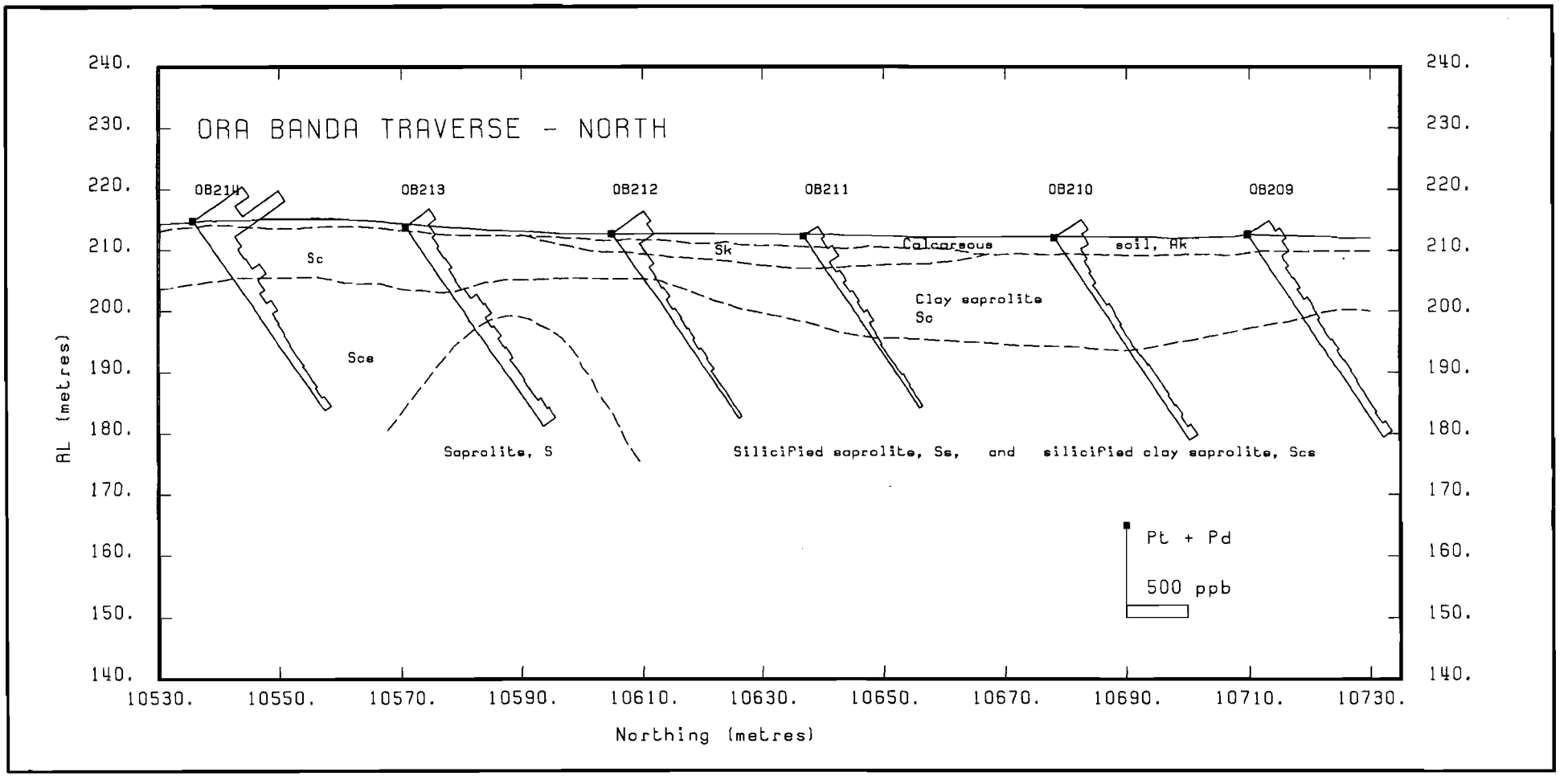

Figure 25. Distributions of platinum ratio (Pt/Pt+Pd%) and total platinum plus palladium in the regolith, Ora Banda traverse north. Data from Carbine Gold N.L.

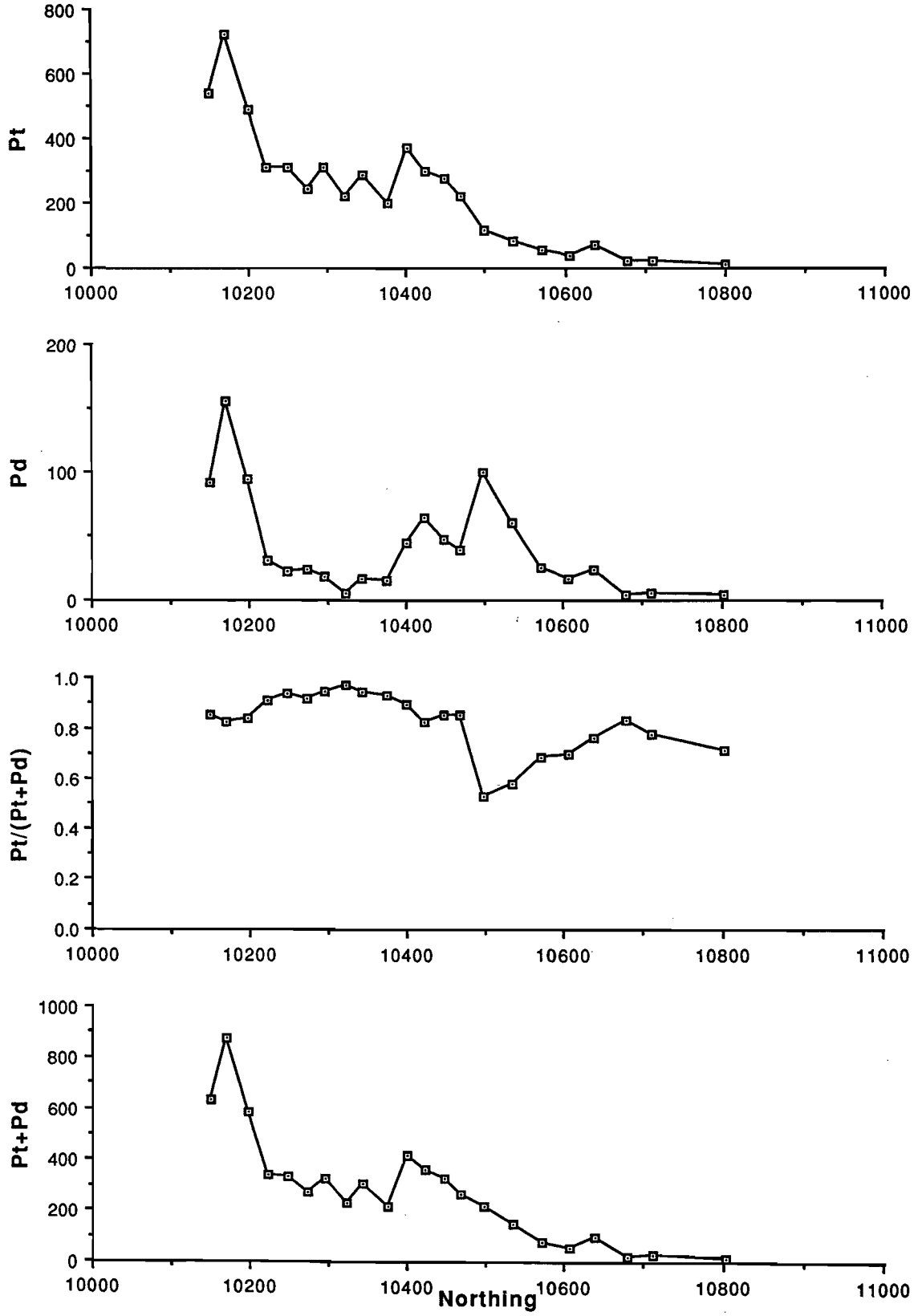

Figure 26. Distributions of platinum, palladium, platinum ratio (Pt/Pt+Pd%) and total platinum plus palladium on traverse 12500E shown by lag sampling.

The greatest concentrations of Fe (>80% Fe_2O_3) occur in the hematite- and maghemite-rich Type A lag and Fe-rich duricrusts over peridotite. Conversely, the type C lags on pyroxenite are richer in Si and Al than the type A lags, indicating that in addition to aluminous goethite and hematite, kaolinite is an important component of the former, although it is poorly crystalline. In a ternary diagram (Figure 27), the black type A lag plots close to the Fe_2O_3 apex whereas the yellow-brown type C lag plots closer to the Al_2O_3 apex. This is identical to the relationship noted by Robertson (1989, Figure 12) between the coarse, black lags and the khaki lag at Beasley Creek; the former is regarded as derived from saprolite and the latter from duricrust. The type B lag, as expected, is intermediate between types A and C. The Fe-rich duricrust is compositionally very similar to the type A lag, as indicated by the petrography. Ignition loss (LOI) is due largely to lattice water and very minor carbonate CO_2. Thus it is directly related to the contents of goethite (α-FeO.OH) and kaolinite ($Al_2Si_2O_5(OH)_4$) and inversely related to the unhydrated Fe oxides, hematite and maghemite. Consequently, type C lag is more hydrous than the type A lag. There is also a very strong correlation between LOI and S which is unexplained. The LOI exceeds S by nearly 2.5 orders of magnitude, so it is not due to gypsum.

Iron in the unweathered rocks is hosted mainly by the ferromagnesian minerals, principally pyroxene and olivine. The amount associated with sulphides is negligible. Both parent lithologies are relatively Fe-rich and this is reflected in the regolith, with mean concentrations in all horizons exceeding 10%. There is minor residual enrichment of Fe in the saprolite but it becomes strongly concentrated in the mottled clay horizon and, over the pyroxenite, the lower nodular horizon of the laterite (24-36% Fe), due to the almost total loss of Mg and Ca, and the apparent partial leaching of silica. The maximum concentrations are comparable to those on ultramafic rocks elsewhere, such as the talc chlorite carbonates of the Hannan's Lake serpentinite at Mt. Percy, although the latter have rather lower initial Fe contents (6.5%) than the pyroxenites (12.2%) (Butt, 1991). The upper part of the laterite and the overlying soil have lower Fe contents, due partly to higher Al contents and partly to dilution by calcrete.

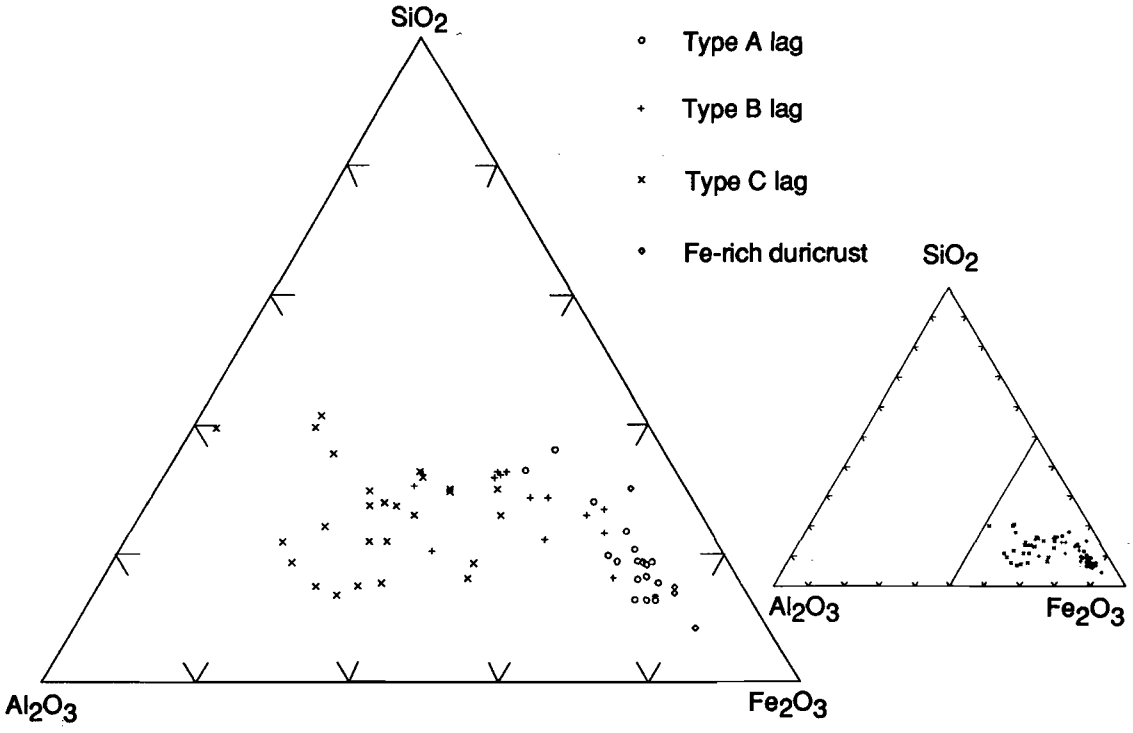

Figure 27. Ternary SiO_2-Al_2O_3-Fe_2O_3 diagram illustrating the compositions of lag and Fe-rich duricrust.

Silicon occurs in ferromagnesian and alumnosilicate minerals in the unweathered rocks; there is essentially no quartz. The silica content of the pyroxenites (mean 53.8%) is, as expected, higher than that of the peridotites (42.6%), but this is not reflected by the composition of the regolith. Over the pyroxenites, there is a marked depletion in silica upwards through the profile, with particularly low concentrations (<20%) in the ferruginous horizons. This decrease in silica content is largely due to leaching, following the weathering and/or replacement of saponite by Fe oxides, and partly due to dilution of residual silica, again by Fe oxides. In contrast, over the peridotites, there is an increase in silica in the saprolite compared to the unweathered rock, manifested by the occurrence of secondary silica, including moss agate. Secondary silica occurs throughout the profile and as surface float, but is particularly abundant below about 10 m in clay-rich saprolite. (Secondary silica is a common weathering product of Al-poor ultramafic rocks, for kaolinite cannot form and thereby retain silica released from primary minerals. It is particularly abundant in regoliths developed on dunites (Butt and Nickel, 1981), where it may form massive units within the saprolite.) The increase in silica content is thus a largely residual enrichment, although possibly supplemented by absolute enrichment from silica derived by leaching from surficial horizons.

Aluminium is present at low concentrations in both lithologies, hosted by plagioclase and minor phases. The Al content is higher in the pyroxenites (mean 3.3% Al_2O_3) than the peridotites (1.8% Al_2O_3). Aluminium appears to be essentially immobile in the regolith, and shows minor (residual) enrichment in the lower horizons (approximately 1.5- to two- fold), increasing to five- to seven fold (18-23% Al_2O_3) in the ferruginous zones over the pyroxenites, where it occurs in gibbsite and aluminous goethite.

6.4 Alkaline earth elements: Ca, Mg, Sr, Ba

Comparative statistical data for these elements in the principal regolith horizons over the two lithologies are given in Table 1, Appendix II. Calcium, Mg and Sr have a number of similarities in their weathering behaviour in this environment. They tend to be leached at the onset of weathering and are almost totally depleted from some horizons of the regolith, but are reconcentrated at or close to the surface as pedogenic calcrete. In comparison, Ba is generally less mobile and is retained throughout the regolith, although there can be some minor secondary accumulation in near-surface horizons, broadly associated with the occurrence of pedogenic carbonates. The good correlation between Mg and Ca and the generally slightly greater content of Mg are consistent with the presence of chips of dolomitic calcrete and magnesite as minor (0-3%) components of the lags. Localized increases in Ca, Ba and Mg contents occur in soil in the lower ground north of the peridotite-pyroxenite contact on 12500N.

Calcium is a minor constituent in both principal lithologies. It is more abundant in unweathered pyroxenites (mean 3.04% CaO) than peridotites (2.39% CaO) and is probably hosted by pyroxenes, plagioclase, tremolite and carbonates. The Ca content declines steadily upwards through the saprolite, with minimum concentrations (<0.10% CaO) in the uppermost clay-rich saprolites and, where present, overlying ferruginous saprolites and mottled clay horizons. The decrease in Ca content is more gradual than elsewhere (*e.g.*, Mt. Percy; Butt, 1991), probably due to the relative resistance to weathering of the primary host minerals pyroxene and tremolite, compared to carbonates and feldspar, and the high buffering capacity of the mineral assemblage. However, in common with other sites, there is a marked concentration of Ca in near-surface horizons, due to the precipitation of pedogenic carbonates as diffuse enrichments in clays, coatings of coarse fragments such as nodules and pisoliths, and as indurated segregations. The carbonates (calcite and dolomite) are present in the top 3-5 m over most of the traverse, so that soils and surficial horizons, except lag, contain 1-20% Ca. The carbonates are thickest and most abundant in the lateritic units developed on the pyroxenites.

The surface enrichment of carbonate corresponds to a similar enrichment of PGE. This is best seen in the northern part of the drill traverse (Figure 25) where the regolith is truncated to the upper saprolite, but is also apparent in the lateritic horizons over the pyroxenites. The association is less pronounced than that for gold in this region and is not confirmed (see Table 6, Section 6.2).

Magnesium has a broadly similar distribution to Ca, except that concentrations are far greater in the fresh rocks (26.6% MgO in pyroxenite, 32.4% MgO in peridotite) and the relative concentration in pedogenic carbonates is less. Magnesium is hosted predominantly by pyroxene and olivine in the fresh rocks, with minor amounts in talc and tremolite. Pyroxene, talc and tremolite are retained through much of the saprolite; talc and, less commonly, pyroxene are present in soils developed on saprolite derived from peridotite. In addition, the principal secondary mineral over both lithologies is the magnesian smectite, saponite, here the principal weathering product of the primary magnesium silicates. Saponite, too, is present in soils developed on saprolitic peridotite. Because of the relative stability of these primary and secondary magnesium silicates, Mg (unlike Ca) is not strongly leached from the saprolites (or derived soils), and concentrations are rarely below 6% MgO. It is, however, strongly leached from the overlying mottled clays and lateritic horizons (on pyroxenite), with minimum concentrations of 0.25-0.50% MgO - which occur within zones that have $<0.20\%$ CaO. Closer to the surface, Mg contents rise, reflecting the occurrence of dolomite in pedogenic carbonate. In the surface horizons over the pyroxenite (*i.e.*, soils, laterites and mottled clay), all the Mg is present as dolomite, so that the CaO/MgO ratio is >1. Calcareous soils and near-surface saprolites on peridotite contain both dolomite and smectite, so that this ratio is always <1.

Strontium abundance in the unweathered rocks is low, but is rather greater in pyroxenite (mean 17 ppm) than peridotite (mean 10 ppm). This distinction is not evident in the regolith, for the Sr distribution is controlled by the occurrence of pedogenic carbonate. Strontium is leached from the saprolite and mottled clays, except where these are invaded by carbonate, but concentrations of both Sr and Ca increase strongly in the calcareous upper horizons over both lithologies. Thus, there is a strong correlation between Sr and CaO ($r=0.92$), with the greatest Sr enrichment in calcareous lateritic material over pyroxenite (mean 350 ppm Sr, 10.05% CaO).

Barium has a rather different distribution pattern to the other alkaline earth elements. Concentrations are again greater in unweathered pyroxenite (mean 36 ppm) than peridotite (16 ppm) and this distinction is evident in comparable regolith horizons. Unlike the other alkaline earth elements, there is no significant depletion from any regolith horizon but a steady increase upwards through the profile, probably due largely to residual concentration. Maximum concentrations do, however, correspond to horizons characterized by pedogenic carbonate, so that some absolute accumulation of Ba may have occurred.

6.5 Alkali elements: Na, K, Cs, Rb.

Sodium. Comparative statistical data for the principal regolith horizons over the two lithologies are given in Table 5, Appendix II. The Na distribution resembles that of Mg in that it is retained in the saprolite but leached from mottled clay and lateritic horizons. The concentrations of Na and *potassium* are very low in lag and show no preferential enrichment in any lag type. *Caesium* and most *rubidium* concentrations are below detection limit (5 ppm). Some soils and upper lateritic horizons contain 5-30 ppm Rb.

Sodium is more abundant in unweathered pyroxenite (0.36% Na_2O) than peridotite (0.15% Na_2O), but this difference is not maintained in the regolith. Concentrations in the saprolite greatly exceed those of the parent rocks, especially over peridotite, where values over 1% Na_2O are common in the more clay-rich material. Such concentration is unusual in deeply weathered profiles, since Na is one of the most mobile elements and is commonly strongly leached.

However, it is also a component of aerosols associated with rainfall and it is probable that the Na in the regolith has accumulated by evaporation in the prevailing arid climate. The higher concentrations occur in the less free-draining clay-rich horizons that are best developed on peridotite. No micas were detected by XRD so, presumably, the alkalis are adsorbed to or occupy exchange sites in smectites; sodium probably also occurs as halite.

6.6 Lithophile elements: Cr, Sc, Ti, V, Zr, Ga.

Comparative statistical data for these elements in the principal regolith horizons over the two lithologies are given in Table 3, Appendix II. These elements commonly accumulate in lateritic regoliths, particularly in the ferruginous horizons. The concentrations are largely residual, due to the stability of their host minerals and the loss of other components. This is evident over both lithologies at Ora Banda, where each element shows a steady increase in concentration upwards through the regolith profile, with the highest abundances in the lateritic horizon over the pyroxenites. Within this horizon, the maximum concentrations tend to occur in the more ferruginous and aluminous zones, thus distributions resemble those of the PGE and Cu. The stable host minerals probably include chromite (Cr), zircon (Zr) and ilmenite and/or anatase (Ti), although only chromite has been positively identified (*e.g.* see Volume III, Chapter 7).

Chromium, Ti and V contents decrease in some upper lateritic horizons, probably due in part to dilution by introduced pedogenic carbonate whereas, in contrast, those of Zr continue to increase. Over peridotite, each of these elements is enriched in the soils compared to the underlying saprolites, with maximum concentrations in the more ferruginous materials (*e.g.*, see data for holes OB 209, 213 and 214, Appendix IV). Both Zr and Ti are enriched in the surface horizons (0-1 m) of these soils, especially in comparison with Cr, even where the soils are highly calcareous. Titanium, V and Zr vary systematically and cyclically along each traverse; this may reflect cryptic layering within the ultramafic rocks or be a function of erosion and exposure of different horizons of the regolith. Gallium is strongly associated with Al and accordingly is most strongly enriched in the laterites and derived soils and lag on the pyroxenite.

Except for Cr, each of these elements is more abundant in unweathered pyroxenite than peridotite. This distinction is maintained in comparable horizons in the regolith although, of course, the relative Cr enrichment of the laterite on pyroxenite has no equivalent over the peridotite. In contrast, the lag over peridotite is much richer in Cr (mean 25850 ppm) than that over pyroxenite (mean 10030 ppm). The lithologies can be distinguished in most regolith horizons quite effectively by binary plots, particularly Ti-Zr, Sc-Cr, Sc-Zr (Figures 28 and 29) and Sc-Ti. A similar distinction is evident in a Ti-Zr plot for lag, with a wide scatter in the mixed type B lag (Figure 32). There is overlap in soils in a Zr-Cr plot due to differential weathering and in the saprolite in most plots with Ti or Zr due to their low initial abundances. In each of these plots, the lower units of the regolith (saprock, saprolite and some mottled clay) fall in quite discrete trends, but there is a wide scatter in laterites and soils. This is shown by comparing Figures 28, 29, 30 and 31. The high variability in these upper units appears to be due to the relative loss of Cr compared to Sc, Ti and Zr during the formation of the lateritic horizons and of Cr and, especially, Sc during the formation of soils from saprolite on the peridotites. The loss of Cr during weathering reflects leaching of Cr from ferromagnesian minerals and to the alteration of chromite (see Section 5.2, Figure 19C). Leaching of Cr has probably been greater over pyroxenite, possibly due to the finer grain size of the chromites and a higher proportion of Cr in silicates such as chromian augite. Some Cr released from these primary minerals has been incorporated in Fe oxides, thus accumulating in the laterite. Indeed, at Mt. Carnage, nearly 80% of the total Cr in the lateritic horizons is dissolved by citrate-dithionite, which is a specific extractant for crystalline Fe oxides, whereas in the saprolite only 20% is soluble (Volume III, Chapter 6, Section 4.4). The higher Cr content of lag over peridotite reflects the greater stability of chromite compared to Fe oxide as a host mineral during continued weathering and the formation of lag, and the greater grain size of the chromite in peridotite than pyroxenite.

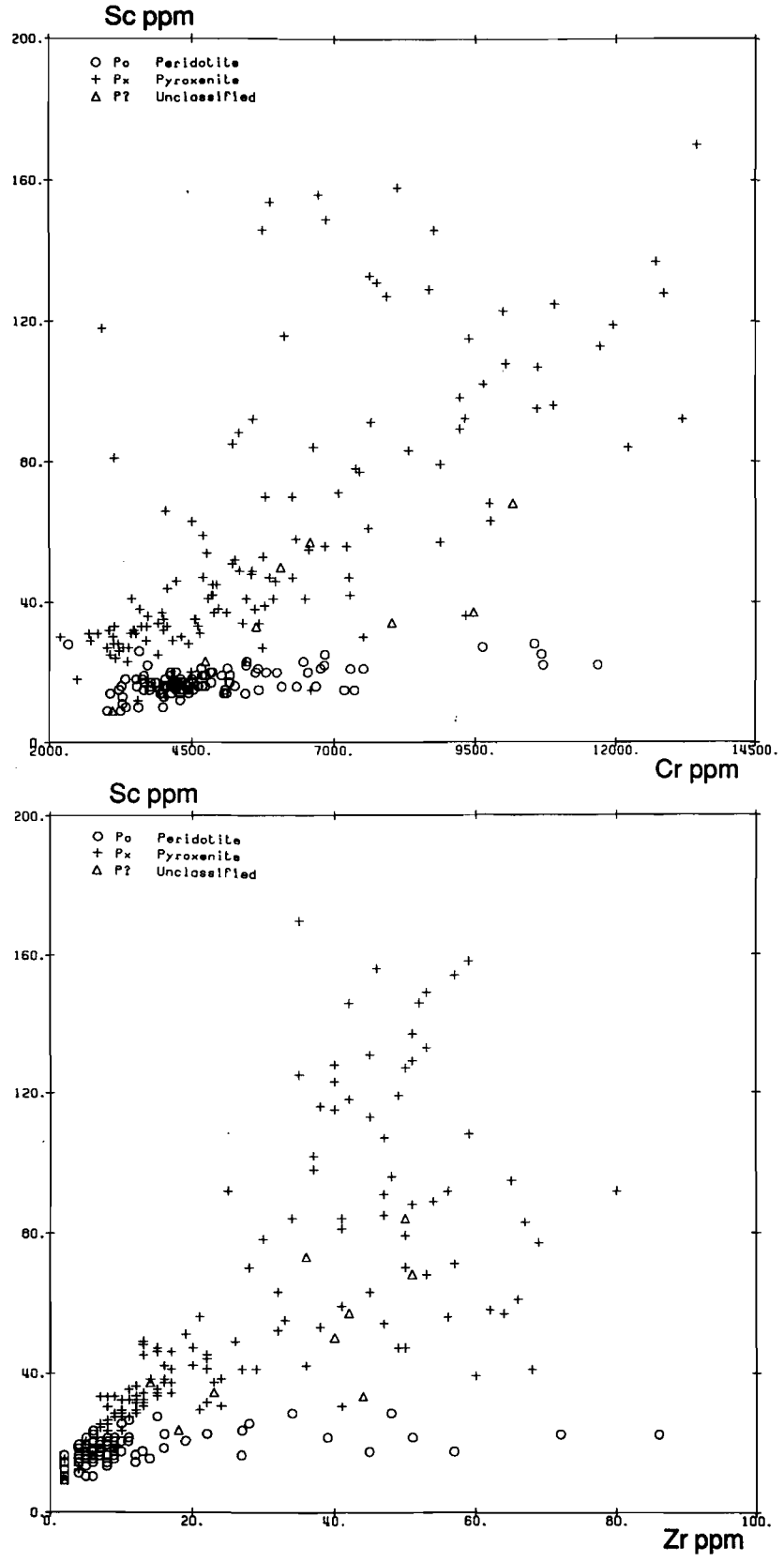

Figure 28. Binary plots illustrating discrimination between peridotite and pyroxenite in regolith samples. Top: Sc and Cr. Bottom: Sc and Zr

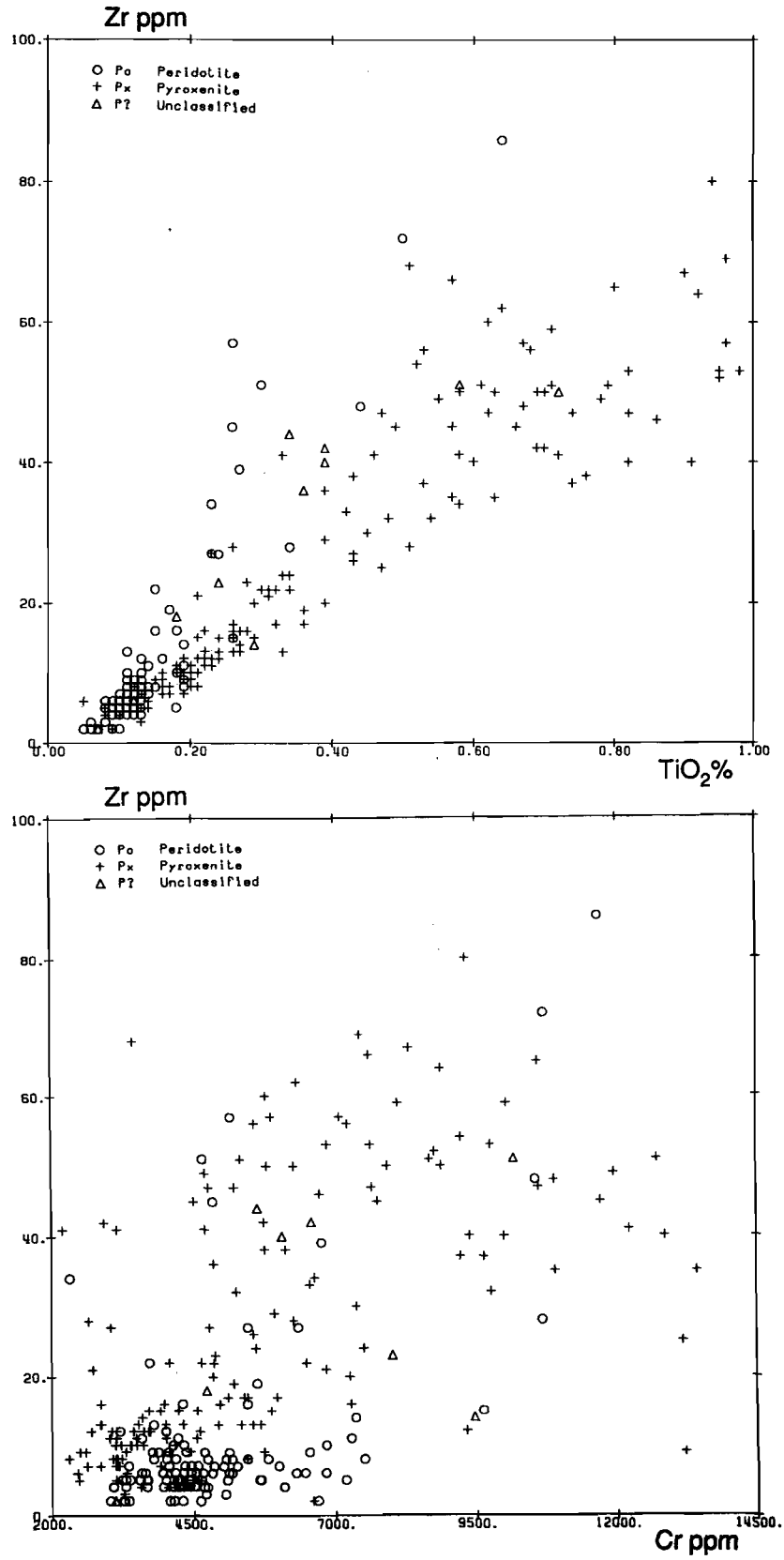

Figure 29. Binary plots showing partial discrimination between peridotite and pyroxenite in regolith samples. Top: Zr and TiO_2. Bottom: Zr and Cr. Note overlaps at low TiO_2 and Zr abundances. The wide scatter, mainly in pyroxenite, is due to relative loss of Cr during laterite and soil formation.

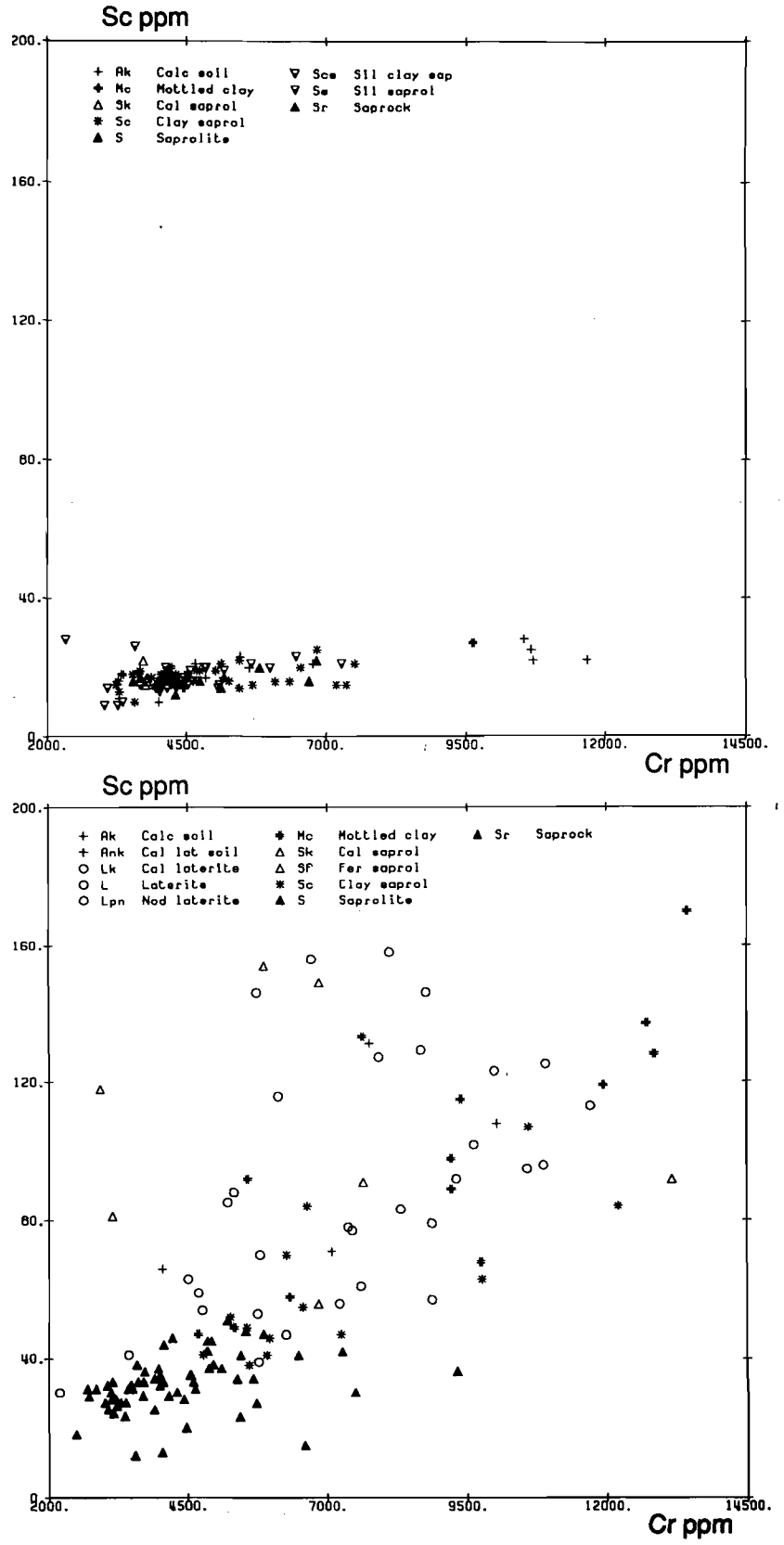

Figure 30. Binary plot of Sc and Cr, illustrating the variability in different horizons of the regolith. Top: Peridotite. Bottom: Pyroxenite. The wide scatter in pyroxenite is due to relative loss of Cr during the formation of the laterite horizon. Both elements have been leached from soil on peridotite.

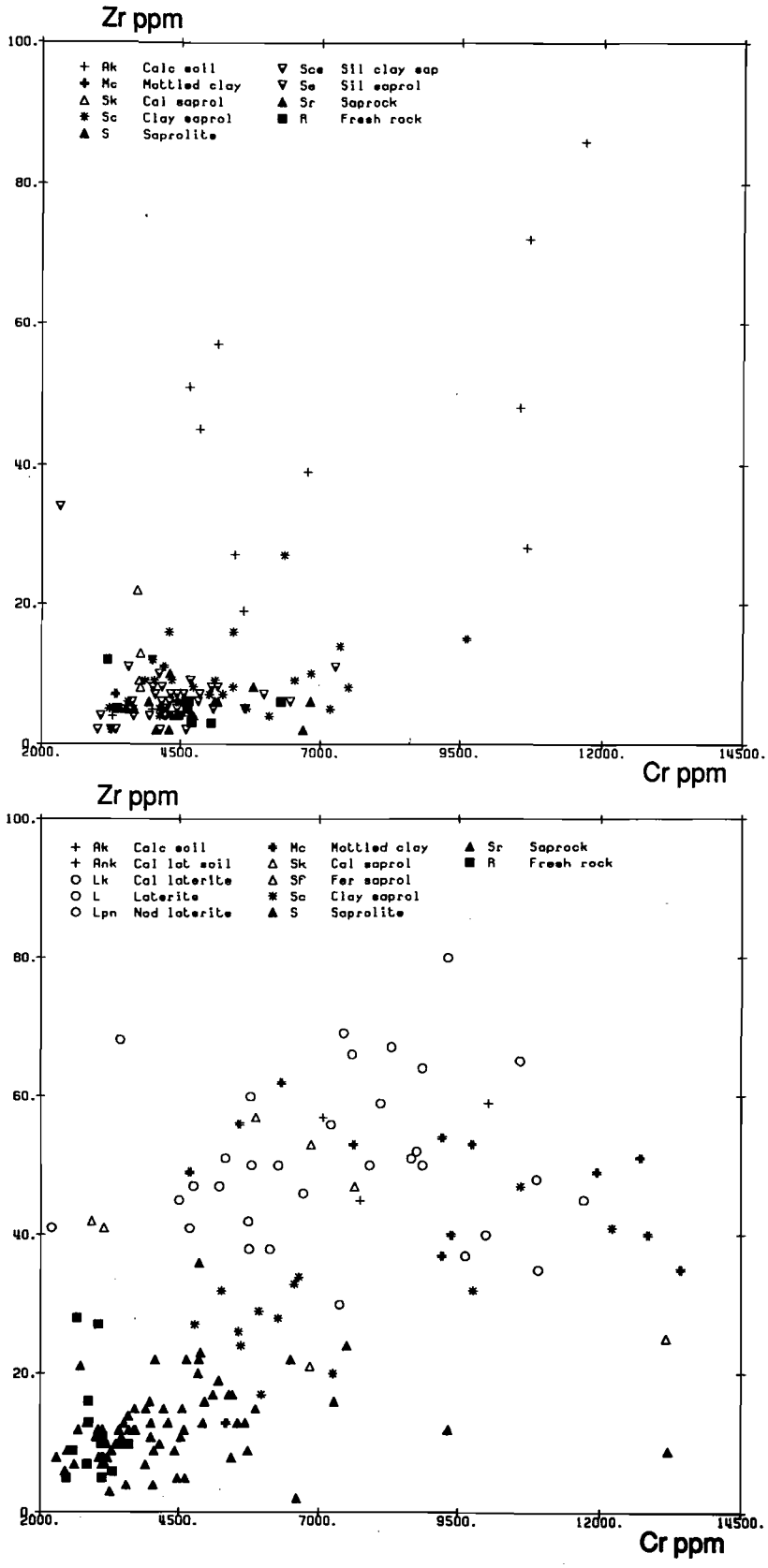

Figure 31. Binary plot of Zr and Cr, illustrating the variability in different horizons of the regolith. Top: Peridotite. Bottom: Pyroxenite. The wide scatters are due to relative loss of Cr during the formation of the laterite horizon and soils.

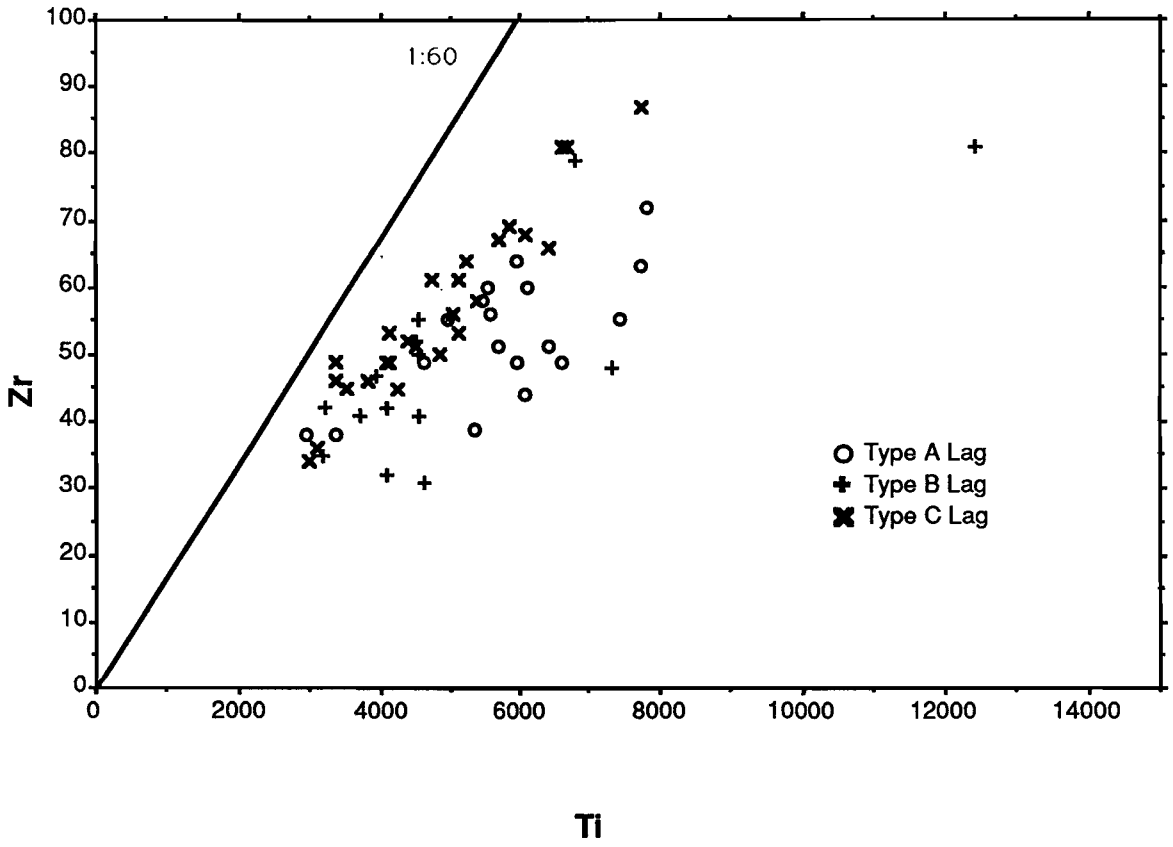

Figure 32. Binary plot of Zr and Ti illustrating discrimination between pyroxenite and peridotite in lag samples.

6.7 Base and transition metals: As, Pb, Co, Ni, Mn, Zn.

Comparative statistical data for these elements in the principal regolith horizons over the two lithologies are given in Table 4, Appendix.II. Cobalt, Ni, Mn and Zn are retained and variably enriched in the saprolite, but strongly leached close to the surface, particularly from the lateritic horizons. Arsenic and Pb abundances are generally very low, commonly at or below detection limits.

Manganese abundances are similar in the unweathered rocks (means 1350 and 1585 ppm in peridotite and pyroxenite, respectively), probably substituting for ferrous iron in olivine and pyroxene. The Mn distribution in the lower regolith is very similar to those of Ca and, in particular, Mg, but there is no surface concentration in pedogenic carbonate. Thus, Mn is retained or weakly enriched in saprolite below a depth of about 20 m, probably due to the occurrence of saponite and relict pyroxene and talc in the saprolite, substituting for Fe, Mg or Ca. Some Mn is also present in Mn and Fe oxides; minor enrichment in the silica-rich saprolites over peridotite may be due to local Mn oxide precipitation associated with perched water-tables. Such precipitation is a feature of strongly silicified regoliths developed on dunite (Butt and Nickel, 1981). Small soft nodules of Mn oxide were found in some samples, most notably in the PGE-enriched interval at 26-27 m in OB 21 (1710 ppm Mn). However, no relationship was found between Mn and PGE contents, although this had been anticipated following previous studies (Butt, 1986). Manganese is mostly leached from the top 20 m of the regolith, with mean concentrations of less than 300 ppm Mn in the clay saprolite, mottled zone and lateritic horizons. The Mn loss corresponds to the disappearance of the Mg silicates; in comparison, Mn concentrations remain high (> 1000 ppm) to the surface where these silicates are also present,

e.g., in OB 19, where pyroxenite saprock outcrops, and in OB 211 and 214, where saponite, orthopyroxene and talc occur in soil and shallow saprolite. The distribution of Mn between oxide and silicate phases is indicated by the partial extraction results from similar materials at Mt. Carnage (Volume III, Chapter 6, Sections 3, 4 and 5).

Nickel distributions in the regolith broadly resembles that of Mn. However, concentrations in the unweathered rocks are rather higher in peridotite (1090 ppm Ni) than pyroxenite (545 ppm Ni) reflecting the common substitution of Ni for Mg in olivine. Some high Ni contents (maximum 3850 ppm) are due to the presence of sulphides. Like Mn, Ni is retained and enriched in the saprolite, particularly on peridotite. This is probably due to continued substitution of Mg by Ni in saponite, similar to that in the primary silicates, possibly enhanced by exchange reactions in which Ni, leached from overlying horizons and released during weathering of olivine, exchanges for Mg as saponite forms. End-member reactions include:

$$\underset{\text{Ni-olivine}}{4Ni_2SiO_4} + 10H^+ \Rightarrow \underset{\text{pimelite}}{Ni_3Si_4O_{10}(OH)_2} + 5Ni^+ + 4H_2O$$

$$\underset{\text{forsterite}}{4Mg_2SiO_4} + Ni^{2+} + 10H^+ \Rightarrow \underset{\text{Ni-saponite}}{Mg_2NiSi_4O_{10}(OH)_2} + 2Mg^{2+} + 6OH^-$$

Some Ni released during olivine weathering is also adsorbed by Fe and Mn oxides. The presence of saponite and relict primary silicates throughout most of the regolith over peridotite results in high Ni abundances in shallow saprolite and some soil. Over pyroxenite, Ni abundances are generally lower, reflecting the primary distribution, with some minor accumulation in upper, clay-rich saprolite - possibly again due to exchange (OB 28 to 32). The immediately overlying ferruginous horizons are relatively depleted in Ni, a common feature of laterites developed on ultramafic rocks. Here, it is due to the absolute loss of Ni during the weathering of saponite, only some of which can participate in exchange reactions at the base of the profile. The distribution in lag reflects the Ni contents of the uppermost horizon of the regolith, so that higher concentrations are evident where saprolitic peridotite rather than lateritic duricrust on pyroxenite form the surface, especially just north of the contact.

Cobalt abundances are greater in unweathered peridotite (130 ppm) than pyroxenite (100 ppm), substituting for Mg and Fe in olivine and pyroxene. The primary distribution is very similar to that of Ni, except that it is not significantly enriched in sulphidic samples. Concentrations are generally lower in the regolith where, unlike Ni, Co does not substitute or exchange for Mg or Fe in secondary silicates such as saponite, but is hosted by relict primary silicates or secondary Mn oxides. Relative to other horizons, there is some enrichment of Co in saprolite on peridotite (with Mn and Ni), which is reflected by the lags, and in mottled clays and lower lateritic horizons on pyroxenite.

Zinc concentrations are very similar in both lithologies (generally 65-75 ppm). There is little variation in the regolith, particularly over peridotite, with similar concentrations to those in the fresh rock, implying that there has been some absolute loss. There is greater variation over pyroxenite, although this may in part reflect primary differences. Concentrations are low (<50 ppm) throughout OB 26 and only 10-30 ppm in the mottled clays and lateritic horizons of holes OB 23 to 28, whereas in these horizons in OB 29 to 33, Zn contents can be as much as 100-260 ppm. The Zn content of lag reflects such variations, although the highest values occur in the lag over peridotite. This distribution could reflect occurrence in a resistant phase such as spinel, with remobilization in the lateritic duricrust where chromite has been destroyed. Selective dissolution experiments on material from Mt. Carnage also suggest that Zn is hosted by a resistant phase.

Arsenic is at or below the detection limit (5 ppm) in most samples, possibly with some minor accumulation (5-12 ppm) in the lateritic horizons. Several samples in holes OB 23, 25 and 26 contain 10-20 ppm As in the mottled and lateritic horizons, and up to 37 ppm As in the saprolite. Arsenic is also present in saprolite in OB 213 (10-80 ppm). These may reflect minor patchy gold enrichment (50-300 ppb Au) in the top 35 m of the peridotite and the bottom 10 m of the pyroxenite.

Lead contents are only above the detection limit (5 ppm) in the soil over the peridotites and the lateritic horizons over pyroxenite (maximum 13 ppm). This distribution suggests residual enrichment as an immobile element.

6.8 Rare earth elements: Ce, La, Y

Comparative statistical data for these elements in the principal regolith horizons over the two lithologies are given in Table 5, Appendix II. Abundances are low, as expected for ultramafic rocks, and the distribution patterns typify those of immobile elements or elements held in resistant minerals. Each demonstrates upward residual accumulation with the highest values in soils (over peridotite) and the lateritic horizons (over pyroxenite), the latter representing three- to five-fold concentration.

7.0 MT. CARNAGE

7.1 Introduction

The Mt. Carnage prospect, situated 8 km WNW of Ora Banda (Figure 2), is less dissected and has lower relief than the Ora Banda prospect, and has a more extensive lateritic cover. The PGE concentrations are rather higher than those at Ora Banda, being in the range 1000-1950 ppb Pt+Pd over thicknesses of 2 to 8 m along 80 m of the principal drill traverse, 14400E. The PGE-enriched material from most of these holes had been removed for metallurgical testing and a complete profile was only available for hole MC 24.

7.2 Regolith mineralogy

The regolith stratigraphy and mineralogy in hole MC 24 are shown in Figure 33. They are similar to those developed on the pyroxenites at Ora Banda, as described in Table 3 and illustrated in Figure 10.

a. *Ferruginous zone (lateritic and mottled horizons)*, 0-13 m. Ferruginous, clay-rich, poorly indurated duricrust and characterized by abundant goethite and hematite and moderate kaolinite. Minor quartz is present at 0-3 m and 10-13 m, and gypsum and calcite occur in the top metre. Trace minerals in panned concentrates (6-7 m depth): barite, baddeleyite (?), chromite, ilmenite with exsolved TiO_2, gold, magnetite, zircon. The zone differs from that at Ora Banda in being poorly cemented, without pisoliths or nodules, and without detectable gibbsite; subdivision into lateritic and mottled horizons is not possible from the drill cuttings.
b. *Saprolite*, 13-39 m. Soft and clay-rich throughout, becoming harder with depth. The clays are green, but strongly oxidized (brown, purple-red), especially above 23 m, in the zone logged as clay saprolite. The saprolite is dominated by the presence of saponite, with minor kaolinite at 23-27 m and above 16 m. Primary talc and tremolite occur below 17 and 23 m, respectively, and trace enstatite at 38-39 m.. The Fe oxides are only minor phases, goethite at 13-15 m and hematite below 26 m. Manganese oxides are abundant at the base of the clay saprolite (20-23m). Trace minerals in panned concentrates, various depths: chromite, magnetite.

7.3 Regolith geochemistry

7.3.1 Major and trace elements

The analytical data for hole MC 24 are listed and summarized in Appendix XI. Selected data are shown in Figure 33. The lateritic ferruginous zone has mean concentrations of 45% Fe_2O_3, 20% SiO_2, 16% Al_2O_3 and 0.2% MgO reflecting the dominant mineralogy (Fe oxides, kaolinite, minor quartz), destruction of primary and secondary magnesium silicates and severe leaching of alkalis and alkaline earth elements. In comparison, the saprolite has mean concentrations of 21% Fe_2O_3, 45% SiO_2, 4% Al_2O_3 and 12% MgO, with the high Mg content due to the presence of saponite and relict primary minerals. The lateritic horizons are also relatively enriched in Cr (mean 10250 ppm) and Cu (1115 ppm), especially at 10-13 m, and depleted in Mn (1290 ppm) and Ni (880 ppm) compared to the saprolite (5980 ppm Cr, 450 ppm Cu, 2985 ppm Mn, 3815 ppm Ni). These trends are similar to those found at Ora Banda, although the abundances are greater. The Si and Fe contents of the clay saprolite and saprolite are similar, but Al and Mg contents (means 8.4% Al_2O_3, 4.1% MgO) are intermediate between those of the saprolite and ferruginous zone, corresponding to the change from saponite to kaolinite as the dominant clay mineral. The clay saprolite is also particularly enriched in Mn, Ni, Co and Zn relative to the other horizons, and in Cr and Cu relative to the saprolite. Maximum concentrations of all these elements except Cr occur in the transition to the saprolite at 20-24 m. The transition,which is marked by Mn oxide precipitation, may occur across a past redox front or water-table, the latter possibly perched at a porosity barrier. Zirconium and Ti concentrations increase upwards through the profile, although doubling from the clay saprolite to ferruginous zones.

7.3.2 Platinum group elements

The concentrations of Pt and Pd show large variations through the profile (Figure 33), with a marked difference in mean abundances between the ferruginous zone (740 ppb Pt and 410 ppb Pd) and the saprolite 128 ppb Pt, 133 ppb Pd). Similar difference are shown by the minor PGE, except Os, which is at the detection limit throughout, and Pt% (see Table 9 and Appendix XI). The highest concentrations tend to occur towards the base of the ferruginous zone, as in holes OB 24 and 25 at Ora Banda, but the apparent enrichment of Pt, Pd and Rh is greater at Mt. Carnage (x4-x7) than Ora Banda (mostly x2-x3). There is a marked difference in Pt% between the ferruginous zone and the saprolite, probably due to preferential leaching of Pd. The proportion of Pt (Pt%) is lower in the ferruginous zone at Ora Banda, but this may reflect a lower initial abundance of Pt, as indicated by the relative abundances in saprolite. The possibility of the decrease in Pt% below 20 m being due to a change in lithology is discussed below.

Attempts to isolate individual PGE minerals at Mt. Carnage were unsuccessful. SEM examination of panned concentrates and magnetic concentrates, and electron microprobe examination of chromites and other minerals yielded negative results - consistent with the finding that Pt and Pd are dominantly hosted by the minus 2 μm fraction and are thus probably very much finer grained than that (Volume III, Chapter 6, Section 5.5). Analyses of Mn oxides occurring as a cobble at surface and separated 22 m in hole MC 24 showed both to be enriched in Pt and Pd, respectively:

	Pt ppb	Pd ppb	Mn %	Ni ppm	Ba ppm	Cu ppm	Co ppm
Cobble	1750	170	26	23400	17400	15600	35100
MC2422	380	2950	nd	nd	nd	nd	nd

The cobble consists of manjiroite (cryptomelane group), with minor barite and cerianite, and has Cu, Ni and Co contents similar to those of Mn oxides in profiles on dunites (*e.g.* at Mt. Keith; see Butt and Nickel, 1981). A chromite-magnetite concentrate from 22 m was also slightly enriched in Pd (560 ppb Pt, 1080 ppb Pd).

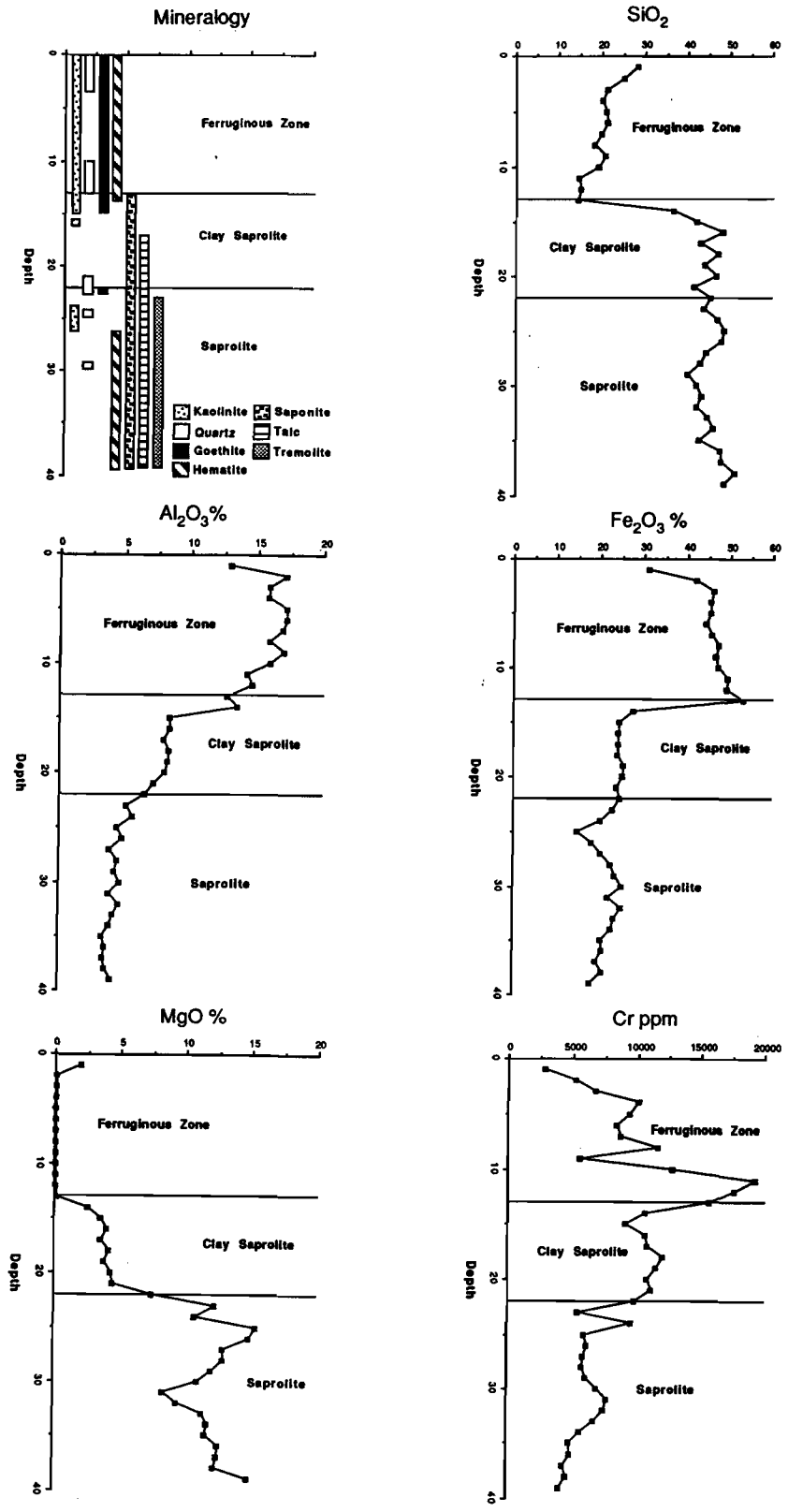

Figure 33. Mineralogy and distributions of selected elements in the regolith, hole MC 24, Mt. Carnage.

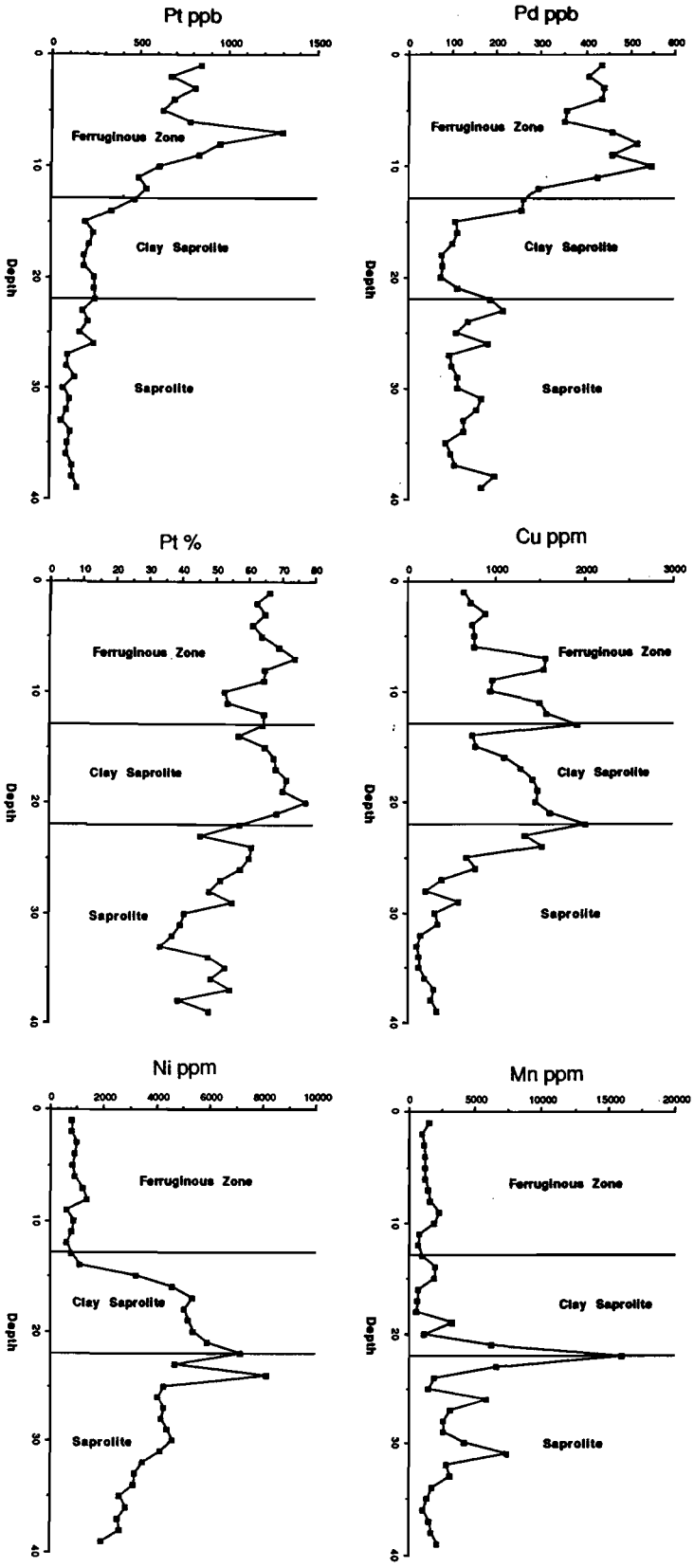

Figure 33 (continued) Mineralogy and distributions of selected elements in the regolith, hole MC 24, Mt. Carnage.

TABLE 9
Platinum group elements in a lateritic profile at Mt.Carnage (analysis by fire assay, NiS collection.

Sample	Depth m	Pt ppb	Pd ppb	Pt/Pt+Pd %	Ru ppb	Rh ppb	Os ppb	Ir ppb
Ferruginous horizons								
MC2401	1	820	480	63	18	43	2	12
MC2403	3	780	450	63	22	54	2	16
MC2405	5	660	400	62	16	40	2	12
MC2407	7	1300	460	74	24	60	2	2
MC2409	9	880	500	64	18	47	2	16
MC2411	11	490	440	53	14	33	2	10
Saprolite								
MC2415	15	175	112	61	8	13	2	6
MC2419	19	195	88	69	8	12	8	4
MC2423	23	180	215	46	16	26	2	4
MC2427	27	86	96	47	14	10	2	4
MC2431	31	94	160	37	14	16	8	4
MC2435	35	96	94	51	14	12	2	2
MC2439	39	140	170	45	12	10	8	4

7.4 Primary lithology of hole MC 24

At Ora Banda, fresh and weathered pyroxenites have >50 Pt% (*i.e.* Pt>Pd), whereas peridotites have <50Pt% (Pd>Pt). This suggests that the ferruginous zone (Pt%=64) in MC 24 at Mt. Carnage is derived from pyroxenite and most of the saprolite (Pt%=48) from peridotite (see Table 9 and Appendix XI). This conclusion is supported by the analyses of chromites from samples MC2407 (laterite), MC2431 and MC2439 (both saprolite), of which MC2431 has the low Pt% value of 37 (Volume III, Chapter 7). There are also marked differences in abundances of many major and trace elements and in mineralogy between the horizons. However, similar mineralogical and geochemical features were observed in profiles developed on pyroxenite at Ora Banda, although the saprolites there are less clay rich. The principal difference is a lower abundance of Pt in the saprolite at Mt. Carnage. Comparisons of binary plots of Zr with Ti and Sc show that most Mt. Carnage samples fall within the pyroxenite field defined by the Ora Banda data (Figure 34). Although there is overlap in some saprolites which have low abundances of these elements, it is concluded that the whole profile, including the saprolite, is derived dominantly from pyroxenite. This implies that the primary Pt/Pt+Pd ratio is lower at Mt Carnage than Ora Banda. Nevertheless, since the hole is drilled almost normal to the presumed dip, it probably passes through layers within the pyroxenite (*e.g.* MC2431) having a more peridotitic composition and this which may be partly reflected in the development and composition of the weathering horizons.

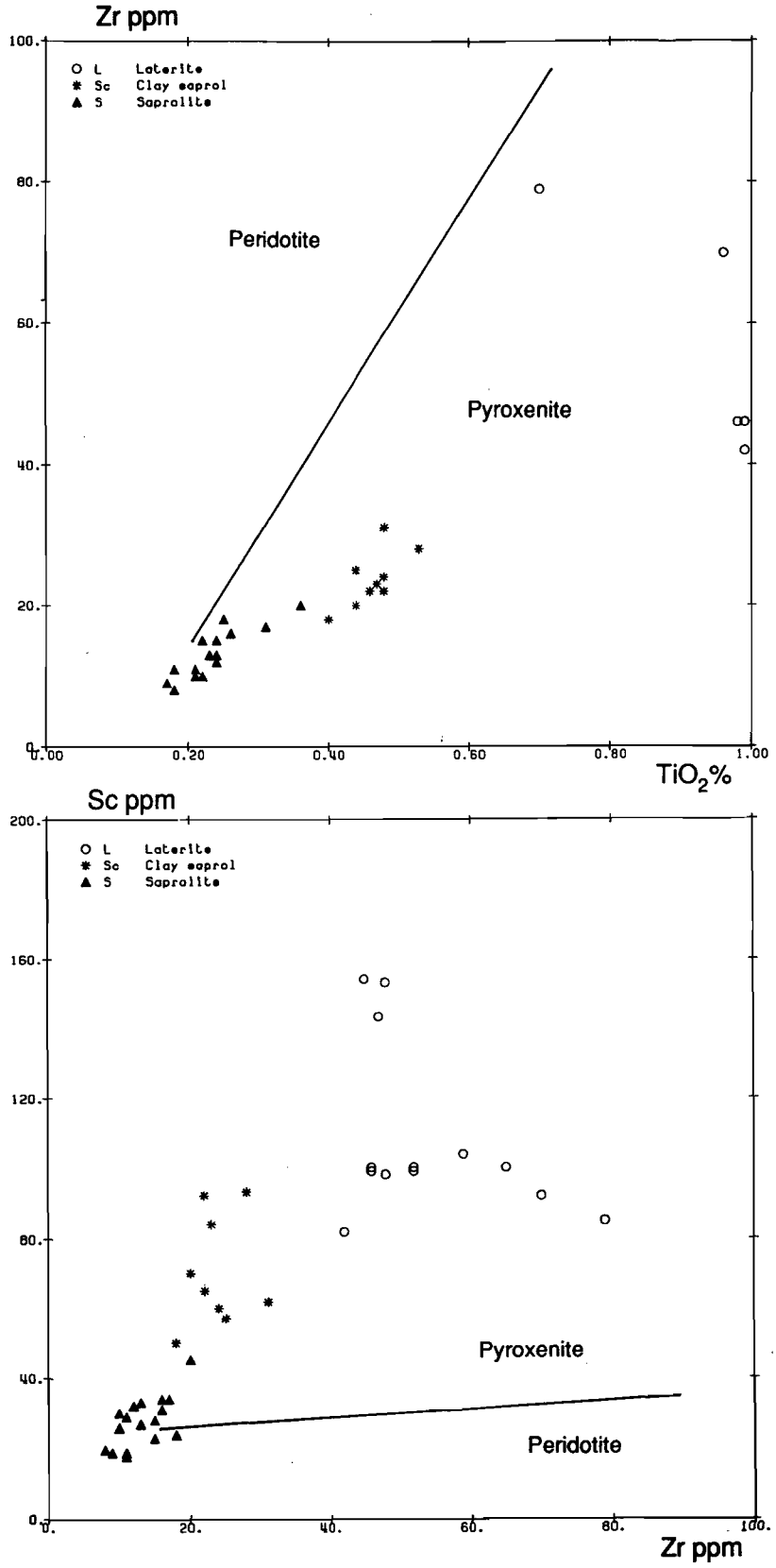

Figure 34 Binary plots of Zr versus TiO_2 and Sc versus Zr for profile MC 24, Mt. Carnage, compared with the fields defined for peridotite and pyroxenite at Ora Banda.

8.0 DISCUSSION AND CONCLUSIONS

8.1 Element distributions and regolith evolution

8.1.1 Introduction

The geochemical data presented in this study are consistent with many of the general features established for the evolution of the regolith in semi-arid regions of the southern Yilgarn Block. The regolith is considered to have developed over a very long period, probably since at least the mid-Mesozoic, during which it has been subjected to several major changes of climate. Two climatic episodes have been of particular importance. These were, firstly, the humid, warm to tropical climates of the Cretaceous to mid-Miocene and, secondly, the drier climates since the Miocene. The former humid climates were probably equivalent to those prevailing in the present wetter savannas and gave rise to extensive, deep lateritic weathering. The later arid to semi-arid climates, which still prevail, have resulted in a general lowering of water-tables and changes to, and slowing of, chemical weathering.

The distribution of each element in the regolith is related to the different weathering processes that prevailed during the principal climatic regimes. In general, only the processes that refer to past regimes of long duration or to extreme or recent regimes have had a significant effect and this is evident in the data from the Ora Banda sill. Thus, many of the dominant geochemical (and mineralogical) characteristics of the regolith can be related to the development of the lateritic profile under humid conditions of higher water-tables, whereas others are due to later events related to more arid environments with lower water-tables and may still be active. The features produced by these later events appear as modifications of the pre-existing lateritic profile and tend to be reflected more by the minor components of the regolith. Finally, the geochemical response in any given location will depend on erosional and depositional processes, which may have removed some horizons and buried others. Accordingly, adequate sampling and successful interpretation of geochemical data require an appreciation of the weathering and erosional history, a key to which is a geomorphological survey of the region being explored.

8.1.2 Lateritic weathering under humid tropical climates

The characteristics commonly associated with lateritic weathering are:

1. *Oxidation of sulphide minerals; strong leaching of alkali and alkaline earth metals.*
   Sulphides are the minerals most susceptible to weathering and this appears to be the case at Ora Banda, being represented in saprock by Fe oxide spotting. Sodium, Ca, Sr and Mg are commonly strongly leached from lateritic regoliths even close to the weathering front. However, at Ora Banda, the preservation of primary orthopyroxene and the formation of saponite and magnesite indicate that weathering conditions were less severe, probably due to the high buffering capacity of the primary minerals maintaining a high pH. Accordingly, Ca and Mg are retained in the lower to mid saprolite and are only strongly leached from the upper saprolite and lower ferruginous horizons. High concentrations of Na throughout the profiles and enrichment of Mg and, especially Ca and Sr, at the surface, are due to secondary accumulation during arid periods. Barium generally has only minor solubility during weathering but some leaching has occurred, because it has not accumulated with other immobile elements in the lower part of the ferruginous horizon.

2. *Retention of less mobile major elements as stable secondary minerals*
   The chemical and mineralogical compositions of lateritic weathering profiles tend to be dominated by the three elements Si, Al and Fe in the form of kaolinite, quartz, Fe oxides (hematite and goethite) and, in places, gibbsite. These phases dominate the secondary mineral assemblages of the upper saprolite, mottled and lateritic zones on the pyroxenites

(except where invaded by later calcrete). However, less severe leaching conditions due to buffering have resulted in Mg being retained throughout much of the saprolite, with smectite as the dominant clay mineral. The distributions of several minor and trace elements (*e.g.*, Cu, Pt, Pd, As, Ga, Ni, V, Sc) are controlled wholly or in part by the distributions of these major elements, especially Fe, and the retention of many of them (*e.g.*, Cu, Mn, Ni) is due in part to the presumed high pH and relatively mild leaching of the saprolite during weathering. In addition, many resistate and immobile elements also tend to accumulate with Fe oxides in the lateritic horizons although, for most, no chemical interactions are involved. Similar, presumably residual, accumulation is evident in soils derived from saprolite on peridotite (*e.g.*, Zr).

Ferruginous laterite is now dominantly present on pyroxenite at Ora Banda, where it occurs as pisolitic duricrust and gravels. The relatively high Al content (mean >17% Al_2O_3) and the presence of gibbsite are important features, given the relatively low primary abundance (3.25% Al_2O_3) and implies considerable residual accumulation. Similar accumulation is evident for other immobile elements or elements concentrated in resistant minerals (see below). The distributions of Co, Mn and Ni, are characteristic of lateritic environments in that they have been strongly leached from the ferruginous horizons of the regolith.

3. *Retention and accumulation of immobile elements and stable minerals*
The distributions of Cr, Ga, Pd, Pt, REE, Ti, V and Zr relate wholly or in part to their chemical immobility during weathering (*e.g.*, PGE, V, Ti) and/or to the stability of their host minerals (*e.g.*, Cr in chromite, Zr in zircon, Ti in rutile and anatase). Like Al, their abundances tend to increase upwards due to the gradual loss of other components, with marked accumulation in the ferruginous horizons, within which lateral dispersion by colluvial action has taken place during the course of profile evolution. Vanadium, some Cr, Ti and, possibly, Pd are released during weathering but become immobilized by precipitation with Fe oxides (Cr, Pd, Ti, V) or as anatase (Ti).

8.1.3 Weathering under semi-arid and arid climates

Characteristics commonly associated with weathering under arid conditions are those related to the excess of evaporation over precipitation, which result in the accumulation of otherwise soluble weathering products within the regolith. The most important of these are the alkali and alkaline earth metals, which concentrate in groundwaters and precipitate as carbonates, sulphates, halides and other salts. In lateritic profiles, this results in the paradoxical accumulation of these highly mobile components in an otherwise highly leached regolith. This is well exemplified at Ora Banda, where there is a marked concentration of Ca, Sr and, to a lesser extent, Mg and Ba as pedogenic carbonates and minor sulphates in the near-surface horizons and high concentrations of Na in the saprolite.

The presence of smectites and secondary silica are generally considered as typical of arid environments, but this may not be the case at Ora Banda, given the nature of the host rocks. Smectites are the initial product of the hydrolysis of silicates but, in most cases, smectites are unstable during lateritization and the reaction continues to form kaolinite. In these Mg-rich and hence highly buffered rocks, the pH remains high during weathering and the initial product, saponite, is stable even during lateritization. Significant production of kaolinite only occurs in the upper saprolite, where buffering is much reduced. Silicification is a feature of weathered ultramafic rocks, particularly dunites, but the mechanisms and conditions of formation are not known. They are presumably related to high Si contents in groundwater that may occur, for example, when Si released during weathering cannot precipitate as kaolinite because of low available Al. This concentration of dissolved Si may be due to aridity but this is not certain

since silicification of dunites is recorded from humid tropical terrains (*e.g.*, in India and Brazil) for which significant aridity is not established.

8.1.4 Regolith evolution

In summary, the principal stages in the evolution of the regolith on the Ora Banda sill are :

1. *Lateritic weathering under warm humid conditions.*

a. In the lower to mid saprolite, progressive weathering of sulphides, olivine, feldspar, tremolite and orthopyroxene and leaching of their mobile constituents (S, Na, Sr).
b. In the saprolite, retention of less mobile constituents hosted by secondary minerals, principally saponite and Fe oxides (Al, Fe, Ca, Mg, Si, As, Ba, Co, Cu, Ga, Mn, Ni, PGE, Sc, V).
c. In the upper saprolite, dissolution of saponite and resistant primary minerals (*e.g*, orthopyroxene, talc) and replacement by kaolinite and, possibly, with precipitation of silica and magnesite deeper in the profile. This was accompanied by remobilization and loss of Si (some), Ca, Mg, Mn, Co and possibly exchange of Mg by Ni during saponite formation.
e. Dissolution and replacement of kaolinite by Fe oxides, loss of Si and some Cr, and the accumulation of Fe and Al in secondary structures during the formation of the ferruginous horizon. Lateral concentration of Fe in depressions, notably on peridotite.
d. Accumulation of immobilized elements in resistant primary minerals (*e.g.*, Zr in zircon; Cr in chromite; REE) or in stable secondary minerals (Ti in anatase; Cu, PGE, Sc, V in Fe oxides).

The thickness and composition of the ferruginous horizon on pyroxenite are typical of lateritic regoliths on ultramafic rocks. However, the relatively thin zone of highly leached material, represented by the mottled zone and kaolinitic clay-rich saprolite, and the abundance of the weatherable minerals orthopyroxene and saponite in saprolite over both lithologies, are atypical. These features imply strong bedrock control in terms of the high buffering capacity attenuating the intensity of weathering and slowing its rate, but with the usual strong transformations occurring in the near-surface, presumably close to the palaeowater-table, where the Mg silicates were destroyed.

2. *Weathering under warm, semi-arid conditions.*

a. Decline of the water-table, with arid conditions leading to vegetation changes which in turn induced instability of the landsurface and initiated the erosion that is still continuing. Slow weathering has continued, mainly at the base of the profile. Dissolved weathering products have gradually accumulated as evaporation exceeded precipitation and have been supplemented by accession of marine salts from rainfall, resulting in progressive salinization of the groundwater and regolith.
b. Dehydration and hardening of lateritic duricrusts over pyroxenite.
c. Continued leaching of base and transition metals (Cu, Co, Pb, Mn, Ni) with minor precipitation in the mid to lower saprolite and possible exchange of Mg by Ni in saponite as weathering continues. Loss of Sc and some Cr during formation of soil from saprolite on peridotite.
d. Accumulation of soluble alkaline earth elements as pedogenic carbonates. These elements are derived, at least in part, from continuing weathering and transported to the surface, probably by evaporation and/or evapotranspiration, and in part by accession in rainfall and as dust.

8.1.5 Origin of Fe-rich lateritic duricrust on peridotite

The general preservation of the ferruginous lateritic horizons over pyroxenite implies that there has been comparatively little erosion over these rocks. However, the equivalent horizons are

absent over the peridotite, except for the massive Fe-rich duricrust and some remnant lag. Widespread ferruginous horizons do develop on peridotites so that it must be assumed they were not susceptible to hardening and have been eroded. The Fe-rich duricrust has a more restricted occurrence, with an approximately linear or lens-like outcrop pattern. It has a pebbly, clastic appearance in outcrop and polished section, although olivine pseudomorphic fabrics within some hematitic clasts indicate that it a largely locally derived, from the peridotite. However, the presence of clasts with lithofabrics foreign to the Ora Banda sill demonstrate it is partly polymictic. In addition, some early, hematitic clasts contain fossil plant material.

Some of the clasts themselves have an internal clastic fabric, implying previous accumulation and cementation of ferruginous detritus, followed by erosion, transport and final incorporation into the Fe-rich duricrust. The clasts have goethite coatings, of varying thickness, thus forming pisolitic and oolitic structures, some of which have been broken and recoated by goethite. The coatings are continuous with goethite that appears to form an incomplete cement to the duricrust, which suggest that it was precipitated in a generally low-energy sedimentary environment, punctuated by episodes of somewhat higher energy, during which coated pisoliths could be fractured. Some of the fossil plant material is also preserved in this later goethite. The assemblage of fossil plant material, containing leaf, moss, fern and bark, suggests a temperate to warm, humid forest environment, *i.e.*, conditions considered conducive to laterite formation. It is suggested that these scattered areas of duricrust represent what were once topographic lows in which pockets of generally locally-derived ferruginous detritus and organic matter accumulated in a drainage system characterized by small ponds, swamps and low-energy streams crossing the peridotites. Decaying vegetation and a high water-table would result in the dissolution of Fe as ferrous-humic complexes and its transport in groundwater, precipitating in the more oxidizing and less acid environment of the stream. Successive periods of erosion and quiescence would alternate physical damage with renewed precipitation. As sedimentation progressed, deeper sediments would become inactive and increasingly cemented and Fe-rich. With a subsequent change to aridity, dehydration, induration and erosion have occurred; on exposure, these materials have been more resistant than any surrounding laterite, resulting in local landscape inversion. This model is similar to that proposed by Ramanaidou *et al.*, (1991) for the origin of the Channel Iron Deposits (*e.g.*, of the Robe River) in the Hamersley Province.

8.2 Implications for exploration

8.2.1 Supergene PGE mineralization

The results obtained by Carbine Gold N.L. during their exploration programme and CSIRO during the course of this project have shown that economically significant concentrations of PGE may develop as a consequence of lateritic weathering. However, neither the PGE concentrations (maximum approximately 2 ppm Pt + Pd) nor the identified resource are sufficiently great to be exploitable, particularly given the low recoveries ($<<50\%$) obtained by preliminary metallurgical tests (J.C Menzies, Carbine Gold N.L., personal communication, 1990). N.B. *Much greater extraction has been obtained under laboratory conditions during this project (Volume III, Chapter 6, Section 4.5).* Nevertheless, the results demonstrate that PGE concentration can occur, given a favourable primary lithology. The concentrations are essentially confined to the lateritic ferruginous zone and appear to be residual. There is no evidence for chemical dispersion within that horizon or for absolute enrichment in the saprolite. Similarly, there is no evidence for depletion of PGE in the upper horizons of the profile. The PGE distribution in the regolith thus resembles that of gold with regard to the physical accumulation within the lateritic horizons, but differs in that there seems not to have been any secondary mobilization, either during or after lateritization, and thus no equivalent to the saprolitic supergene Au deposits. For the supergene PGE concentrations in lateritic regoliths to be economic would probably require a rather higher initial PGE content and the possibility of chemical mobilization and reconcentration during weathering. Such mobility might be promoted

in rocks that have a higher sulphide content, or in sites where the regolith is saturated by hypersaline groundwater, thus permitting mobilization as thiosulphate and chloride complexes, respectively. Local PGE enrichment in Mn oxides occurs locally at Mt. Carnage and is also present in the lateritic regolith at Mt. Keith, overlying silicified zones in dunite-derived profiles (Butt, 1986; 1992). Such Mn-rich horizons appear to form at perched water-tables or redox fronts above porosity barriers. They are commonly thin and restricted in occurrence, so the potential for economic mineralization is not high; the PGE-Mn oxide association does, however, suggest that the possibility for distal concentrations.

8.2.2 Primary PGE mineralization

Inspection and analysis of the diamond drill core show that there is no economic concentration of PGE in the Ora Banda Sill, but a general enrichment throughout the upper peridotite and the pyroxenite. Data from the regolith, however, suggest that there may be local zones of enrichment, characterized by enrichment not only of Pt and Pd (to 3000 ppb Pt + Pd), but also in the minor PGE (maxima 52 ppb Ru, 114 ppb Rh, 6 ppb Os, 20 ppb Ir). Such an enrichment was found in the upper peridotite in the saprolite but, due to faulting or lack of continuity, it was neither intersected by the diamond core, nor, apparently, does it outcrop. The presence of the full PGE suite suggests that this represents local primary concentration, but further exploration would be necessary to determine its significance.

8.2.3 Exploration procedures

The Ora Banda sill generally occupies relatively high ground and, although deeply weathered, the ultramafic zones have predominantly residual regolith at surface. Accordingly, the routine surface exploration procedures of soil and lag sampling have been effective in exploration for lateritic PGE mineralization. Direct sampling of the laterite itself by shallow drilling would be the best procedure. Similar procedures would also be effective for exploration for primary mineralization, although care would be required to identify such mineralization within or close to areas of laterite. High Pt and Pd concentrations are themselves insufficient indicators so that it would probably be necessary to analyse selected samples for the other PGE. Copper, Cr and Ni are not effective pathfinder elements. None is necessarily associated with primary enrichments (*e.g.*, sample OB 2127, which has 3 ppm Pt + Pd and elevated Ru, Rh and Ir contents, has only 52 ppm Cu, 5120 ppm Cr and 1920 ppm Ni), and both Cu and Cr are residually enriched in lateritic horizons. The apparent lack of chemical mobility of the PGE may pose problems to effective exploration of areas of saprolite, since the target will be restricted in size and any enlargement is thus dependent on limited physical transport at surface. In extreme cases, where there is little regolith, element abundance will also be much lower, as reported by Harrison (1990) at the Windimurra Complex, where thresholds of 8 ppb and maxima of 43 ppb Pt and 52 ppb Pd were found in the minus 180 μm fraction of shallow lithosols. Such situations exist on non-prospective upper parts of the Ora Banda sill.

No data were obtained that could assist in exploration of areas of transported overburden except that, by analogy with gold exploration, the most effective procedure would be to sample buried lateritic residuum by shallow drilling. Where the buried residual profile is partly truncated, however, the apparent absence of lateral dispersion of PGE in the saprolite means that exploration must rely on close-spaced drilling, preferably using overlapping angle holes, over carefully defined targets. The possibility that Pd in particular may be mobile in the soil and concentrating in pedogenic carbonates may imply that, under certain conditions, these may offer a preferred sample medium, again by analogy with gold. However, the association is less well established than for gold and the conditions under which it may be enhanced are not established.

The high concentrations of Pt, Pd and Cu present in lags and lateritic horizons is similar to that which might be expected to indicate the presence of significant Ni sulphide mineralization and to be used in gossan discrimination. In the absence of other geological information, the most

effective additional geochemical discriminant for Ni sulphides would probably be analysis for Ir and, possibly, Te.

8.2.4 Lithological discrimination

Various binary plots of Ti, Zr, Sc and Cr are effective in discriminating between the peridotites and pyroxenites in the regolith at Ora Banda (Figures 28 and 29), although differential leaching from laterite (Cr) and soil (Cr, Sc) tends to give a wide scatter and some overlap in these upper horizons (Figures 30 and 31). There is also overlap in the saprolite, saprock and fresh rock due to the low abundances of Ti and Zr. The possibility of incorrect identification of the parent lithology of clay-rich samples in holes OB 20-23 was tested by discriminant analysis. This possibility arose because the top 5 m of OB 20 is pyroxenite saprolite/saprock and hence these holes should also either intersect the contact at depth or be wholly in pyroxenite. Using training sets of *saprolite* from holes OB 209-214 and OB 19 (peridotite) and *saprolite* and aluminous *mottled clay* from OB 24-33 (pyroxenite), the analysis classified most of the samples as peridotite (Figure 35A), confirming the interpretation of the pyroxenite at the top of OB 20 as a fault block. This interpretation is shown in Figure 36. A similar conclusion was derived from the analyses of the chromites (Volume III, Chapter 7). The lateritic horizon in OB 23 has not been classified for, although it has the characteristics of pyroxenite, it is uncertain whether it is *in situ*, and hence marking the contact, or whether it contains material transported downslope from the south. The elements most important for the classification were Ti > Mg > Si > Sc > Ca (Figure 35B), *i.e.*, a combination of relatively mobile alkaline earths that have been retained in the saprolite in magnesite (Mg) and, unusually for the region, smectite (Mg, Ca), immobile minor and trace elements (Ti, Sc) and Si, which occurs in smectites and also as free silica over peridotite.

ACKNOWLEDGEMENTS

Mr. J.C. Menzies and Mr. W. Fortune are thanked for their cooperation in allowing initial access to the leases held by Carbine Gold N.L. and for making the diamond drill core from Ora Banda available. Sample preparation was by G.D. Longman and R.J. Bilz. XRD data were collected by M. Cheeseman and G.D. Longman. XRF analyses were by M.K.W. Hart and M. Cheeseman and I.C.P. analyses by J.E. Wildman. Thin and polished sections were prepared by A.G.Bowyer and R.J. Bilz. R.C. Morris advised on the identification of opaque minerals in the lag and S.J. Barnes assisted with the interpretation of the geology and primary geochemistry of the Ora Banda Sill. R.R Anand and E.R. Ramainaidou confirmed the presence of fossil wood and J.K. Marshall advised on its identification. N.A. Campbell and M.J. Palmer (CSIRO Division of Mathematics and Statistics) provided access to and assistance with multivariate statistics programs. Some of the data processing and plotting has been carried out using a demonstration copy of the GDM program, supplied by BRGM, Orléans, France. Additional drafting and artwork was by C.R. Steel and A.D. Vartesi. This collaboration and assistance is all gratefully acknowledged.

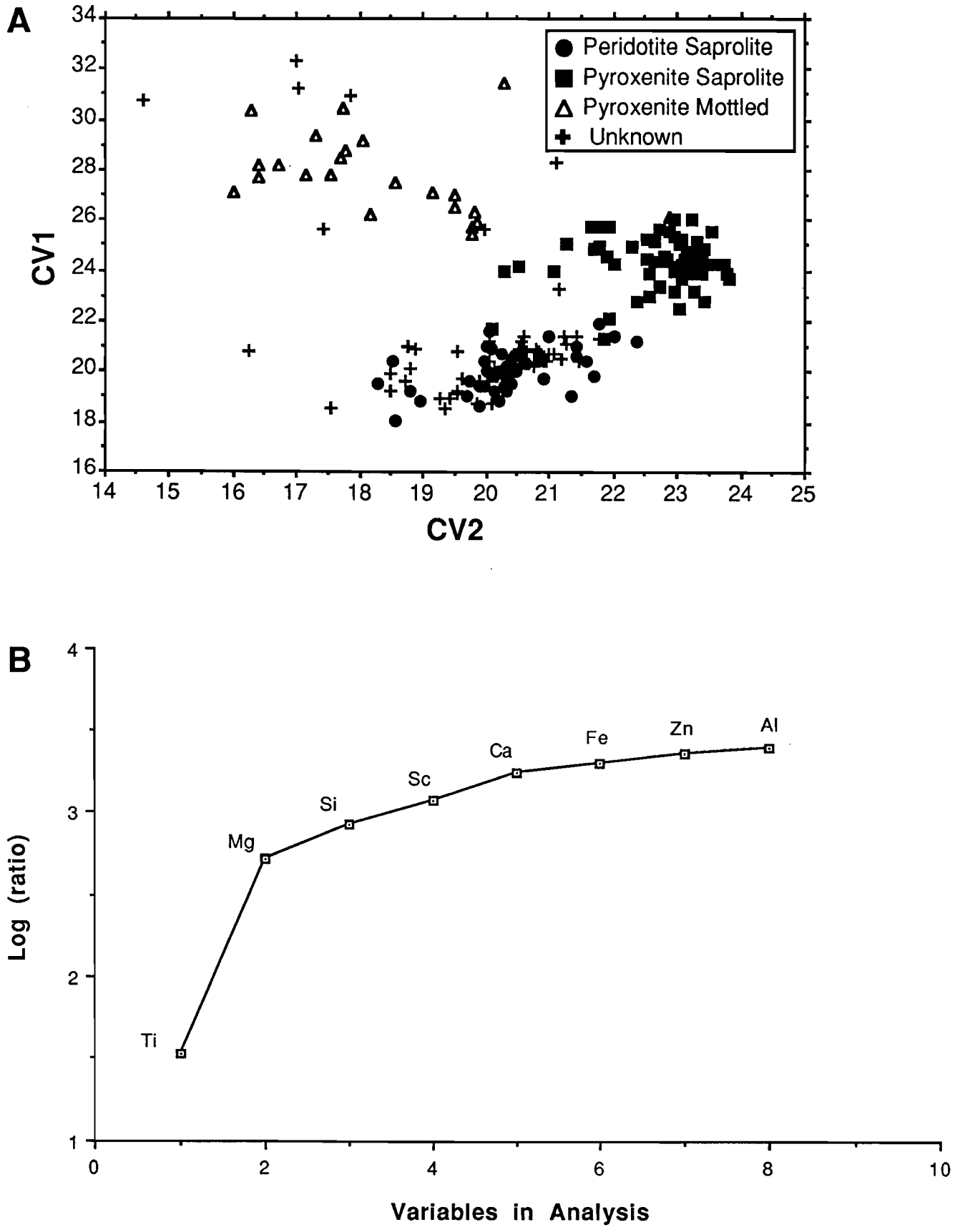

Figure 35. Results of discriminant analysis of saprolites from holes OB 20-23. A: Plot of canonical variates. B: Variables in the discriminant analysis.

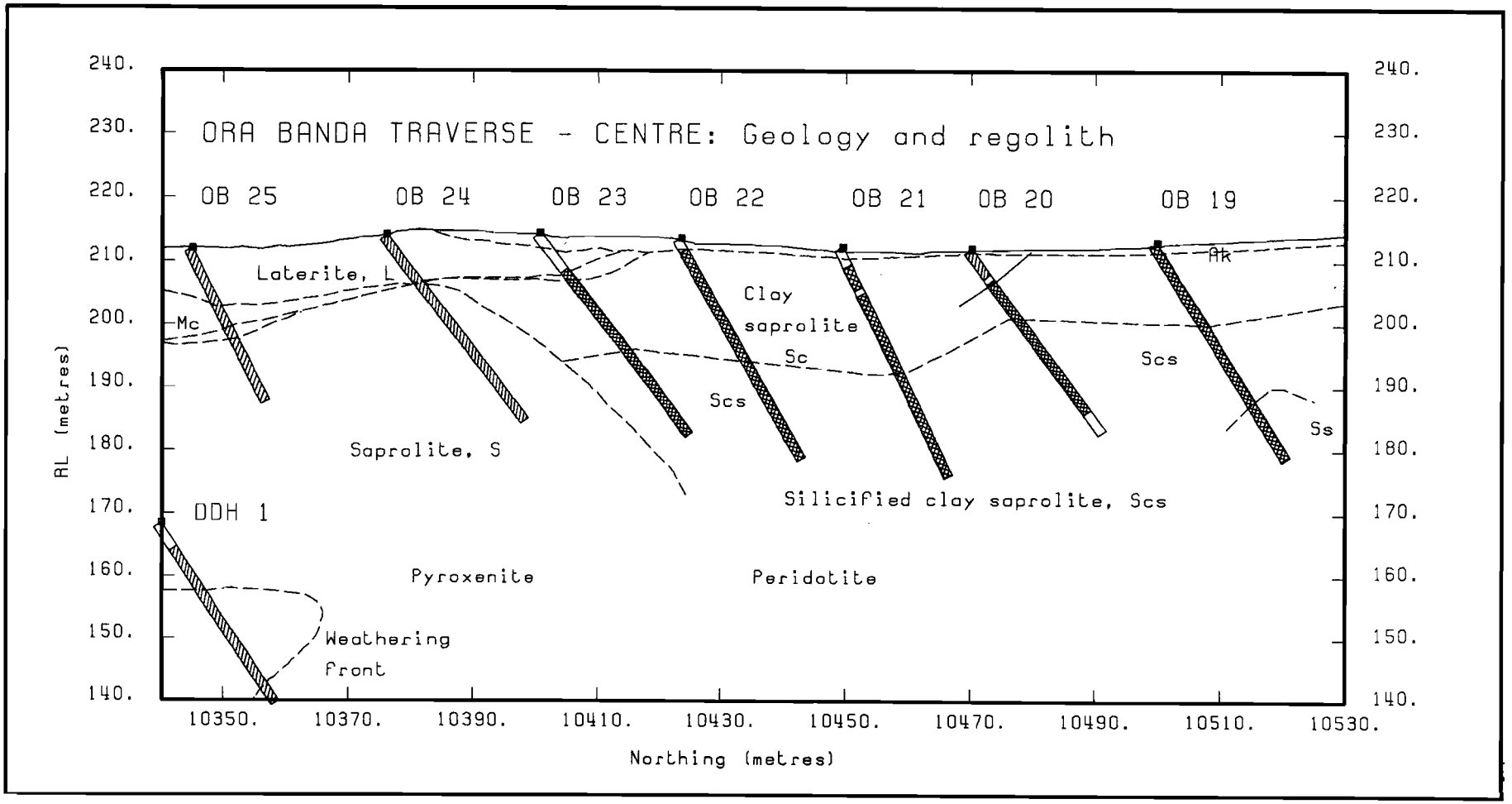

Figure 36. Central section of the drill traverse at Ora Banda, with lithology in holes OB 21-23 classified by discriminant analysis. Intervals left blank fell outside the areas defined by the training sets. Note the fault block of pyroxenite at the top of OB 20.

REFERENCES

Anand, R.R., Smith, R.E., Innes, J., Churchward, H.M., Perdrix, J.L. and Grunsky, E.C. 1989. Laterite types and associated ferruginous materials, Yilgarn Block, WA. CSIRO Division of Exploration Geoscience Report 60R.

Anand, R.R., Churchward, H.M. and Smith, R.E. 1990. Regolith/landform relationships and the petrological, mineralogical and geochemical characteristics of lags, Lawlers District, Western Australia. CSIRO Exploration Geoscience Restricted Report 106R. 105 pp.

Anand, R.R., Churchward, H.M., Smith, R.E. and Grunsky, E.C. 1991. Regolith-landform development and consequences on the characteristics of regolith units, Lawlers District, Western Australia. CSIRO Exploration Geoscience Restricted Report 166R. 160 pp.

Barnes, S.J., Hill, R.E.T., Hoatson, D.M., Perring, R.J., Witt, W.K., Mathison, C.I. and Bunting, J.A. 1991. Layered mafic-ultramafic complexes of Western Australia: Introduction. In: S.J. Barnes and R.E.T Hill (editors), Mafic-ultramafic complexes in Western Australia, Geological Society of Australia, WA Division Excursion Guidebook 3. pp. 1-13.

Brindley, G.W. 1980. Quantitative X-ray mineral analysis of clays. In: G.W. Brindley and G. Brown (editors). Crystal structures of clay minerals and their X-ray identification. Mineralogical Society Monograph No 5. 411-438.

Butt, C.R.M., 1986. Platinum group elements in weathered ultramafic rocks at Mt. Keith. Restricted Report, MG 3R. CSIRO Australia, Division of Minerals and Geochemistry, Perth, 17 pp.

Butt, C.R.M., 1991. Dispersion of gold and associated elements in the lateritic regolith, Mystery Zone, Mt. Percy, Kalgoorlie, Western Australia. CSIRO/AMIRA Weathering Processes Project P241. CSIRO Australia, Division of Exploration Geoscience, Restricted Report 156R. Volumes I and II. 226pp.

Butt, C.R.M., 1992. Semiarid and arid terrains. In: C.R.M. Butt and H.Zeegers (Editors): Regolith Exploration Geochemistry in Tropical and Subtropical Terrains: Handbook of Exploration Geochemistry 4. Elsevier, Amsterdam, pp. 324-328

Butt, C.R.M. and Nickel, E.H., 1981. Mineralogy and geochemistry of the weathering of the disseminated nickel sulfide deposit at Mt Keith, Western Australia. Economic Geology, 76: 1736-1751.

Butt, C.R.M., Gray, D.J., Lintern, M.J., Robertson, I.D.M., Taylor, G.F. and Scott, K.M. 1991. Gold and associated elements in the regolith - dispersion processes and implications for exploration. Final Report. CSIRO/AMIRA Weathering Processes Project P241. CSIRO Australia, Division of Exploration Geoscience, Restricted Report 167R.114pp.

Carver, R.N., Chenoweth, L.M., Mazzucchelli, R.H., Oates, C.J. and Robbins, T.W., 1987. "Lag" - A geochemical sampling medium for arid terrain. In: R.G. Garrett (Editor), Geochemical exploration 1985. Part I. Journal of Geochemical Exploration, 28: 183-199.

Deer, W.A., Howie, R.A., and Zussman, J. 1967. An introduction to the rock forming minerals. Longmans, Green and Co. Ltd. London. 528 pp.

Hallberg, J.A., 1984. A geochemical aid to rock type identification in deeply weathered terrain. Journal of Geochemical Exploration, 20: 1-8.

Harrison, P.H., 1990. Platinum group elements. Review of exploration techniques and targets. In: Mineral exploration, geology and geophysics: Quo vadis? Proceedings of 30th Annual Technical Meeting, Australian Mineral Industries Research Association, Melbourne, pp. 1-15.

Hart, M.K.W., 1989. Analysis for total iron, chromium, vanadium and titanium in varying matrix geological samples by XRF, using pressed powder samples. In: Standards in X-ray analysis. Fifth State Conference, Australian X-ray Analytical Association (WA Branch), Perth, pp. 117-129.

Hoatson, D.M. and Keays, R.R. 1989. Formation of platiniferous sulfide horizons by crystal fractionation and magma mixing in the Munni Munni layered intrusion, west Pilbara Block, Western Australia. Economic Geology, 84: 1775-1804

Menzies, J.C., 1988a. Second annual report, Ora Banda Prospect, Broad Arrow Mineral Field, Western Australia. Unpublished Report, WA Mines Department. 18 pp.

Menzies, J.C., 1988b. Second annual report, Mt. Carnage Prospect, Broad Arrow Mineral Field, Western Australia. Unpublished Report, WA Mines Department. 15 pp.

Norrish, K. and Chappell, B.W., 1977. X-ray fluorescence spectrometry. In: J. Zussman (Editor), Physical methods in determinative mineralogy. Academic Press, London, pp. 201-272.

Ramanaidou, E.R., Horwitz, R.C. and Morris, R.C. 1991. Channel iron deposits - Progress Report No 2. CSIRO Exploration Geoscience Restricted Report 162R. 63 pp.

Robertson, I.D.M., 1989. Geochemistry, petrography and mineralogy of ferruginous lag overlying the Beasley Creek gold mine - Laverton, W.A. CSIRO/AMIRA Weathering Processes Project P241 and Laterite Geochemistry Project 240. CSIRO Australia, Division of Exploration Geoscience, Restricted Report 27R. Volumes I and II. 181pp.

Schulze, D.G. 1984. The influence of aluminium on iron oxides. VIII. Unit-cell dimensions of Al substituted goethites and estimation of Al from them. Clays and Clay Minerals: 32, 36-44.

Thornber, M.R.and Wildman, J.E., 1979. Supergene alteration of sulphides, IV, Laboratory study of the weathering of nickel ores: Chemical geology, 24: 97-110.

Travis, G.A., Keays, R.R. and Davison, R.M., 1976. Palladium and iridium in the evaluation of nickel gossans in Western Australia. Economic Geology, 71: 1229-1243.

Witt, W.K. and Barnes, S.J. 1991. The Ora Banda Sill. In: S.J. Barnes and R.E.T Hill (editors), Mafic-ultramafic complexes in Western Australia. Geological Society of Australia, WA Division Excursion Guidebook 3. pp.31-35